

THE UNIVERSITY OF SHEFFIELD
DEPARTMENT OF CHEMISTRY



The Synthesis and Application of Hyperbranched Copolymers

HAMZA AHMED QASEM

PhD Thesis

2017

Supervised by

Dr. LANCE J. TWYMAN

The Synthesis and Application of Hyperbranched Copolymers

Hamza Ahmed Qasem

A thesis submitted for the degree of Doctor of Philosophy

The University of Sheffield
Department of Chemistry
Sheffield, S3 7HF
England

November 2017

إلى الوالدة والوالد

﴿..... وَقُلْ رَبِّ ارْحَمْهُمَا كَمَا رَبَّيَانِي صَغِيرًا﴾*

To Mum & Dad

*“My Lord, bestow on them Thy Mercy even as they Cherished me in childhood”***

* The Holy Qur-Ān.

** The Holy Qur-Ān, English translation of the meanings and Commentary, King Fahd Holy Qur-ān Printing Complex.

Acknowledgement

I would like to acknowledge Dr Lance Twyman for his supervision, great help and advice throughout the time it took me to complete my research.

I am also very grateful to have met wonderful people who were always with me during the four years and available to assist me. Special thanks must go to Ms Devanshi Singh, Ms Alaa Kadhim, Mr Greg Clixby and Mrs Fatema Aboshnaf. I would also like to thank Dr Meshari Alsharif, Dr Muhammad Azrul and Dr Kuljit Dyal for their assistance during the early part of my PhD research. My thanks also extend to Ms Heather Grievson for running GPC and Mr Robert Hanson for running GC.

It would be impossible to proceed any further without the mention of some individuals whom I met through serendipitous circumstances and who made my years as a postgraduate student unforgettable; they are Mr Ibrahim Althobiti, Mr Talal Algassab, Mr Bunian Shareef, Mrs Azrah Abdul Aziz, Ms Samira Hussein, Mr Meng Fan, Ms Neelam Mughal, Mr Bader Altayeb, Dr Bakaet Alqurashy and Mr Jawad Abaies.

Without their love, support and prayers this work would not be accomplished. I offer my deepest gratitude to my wife, son and daughter. This gratitude also extends to my brothers and sister for their unlimited support during my PhD. In addition, not to forget Dr Mouslim Messali who encouraged me to proceed my higher education.

Finally, special thanks also go to Taibah University for its financial support throughout the period of my PhD study.

Abstract

Incorporation of comonomers into hyperbranched poly(3,5-diacetoxybenzoic acid) is explored in this thesis. Hyperbranched polymers with up to 20% of comonomers retained their dendritic properties and physical behaviour. These findings were then applied to study the application of hyperbranched copolymer as catalyst and light-harvesting models.

Chapter 2 reports the development of a simple one-pot methodology for the functionalisation of a hyperbranched copolymer. This was used to prepare HBPs with multiple peripheral units. These units significantly increased the solubility, which enabled the hyperbranched copolymer to be used to study binding and catalysis in a range of solvents. Initial binding experiments in toluene and chloroform showed there was a steric barrier, which might be exploited in terms of catalysis. However, all HBP catalysed reactions in all the solvents performed identically to those performed in the control reactions.

Techniques developed in chapter 2 were used in chapter 3 in an attempt to prepare a photosynthetic model for possible application for light harvesting. Incorporation of multiple ligand functionalities into the polymer was achieved, and these need to bind a number of porphyrin units. Binding constants were $1 \times 10^3 \text{ M}^{-1}$ and $1 \times 10^5 \text{ M}^{-1}$ for a monomeric porphyrin and a dimeric porphyrin respectively. The position of the ligands and the number of ligands were confirmed using NMR and UV titrations. Moreover, a self-assembly process led to the formation of a multi-porphyrin array, which was confirmed via diffusion NMR and DLS.

Abbreviations

Standard Abbreviations

^{13}C NMR	Carbon Nuclear Magnetic Resonance Spectrometry
^1H NMR	Proton Nuclear Magnetic Resonance Spectrometry
DB	Degree of Branching
ESMS	Electrospray Ionisation Mass Spectrometry
GPC	Gel Permeation Chromatography
IR	Infrared Spectrophotometry
UV/Vis	Ultraviolet, Visible Light Spectrophotometry
L	Linear unit
T	Terminal unit
D	Dendritic unit
-Co-	Copolymerisation
K_a	Binding Constant
GC	Gas Chromatography
MgSO_4	Magnesium Sulphate
DCM	Dichloromethane
THF	Tetrahydrofuran
DMSO	Dimethyl Sulphoxide
Ethyl OAc	Ethyl Acetate
DMF	Dimethylformamide
DME	Dimethoxyethane
DLS	Dynamic light scattering

NMR Abbreviations

s.....	singlet
d	doublet
t	triplet
q	quartet
m	multiplet
dd	Doublet of Doublets
dt	Doublet of Triplets
br	broad

o- ortho

m- meta

p- para

Nomenclature

HBP_s Hyperbranched Polymers (Hyperbranched Polyarylesters)

SA Stearic Acid

NPA 4-Nitrophenyl Acetate

HBP-SA Poly(3,5-Diacetoxybenzoic Acid)-co-(Stearic Acid)

NPA-HBP 4-Nitrophenyl Acetate cored Hyperbranched Poly(3,5-Diacetoxybenzoic Acid)

NPA-HBP-SA 4-Nitrophenyl Acetate cored Hyperbranched Poly(3,5-Diacetoxybenzoic Acid)-co-(Stearic Acid)

AMPy 3-(Acetoxymethyl) Pyridine

AMPy-HBP-SA 3-(acetoxymethyl) Pyridine cored Hyperbranched Poly(3,5- Diacetoxybenzoic Acid)-co-(Stearic Acid)

AMPy-HBP 3-(Acetoxymethyl) Pyridine cored Hyperbranched Poly(3,5- Diacetoxybenzoic Acid)

Py 3-Acetoxy pyridine

Py-HBP-SA (Py-HBP) 3-Acetoxy pyridine cored Hyperbranched Poly(3,5-Diacetoxybenzoic Acid)-co-(Stearic Acid)

ATPP 4-Acetoxyphenyl Porphyrin

ZnTAPP Zinc functionalized 4-Acetoxyphenyl Porphyrin

DMAD Dimethyl Acetylene Dicarboxylate

DMAP 4-Dimethylaminopyridine

INA Isonicotinic Acid

HBP-INA Poly(3,5-Diacetoxybenzoic Acid)-co-(Isonicotinic Acid)

ZnTPP Zinc Functionalized Monomeric Porphyrin

ZnTPP-ZnTPP Zinc Functionalized Dimeric Porphyrin

TAPP-HBP-INA 4-Acetoxyphenyl Porphyrin cored Hyperbranched Poly(3,5- Diacetoxybenzoic Acid)-co-(Stearic Acid)

Table of Contents

ACKNOWLEDGEMENT	I
ABSTRACT	II
ABBREVIATIONS.....	III
1. INTRODUCTION.....	2
1.1. Preface.....	2
1.2. Dendritic Polymers	4
1.2.1. Introduction	4
1.2.2. Dendritic Structure	4
1.2.3. Dendritic Polymer Terminology.....	5
1.2.4. Molecular weight of Polymer	7
1.3. Dendritic Polymers Properties	10
1.3.1. Preface	10
1.3.2. Viscosity.....	10
1.3.3. Solubility.....	11
1.3.4. Hydrodynamic Volume	11
1.3.5. Dense Shell and Dense Core.....	12
1.4. Dendritic Polymer Preparation	13
1.4.1. Dendrimer Synthesis	13
1.4.2. Hyperbranched Polymer Synthesis	14
1.5. Dendritic Polymers Applications	17
1.6. Porphyrin	19
2. HYPERBRANCHED COPOLYMER SYSTEMS AS A CATALYTIC SUPPORT	21
2.1. Introduction.....	21
2.1.1. Single Cored Hyperbranched Polymers.....	23
2.1.2. High Loading Peripheral Hyperbranched Copolymers	25
2.1.3. Probing Effect of Comonomers on Hyperbranched Copolymer Properties	27

2.1.4. Effect of Branching on Viscosity	30
2.1.5. Effect of Branching of the Packed Limits within a Hyperbranched Copolymer via Ligand Binding.....	31
2.2. Aims.....	33
2.3. Synthesis.....	35
2.3.1. Summary	35
2.3.2. Polymerisation of 3,5-Diacetoxybenzoic acid, 2HBP	36
2.3.3. Copolymerisation of 3,5-Diacetoxybenzoic acid and Stearic acid, 4HBP-SA	41
2.3.4. Controlling the Molecular Weight of the Hyperbranched Copolymer by Adding 4-Nitrophenyl Acetate as Core, 7NPA-HBP-SA	45
2.3.5. Synthesis of Pyridine 3-(Acetoxymethyl) Cored Hyperbranched Copoly (3,5-Diacetoxybenzoic acid) and (Stearic acid), 8AMPy-HBP-SA	51
2.3.6. 3-Acetoxy-pyridine Cored Hyperbranched Copoly (3,5-Diacetoxybenzoic acid) and (Stearic acid), 11Py-HBP-SA.....	53
2.4. UV/Vis Study.....	57
2.4.1. Preface.....	57
2.4.2. Synthesis of 4-Acetoxyphenyl Porphyrin, 15TAPP	59
2.4.3. Porphyrin Zinc Complex, 16ZnTAPP	61
2.4.4. Binding study	62
2.5. Catalysis.....	66
2.5.1. Catalysis Reaction of an Alkyne with an Aromatic Aldehyde, Monitored by GC.....	66
2.5.2. Catalysis Reaction in Standard Solvent, Monitored by NMR	71
2.5.3. Direct NMR Analysis for Catalysis Reaction, using Deuterated Solvents	73
2.6. Conclusion	82
3. LIGHT HARVESTING HYPERBRANCHED COPOLYMER MODEL.....	85
3.1. Introduction.....	85
3.1.1. Multi-Porphyrin Arrays as Model Compound	87
3.1.2. Dendritic Polymers in Light Harvesting Systems	89
3.2. Aims.....	94
3.3. Copolymerisation of 3,5-Diacetoxybenzoic Acid and Isonicotinic Acid, 17HBP-INA	98

3.4. Complexation of Multiple Zinc-Metalled Porphyrins with Pyridine Ligand containing Hyperbranched Polymer	100
3.4.1. Synthesis of Metal Functionalised Monomeric Porphyrin (19ZnTPP), and Metal Functionalised Dimeric Porphyrin (20ZnTPP-ZnTPP)	100
3.4.2. Binding Study.....	102
3.4.3. Proof of Stoichiometry and Availability.....	103
3.4.4. Proof of Self Assembled System	108
3.5. Copolymerisation of 3,5-diacetoxybenzoic acid with Isonicotinic Acid (INA) and Tetraacetoxyphenyl Porphyrin (TAPP); 21TAPP-HBP-INA	112
3.6. Conclusion	115
4. EXPERIMENTAL DETAILS	118
4.1. General experimental Conditions	118
4.1.1. Chemicals and Instruments	118
4.1.2. Nuclear magnetic resonance spectroscopy (NMR)	118
4.1.3. Infra Red Spectroscopy (IR)	118
4.1.4. Ultra Violet-Visible (UV/Vis) Spectroscopy.....	118
4.1.5. Analytical Gel Permeation Chromatography (GPC).....	118
4.1.6. Mass Spectroscopy (MS)	119
4.1.7. Gas Chromatography (GC).....	119
4.2. Synthesis	120
4.2.1. General Procedure 1: Polymerisation/Copolymerisation	120
4.2.2. General Procedure 2: Synthesis of Porphyrins.....	120
4.2.3. General Procedure 3: Synthesis of Zinc Functionalized Porphyrins	120
4.2.4. Synthesis of 3,5 Diacetoxybenzoic Acid 1, AB ₂ monomer	121
4.2.5. Polymerisation of 3,5-Diacetoxybenzoic Acid, 2HBP.....	121
4.2.6. Copolymerisation of 3,5-Diacetoxybenzoic acid and Stearic acid, 4HBP- SA%	122
4.2.7. 4-Nitrophenyl acetate Cored Hyperbranched Copoly (3,5-Diacetoxybenzoic acid) and (Stearic acid), 7NPA-HBP-SA%	123
4.2.8. Polymerisation of 3,5-Diacetoxybenzoic Acid with 4-Nitrophenyl acetate core, 6NPA-HBP%	124
4.2.9. Synthesis of Pyridine 3-(Acetoxymethyl), AMPy9	124
4.2.10. 3-Acetoxy-pyridine Cored Hyperbranched Copoly (3,5-Diacetoxybenzoic acid) and (Stearic acid), 11Py-HBP-SA.....	125
4.2.11. Preparation of 2-oxo-3-benzylidenesuccinate, 13.....	126
4.2.12. Preparation of 4-Acetoxybenzaldehyde, 14	126

4.2.13. Synthesis of 4-Acetoxyphenyl Porphyrin, 15TAPP	127
4.2.14. Porphyrin Zinc Complex, 16ZnTAPP	127
4.2.15. Pyridine Catalysed Control Reaction of DMAD with 3-Nitrobenzaldehyde (in 5 mL standard solvent).....	127
4.2.16. Pyridine Catalysed Control Reaction of DMAD with 3-Nitrobenzaldehyde (in 1 mL deuterated solvent).....	128
4.2.17. Cored Pyridine Catalysis Reaction of DMAD with 3-Nitrobenzaldehyde (in 1 mL deuterated solvent).....	128
4.2.18. Recovery Experiment of Cored Pyridine Catalyst (in 3mL normal solvent).....	129
4.2.19. Copolymerisation of 3,5-Diacetoxbenzoic Acid and Isonicotinic Acid, 17HBP-INA	129
4.2.20. Synthesis of Tetraphenyl Porphyrin, TPP	130
4.2.21. Synthesis of Tetraphenyl Porphyrin, 19ZnTPP	130
4.2.22. Copolymerisation of 3,5-diacetoxybenzoic acid with Isonicotinic Acid (INA) and Tetraacetoxyphenyl Porphyrin (TAPP); 21TAPP-HBP-INA	130
5. REFERENCE	132

Chapter 1

1. Introduction:

1.1. Preface:

Polymers are a class of materials that are composed of many small molecules connected together. These small molecules, termed monomers, can be linked together by covalent bonds to form long chains. The terms polymer and monomer were created from the Greek words: poly (many), mono (one), and mer (unit).¹ Generally, polymers can be split into four main classes according to their properties and architecture: (i) linear and random coil thermoplastics, such as nylon; (ii) cross-linked architectures and thermosets, such as epoxy resins; (iii) branched systems based on long chain-branched in polyolefins, such as low-density polyethylene; and, (iv) dendritic (highly branched) polymers (**Figure 1.1**).^{2,3}

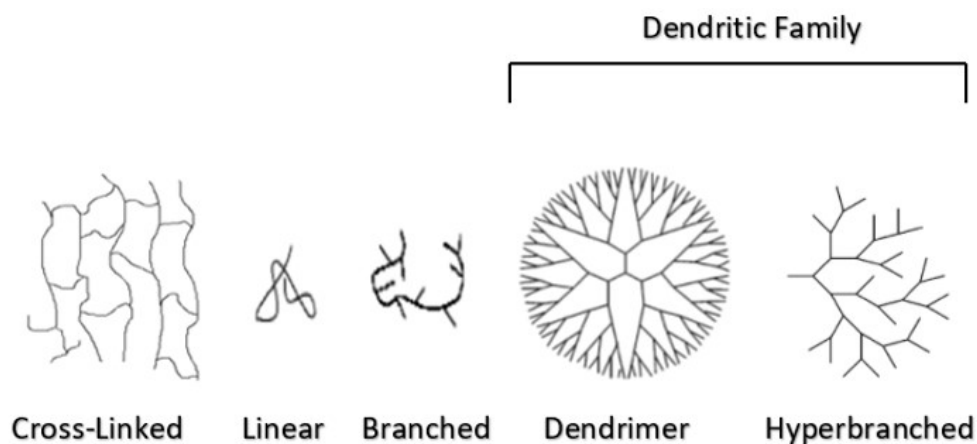


Figure 1-1. General architectures of polymers.^{4,5}

Dendritic architectures are perhaps one of the most dominant topologies observed on our planet and represent a new promising aspect of macromolecular chemistry to replace conventional polymers. Many examples of these patterns can be found in abiotic systems and in the biological world, including lightning patterns, snow crystals, tree roots, and neurons. This thesis is focused on the fourth class and its subclasses. The aim of this review is to provide the reader the essential knowledge to understand the topic and concept that is applied in this research. Moreover, a number of excellent references in the literature are provided in case more information is required in more detail.⁶⁻¹³

In addition, a brief introduction about porphyrins is also provided, as metalloporphyrins were utilized in this research to generate coordination complexes with pyridyl ligand (within hyperbranched polymer in order to probe the microenvironment of this system). Furthermore, porphyrins were employed as a unit within hyperbranched polymers to mimic natural light harvesting systems. This hyperbranched model contains the free-based/unmetallated porphyrin at core, which can act as an acceptor and peripheral pyridine. Metal functionalized porphyrins can interact with pyridines through non-covalent chemistry and act as a donor.

1.2. Dendritic Polymers:

1.2.1. Introduction:

Dendritic polymers are highly branched polymers (macromolecules) with three dimensional architectures and are a new attractive field in polymer chemistry. Meanwhile, linear polymers up to the present time play a focal point in research. Moreover, these linear macromolecules sometime contain some small branches however, dendritic polymers have become more interesting, due to their structure having a great impact on their application, since Vögtle,¹⁴ Tomalia,¹⁵ and Newkome¹⁶ reported the first synthesis of a highly branched system.

1.2.2. Dendritic Structure:

Dendritic chemistry is an independent research field, which has led to its own nomenclature. Dendritic architecture composed of six subclasses: dendrimers (dendrons), linear-dendritic hybrid, dendrigraft polymers, hyperbranched polymers (HBPs), star polymers, and hypergrafted polymers.⁵ This review is intended to cover two types of dendritic polymers, dendrimers and hyperbranched. The interest in dendrimers and hyperbranched polymers has risen since both show unique properties that make them very attractive materials for academic and industrial researchers.

Generally, AB_n monomers (where $n \geq 2$) are required to construct dendritic polymers (**Figure 1.2**). Consequently, the stepwise reaction of AB_2 monomers leads to perfectly branched and monodisperse dendrimers. In contrast, the polymerisation of AB_2 monomers generates imperfectly branched and polydisperse hyperbranched polymers. The less ordered structure of hyperbranched polymers is caused by incomplete reactions of the monomer.

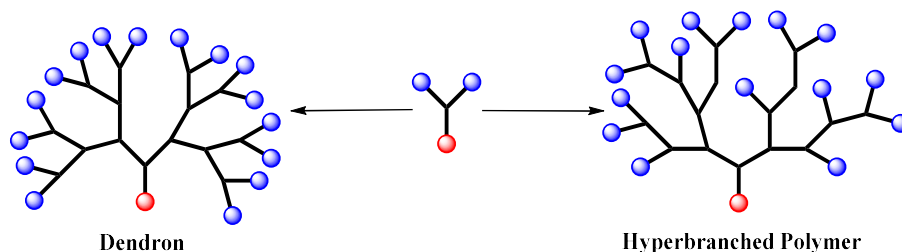


Figure 1-2. Dendritic growth vs random growth through AB_2 monomer.

1.2.3. Dendritic Polymer Terminology:

Dendritic polymers with highly branched 3D structures require a new way to describe them. Conventional polymer nomenclature cannot express certain aspects of dendritic structure. This has led scientists to develop specific terminology suited to dendritic polymers, where “dendrimer” and “hyperbranched polymers” are clear examples that illustrate branched terminologies. Dendrimers and hyperbranched polymers share two distinct types of dendritic units: (1) monomers contributing to total branching are termed *dendritic units* (D); (2) monomer residues at the periphery of the compound are termed *terminal units* (T). Whereas hyperbranched polymers possess one further unit; (3) when the monomer contributes linear character to polymer structure, due to its partial reaction, which is termed *linear units* (L) (**Figure 1.3**).

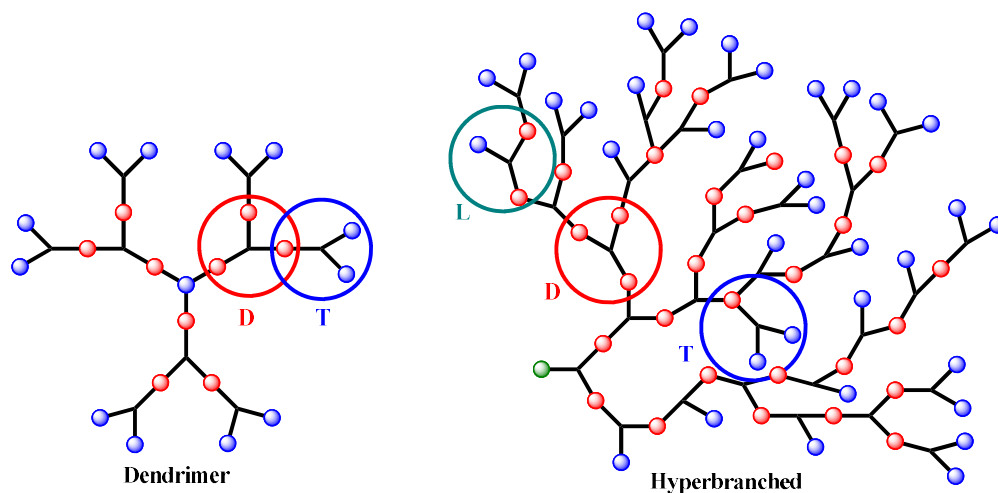


Figure 1-3. Dendrimer structural units and Hyperbranched polymer structural units.

Dendrons is also a common term used in polymer science, which are dendritic wedges without a core. Dendrons have high regular structure (monodisperse), and the capability to control their molecular weight. Typically, assembling two or more dendrons together leads to preparing the dendrimers. The term *generation* is used to define the different levels or stages of synthesis as you move from the core to the surface. In addition, dendritic polymers have a large number of *end groups*, whereas linear polymers have only two end groups. These end, or terminal, groups are functionalized units at the extremity of a macromolecule, which can be further functionalised (**Figure 1.4**).

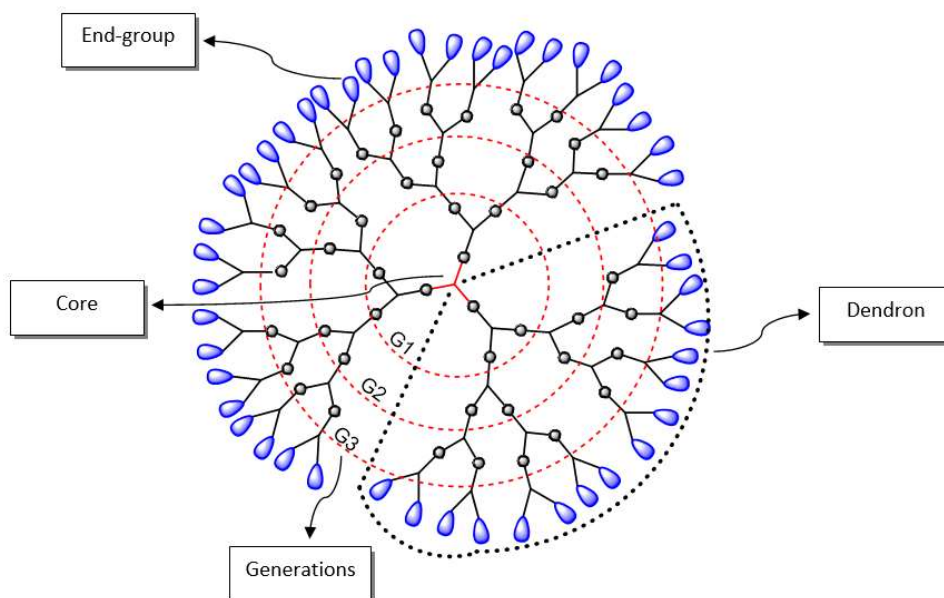


Figure 1-4. Different structural components of the dendrimer.

The *degree of branching* (DB) was described by Fréchet in 1991 to compare hyperbranched polymers with perfectly branched dendrimers **Equation 1**.¹⁷ Generally, this equation is appropriate for hyperbranched polymers synthesised via AB_2 units. The ratio of linear (L), dendritic (D), and terminal (T) units is 2:1:1 respectively, which equals to a DB of 50%, while, DB for perfectly structured dendrimers is 100% and 0% for linear polymers.

$$DB = \frac{D + T}{D + L + T} \dots \text{Equ. 1}$$

Later Frey et al. developed a second equation for the DB, modification was reported as shown in **Equation 2**.¹⁸

$$DB = \frac{2D}{2D + L} \dots \text{Equ. 2}$$

1.2.4. Molecular Weight of Polymer:

Like small molecules, the molecular weight is important to determine the physical properties of the polymer. Such as glass transition temperature (T_g) (including transition from liquid to wax to rubber to solid) and mechanical properties (stiffness, strength and viscosity). However, polymeric substance contains molecules of various sizes or/and existence of a distribution of chain lengths. Polymers of uniform molecular size are comparatively rare (such as a protein), therefore, the repeating unit of the polymer molecule is more fundamental significant than the molecule itself. The way applied to characterise the mass of the polymeric molecule could be by molecular weight distribution or a molecular weight average. Typical molecular weight molecular distribution can be illustrated by plotting the weight of polymer of a given molecular weight against the molecular weight, as shown in **Figure 1.5**.

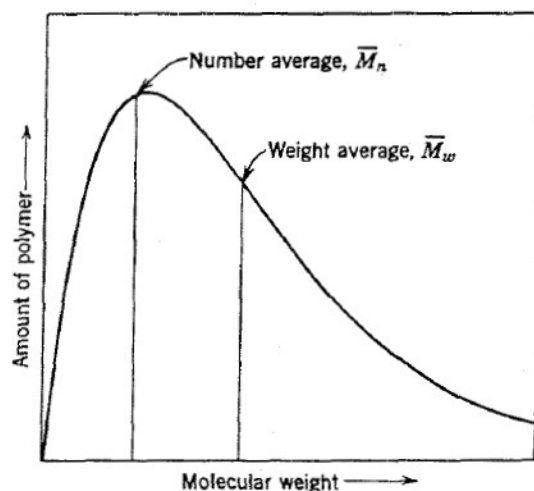


Figure 1-5. Distribution of molecular weights with various average molecular weight.

Because of the existence of the distribution in any sample of polymer, the experimental measurement of molecular weight can give only an average value. However, average molecular weight can be calculated in many ways, and the formal definitions of some common molecular weight average are as follows:

Number average molecular weight: M_n

$$M_n = \frac{\sum N_i M_i}{\sum N_i} \dots \text{Equ. 3}$$

Where M_i is the molecular weight of a chain and N_i is the number of chains of that molecular weight. The number average molecular weight (M_n) is the statistical average molecular weight of all the polymer chains in the sample which means M_n is sensitive to the number molecules present in mixture. M_n is also highly sensitive to small number of low molecular weight fraction. Whereas, M_n can be predicted by polymerization mechanisms.

Weight average molecular weight: M_w

$$M_w = \frac{\sum N_i M_i^2}{\sum N_i M_i} \dots \text{Equ. 4}$$

M_w depends on the size/weight of each polymer molecule, not just on the number of polymer molecules such M_n . M_w is sensitive to small amounts of high molecular weight material by weight.

The polydispersity index (PDI) is used as a measure of the broadness of a molecular weight distribution of a polymer, and is defined by:

$$PDI = \frac{M_w}{M_n} \dots \text{Equ. 5}$$

The narrow molecular weight distribution is a monodisperse polymer, which implies all the chain lengths are equal and has $PDI = 1$. The larger PDI, the broader the molecular weight distribution and has $PDI > 1.20$.

There are several methods to measure these molecular weights of the polymers and GPC is one of the most important and convenient ways. GPC is a process whereby polymer molecules can be separated on a size basis by permeation/filtration through the gel. The gel is in the form of the column and consists of a highly crosslinked polymer. The polymer in solution passes from the top of the column, and the column is eluted with a steady stream of the solvent which is mobile phase. Polymer molecules are separated by size because of their ability to penetrate pore of the gel particles which is the stationary phase. As the sample moves along the column, the largest molecules are almost entirely passed the stationary phase and collected first, while the smallest molecules are found stuck on the gel's pore. Thus, small molecules fall behind larger ones and are collected later (**Figure 1.6**).

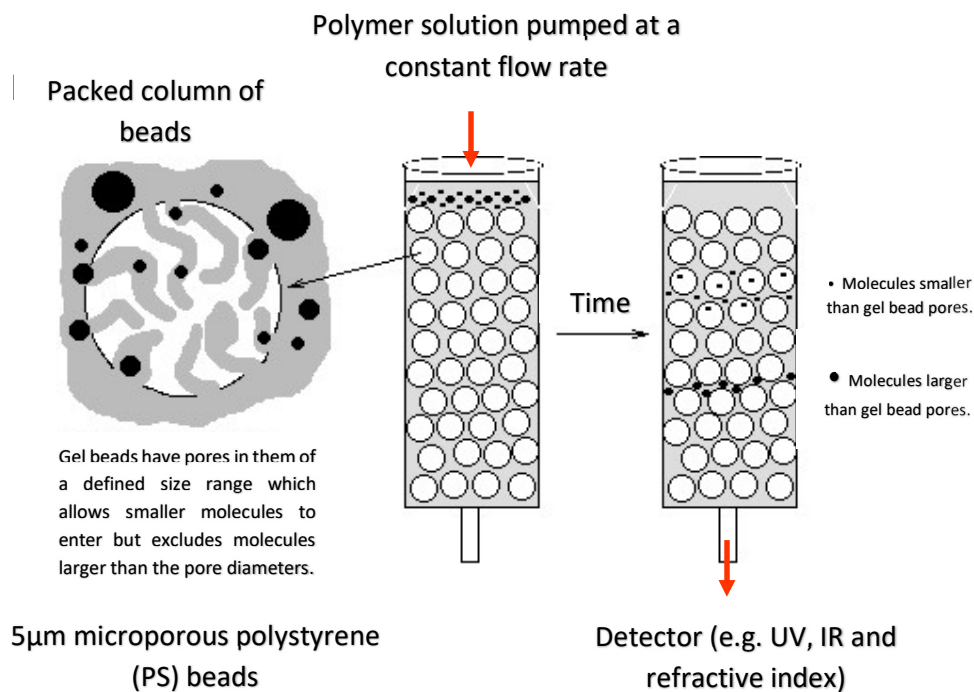


Figure 1-6. The size separation mechanism and schematic of pore vs analyte size.¹⁹

The common GPC equipment consists of column, flow system (solvent reservoir, pump and associated devices) and detector. UV absorbance, light scattering and viscometer can be used as detectors, but differential refractometer is regularly used.

1.3. Dendritic Polymers' Properties:

1.3.1. Preface:

Polymer chemistry and technology has used linear polymers containing small or long branches in many different applications. Recently, it has been found that the properties of highly branched macromolecules can be very different to traditional polymers, which enables them to be used in several applications. In this section, dendritic polymers will be compared with linear polymers to demonstrate their unique features.

1.3.2. Viscosity:

The elongated structure of linear polymers results in a number of attractive secondary forces along their chain, which can be higher than those of a globular structure of dendritic polymers. Subsequently this leads to a significant decrease in chain entanglement for a globular structure and a significant increase in chain entanglement for an elongated structure. This means a dendritic polymer possesses low viscosity due to it being less entangled than linear polymers. On the other hand, the relationship between the molecular weight and viscosity of linear polymers, dendrimers, and hyperbranched polymers is illustrated schematically in **Figure 1.7**. The graph displays that as the molecular weight increases the viscosity of linear polymers also increase. Whereas, dendrimer viscosity reaches a maximum before it is falling at a higher dendrimer generations. This occurs as higher generation dendrimers have a compact globular structure, leading to a decrease in the degree of entanglement.²⁰ Hyperbranched polymers have a viscosity intermediate between linear polymers and dendrimers, however, the viscosity of hyperbranched polymers is not as dramatic as the rise for dendrimers.²¹

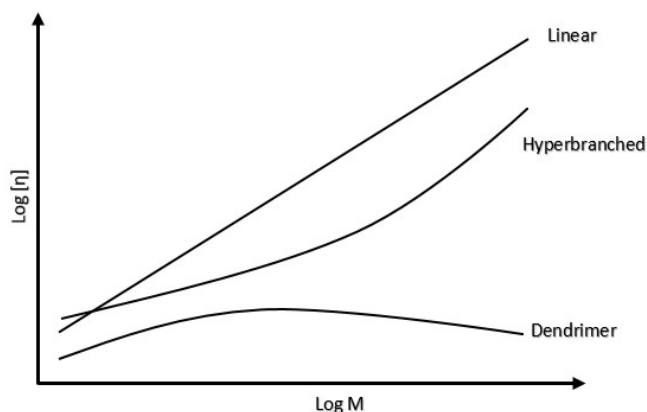


Figure 1-7. Schematic plot of $\text{Log } [\eta]$ (Intrinsic Viscosity) against $\text{Log } M$ (mass) for polymers.

1.3.3. Solubility:

Solubility is dependent on the structure of a polymer, its branching and the nature of their terminal groups. Dendritic polymers have many end groups that help control solubility. Considering that a large number of end groups are exposed to solvent explains why the solubility of dendritic polymers is different to classical linear polymers. In addition, the terminal functional groups of dendrimers and hyperbranched polymers can be tailored to reach the required solubility in certain solvents. This means that end groups play a significant role in solubility, which is an important factor to impact polymer applications.²²

1.3.4. Hydrodynamic Volume:

Dendritic polymers have a smaller hydrodynamic volume compared to equivalent linear polymers, as a consequence of their highly-branched architecture. As this branching gets larger, from one generation to another, the dendritic polymers form a more compact structure. This compact structure leads to difficulty in measuring the molecular weight by gel permeation chromatography (GPC). The GPC instrument is usually calibrated using linear polymers, such as polystyrene. This is a problem when analysing compact dendritic molecules. For example Kampf and co-worker showed that the hydrodynamic volume of dendrimers was almost 40% smaller than the linear polymer analogue, both of which possess the same molecular formulas and molecular weight.²³

1.3.5. Dense Shell and Dense Core:

Dendrimers have regular and well-defined structures, which means they are typically symmetrical. The terminal functional units of dendrimers, which form the surface, are presented facing outwards. This implies the dendrimer has a spherical shape. According to De Gennes et al, the periphery of a dendrimer has a high dense shell as the terminal groups are positioned in a concentric circle around the focal point of the dendrimer.²⁴ This could occur in some specific conditions, such as when the terminal groups have a strong interactions between them, or the structure of the dendrimer is constructed of stiff repeat units.^{25,26} However, computational investigations have revealed that terminal groups are not found exclusively at the dendrimer surface but may also be folded back to within the dendrimer core.²⁷ Depending on the size and chemical nature of dendrimer, these terminal groups can be found throughout the dendrimeric entity, which relieves the steric crowding on the dendritic surface and causes the core of the dendrimer to exhibit the highest density (**Figure 1.8**).²⁸ In contrast, hyperbranched polymers with irregular structure have reduced interactions between their terminal groups. As a result, these terminal groups would be found throughout the hyperbranched polymer's structure.

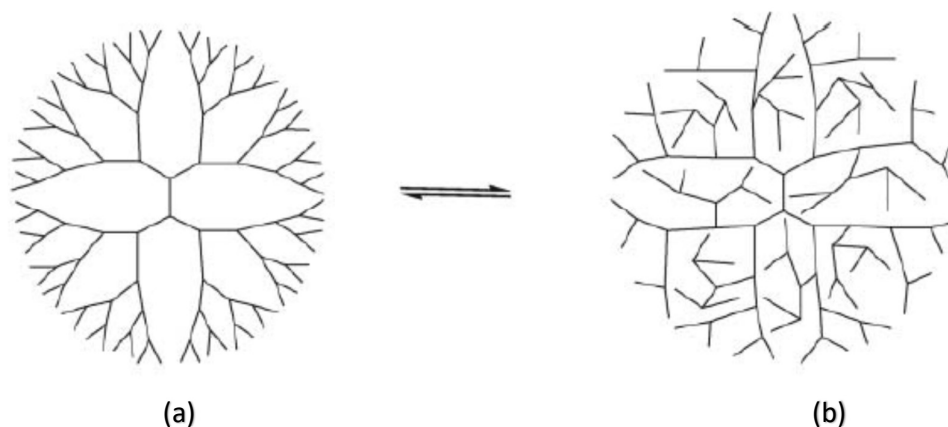


Figure 1-8. (a) Dense shell packing resulting of attractive forces between the surface or synthesized of stiff repeat units. (b) Folded back conformation depending on size and nature of repeat units which consequence increased core density of the dendrimer.²⁸

1.4. Dendritic Polymer Preparation:

1.4.1. Dendrimer Synthesis:

Dendrimers are synthesized by iterative synthetic methods, which make syntheses of dendrimers extremely laborious. They often require a series of activation and/or protection and deprotection steps, as well as separation and purification of the products after each synthesis step. The divergent method was the first method used to prepare dendrimers and was developed by Tomalia in 1985.²⁹ The concept of this method involves growth from a central core, where branching is aided by a series of repetitive steps. This method is characterized via reactions occurring at an ever-rising number of sites with the dendrimer being constructed from the inside out. After 5 years, a new method was developed by Hawker and Fréchet and was termed the convergent method.³⁰ This new concept involves the synthesis of small dendrons, which can be converged together on a central core to give the final dendrimer. This method is characterized by reactions occurring at only one site, the core or the focal point (**Figure 1.9**).^{13,31}

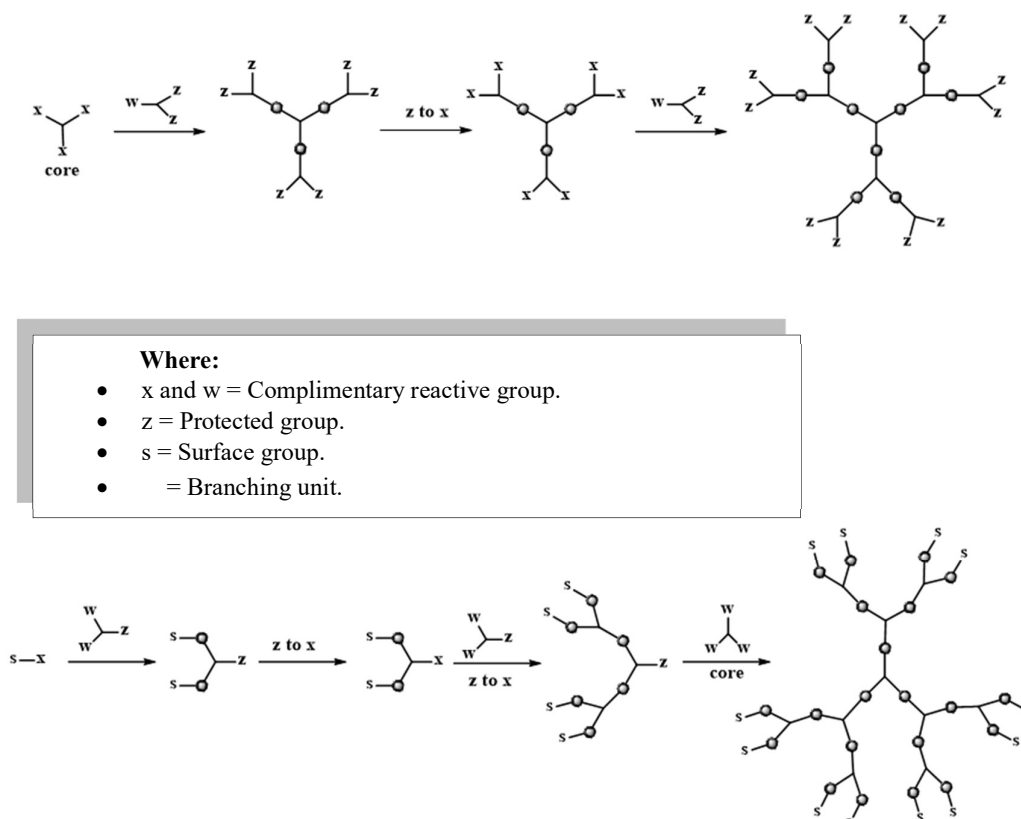


Figure 1-9. Dendrimer synthesis, in the top divergent method, and the bottom convergent method.

1.4.2. Hyperbranched Polymer Synthesis:

Many approaches have been investigated to generate branched polymers in order to avoid the complicated multistage synthetic procedure and unwanted side-reactions. These studies resulted in irregular architectures with incomplete branch points. However, in 1952 a new class of synthesis was proposed by Flory that could synthesise highly branched polymers by polycondensation of a monomer containing one A functional group and two or more B groups, where one of them can react with A (AB_n monomer, $n \geq 2$).³² Many years after Flory proposed this theory, the first hyperbranched polymer was synthesized by Kim and Webster.³³

The final properties and applications rely on the structure of repeating units of the A and B functionalities and the nature of the resulting end groups.³⁴ In contrast with dendrimers, HBPs offer a significant time, cost, and synthesis advantages *via* their one-pot processes, while dendrimers require multiple step reactions, including purification, protection, and deprotection processes. In addition, HBPs retain exceptional physical and chemical properties of their counterparts. Consequently, such molecules are easily obtained on a large scale, are less costly, and are often put forward as realistic alternatives to dendrimers in some applications.³⁵

Generally, HBPs can be synthesised by three main methodologies: step-growth polycondensation of AB_x and $A_2 + B_3$ monomers, self-condensing vinyl polymerisation of AB^* monomers, and multi-branching ring-opening polymerisation of latent AB_x monomers.^{8,9}

The principle of the step-growth polycondensation method is polymerisation of AB_x , where $x \geq 2$, monomers by a one-step polycondensation. Using AB_2 as an example, when a functional A group reacts with one molecule of a functional B group, the result is for linear units to be produced. Whereas, another A functional group reacts with a second B molecule then the branched unit would be generated. AB_2 class monomers are a popular route due to their easy preparation (**Figure 1.10**). This route can be used to synthesise hyperbranched polymers of polyester,³⁶ polyether,³⁷ and polyamide.³⁷ Whereas AB_3 , AB_4 , AB_5 , and AB_6 monomers have been used to synthesise polyester,³⁸ and polysiloxanes.³⁹ Although, step-growth polycondensation is a good method of

synthesis, gelation can occur, and purification of products is difficult, which can produce unwanted side reactions.⁴⁰

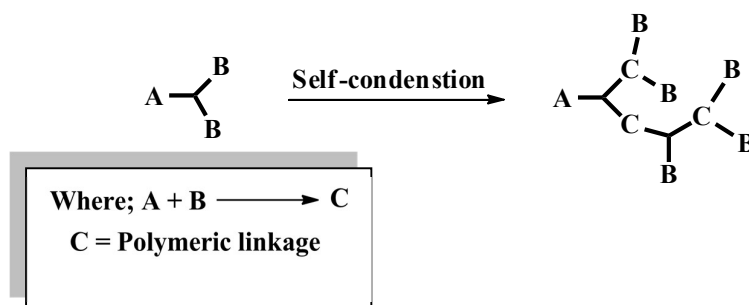


Figure 1-10. Step growth polycondensation AB_2 monomers.

The use of A_2+B_3 monomers can be an alternative route of polycondensation if the AB_2 units are not available (**Figure 1.11**). Nevertheless, there are many factors that should be considered in order to obtain a successful hyperbranched polymer. These include the ratio of functionalities, solvent, reagent purity, reaction time, and temperature. The main drawback in this strategy is that gelation may occur when direct polycondensation is applied. To avoid this problem, the polymerization can be stopped through precipitation, or end-capping, before reaching the critical point of gelation, such as adding monomer slowly, or by using specific catalysts and condensation agents. Generally, the polymerisation process is difficult to control and will often produce a high molecular weight. Various polymers have been prepared through this method such as polyamides.⁴¹

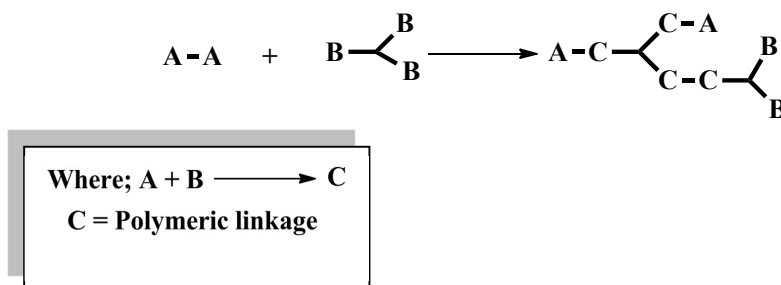


Figure 1-11. Step growth polycondensation A_2+B_3 monomers.

Self-condensing vinyl polymerisation is the second category to prepare hyperbranched polymers. The strategy of this method involves the use of monomers that aspect one double bond group and one initiating moiety (AB^* monomers). The initiating moiety could be activated as a cation, radical, and carbanion species, which then reacts with a double bond to generate a covalent bond. Another covalent bond could also be generated from the new active site on the second carbon (**Figure 1.12**). The disadvantages of this approach are crosslinking side reactions and chain transfers, which lead to gelation. In order to overcome these problems living/controlled polymerization can be used, such as atom transfer radical polymerization (ATRP). The hyperbranched polymers prepared with this method include polystyrenes,⁴² and polyacrylate.⁴³

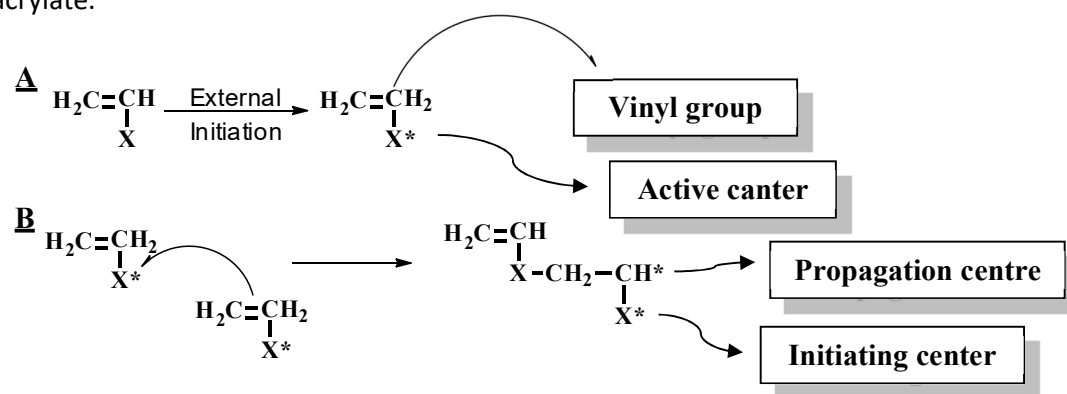


Figure 1-12. Self-condensing vinyl polymerization.

The third major category of hyperbranched polymerisation is the latent AB(B) method, of which ring-opening polymerisation is the most common form. In this technique, the terminal unit of the polymer acts as a reactive centre where additional cyclic monomers can react to form a larger molecule chain (**Figure 1.13**). The hyperbranched polymers formed via this method include polyamines,⁴⁴ polyethers,⁴⁵ and polyesters.⁴⁶

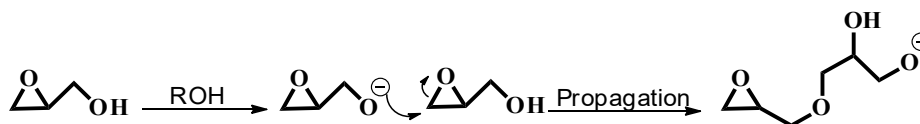


Figure 1-13. Synthesis of a hyperbranched polyglycerol by the ring opening polymerisation of glycidol.

1.5. Dendritic Polymers' Applications:

Originally the aim of first dendrimer research was to develop the methods of synthesis and the characteristics of these macromolecules. More recently these molecules have been used in a number of applications that exploit their unique architecture and construction. This includes their unparalleled molecular uniformity, multifunctional terminal group, and the presence of internal cavity dendrimers. Alternatively, HBPs have similar structure and properties, which means they can also be applied to a number of areas that can exploit their structure. Both dendrimers and HBPs have been used in a wide variety of applications, such as biomedical and industrial. This includes drug delivery, catalysis and light harvesting.^{45–50}

Dendritic polymer systems have been employed as promising scaffold in biomedical areas due to their unique three-dimensional designs and multi-end group functionality. For instance, Zhu and co-worker developed charge-tunable dendritic polycations for gene delivery via modification the end group of hyperbranched polyglycerol (HPG) with adamantane (AD) to obtain HPG-AD guest. Through host-guest interactions between HPG-AD and β -cyclodextrin (β -CD) derivative (primary- or tertiary- amine-functionalized) hosts and alteration of the molar ratios of these two cationic β -CD derivatives, the surface charge and molecular functionality of the resulting polycations can be efficiently regulated or optimized (**Figure 1.14**).⁵³

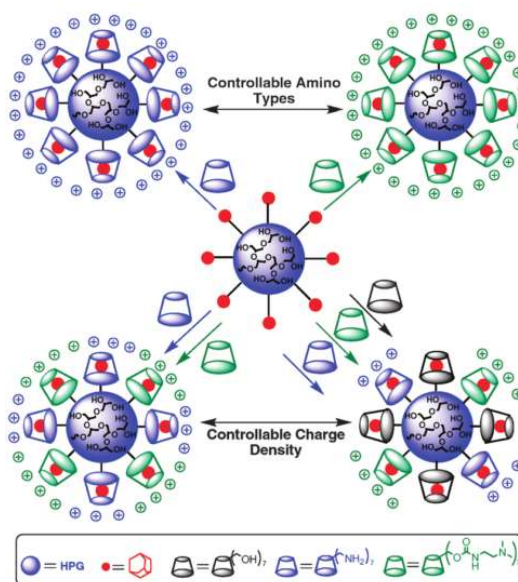


Figure 1-14. Construction of charge-tunable dendritic polycations via β -CD/AD host-guest interactions.⁵³

Furthermore, same group proposed the dendritic polymer to be important candidates in nanotechnology. This was done via obtaining CdS nanocrystals which could be readily realized from organic phase into aqueous phase through the electrostatic interaction between palmitic acid (PA) and hyperbranched polyethyleneamines (HPEI) or Hyperbranched polyamidoamine (HPAMAM).⁵⁴ Employing similar technique using star-copolymer (HPEI-star-mPDMS), Au@mesoporous silica nanoparticle (Au@MSN) nanocomposites was prepared via the in situ reduction of chloroauric acid (**Figure 1.15**), and these nanocomposites demonstrated brilliant catalytic performance.⁵⁵

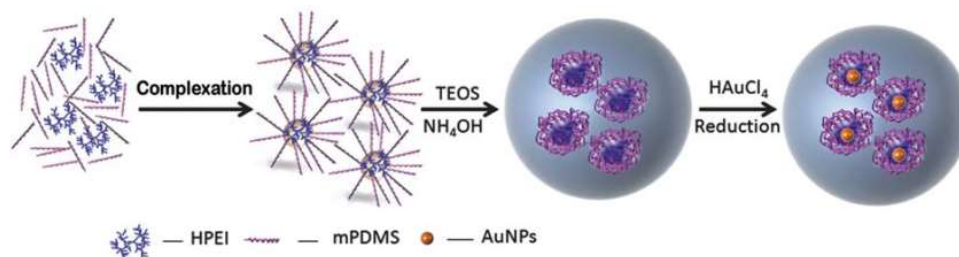


Figure 1-15. Construction of Au@MSN nanocomposites with a supramolecular star-copolymer template.⁵⁵

Another application which has received attention is the use of hyperbranched polymers as surface coatings, especially polymer films. Möller produced ultra-thin films from arborescent graft polystyrenes. The films produced were of even thickness and the overall thickness was found to be dependent on the molecular weight and branching density of the hyperbranched polymer in question.⁵⁶ Asif *et al.* investigated a waterborne coating using ultraviolet curing technology. Waterborne coatings have achieved a great deal of interest, as they are known to reduce air pollution, lower the risk of fire and improve numerous areas of occupational health and safety. A succession of waterborne hyperbranched polyurethane acrylates for aqueous dispersion based upon hydroxy functionalised polyester Boltoron H₂O were shown to display good dispersability.⁵⁷

1.6. Porphyrin:

Porphyrins are heterocyclic macrocycles composed of four pyrrole rings attached through α -carbon positions via four methylene bridges. 18 π -electrons conjugate easily through the porphyrin structure ring. As a consequence, porphyrin conforms to Hückel's rule ($4n + 2$), where n is 4, and are aromatic compounds. However, porphyrins and some related compounds are derived formally from porphines by substitution of several or all the hydrogen atoms 1-8 by diverse side-chains (**Figure 1.16**).

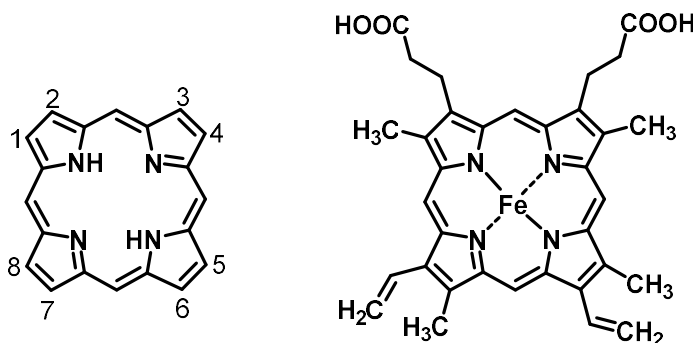


Figure 1-16. Porphine (left) heme (right).

Complexation chemistry is a property often exploited, as porphyrins possess a unique central cavity that can host numerous transition metals including iron, magnesium, and cobalt (in haemoglobin, chlorophyll, and vitamin B₁₂ respectively). This complexation is important and has an essential role in a number of biological systems, including oxygen transfer and electron transfer. The most illustrious example is haemoglobin, which is based on porphyrin hosting an individual iron atom. The porphyrin's metal is responsible for binding and transporting the oxygen in red blood cells of vertebrates and other animals.⁵⁸

Scientists are interested in porphyrins as they have wonderful biological, photonic, and electronic characteristics. When attached to dendritic polymers porphyrins have been involved in a number of applications, such as catalysts,⁵⁹ hemeprotein,⁶⁰ and light-harvesting.^{61,62} The fundamental concept of these examples is where the porphyrin is located either at the core and/or surface, or even at the repeat units.

Chapter 2

Results and Discussion (I)

2. Hyperbranched Copolymer Systems as a Catalytic Support:

2.1. Introduction:

Dendritic polymers have received great attention as catalytic supports. This interest has emerged because these three-dimensional branched macromolecules display various specific properties that improve compared to classical catalyst support. For example, the terminal groups along the dendritic surface can be adjusted to make them soluble in different solvents, including environmentally-friendly solvents. In addition, these globular-shaped polymers can be easily separated and purified using several methods, such as membrane separation techniques, size exclusion chromatography, and precipitation after reaction.⁶³ A distinct characteristic of dendritic macromolecules is their ability to narrow the gap between homogenous and heterogeneous catalytic systems.⁶⁴ A specific advantage is catalyst recovery and recycling, particularly in recovering expensive and toxic molecules from the reaction mixture at the end of the procedure, which can rival the advantages of heterogeneous catalysts. These dendritic materials have therefore be targeted to combine the inherent advantages of both homogenous and heterogenous catalysts.⁶⁵

Various insoluble polymers have been used as stationary phases to immobilise homogeneous catalysts, such as resins⁶⁶ and membranes.⁶⁷ Notwithstanding, these systems were limited by difficulties in characterisation and the reactants reaching the catalytic centres. It was suggested that soluble support scaffolds could overcome such problems, extending from linear polymer⁶⁸ to dendritic polymers,^{31,69} and that they can be separated from the reaction mixture by either physicochemical methods and/or polymer sizing methods. Nevertheless, the location of the catalysts is a key reason why dendritic polymers may be more useful than linear polymers, because they can improve the selectivity, stability and activity of the catalysts. Despite the regular structure of the macromolecular dendrimers, the use of hyperbranched polymers (HBPs) as platforms for catalysts can be justified by their increased accessibility, lower cost, and the fact that they have similar properties to their dendrimer counterparts

including high thermal and chemical stability. These features make HBPs extremely significant in catalysis support for large-scale synthesis.⁷⁰

2.1.1. Single Cored Hyperbranched Polymers:

Hyperbranched polyarylesters synthesised from the AB₂ branching monomer, 3,5-diacetoxybenzoic acid, have been used in several applications by Twyman and coworkers. Most of their research used a metal-functionalised, B₄ unit, 4-tetracetoxypheyl porphyrin (TAPP), as a reagent in the core of the HBPs, either to probe the dense packing of the HBPs, or to synthesise a model haemoglobin system (**Scheme 2.1**).^{60,71} In addition, this metallic porphyrin cored HBP was applied as a catalyst support to evaluate catalytic efficiency. For these experiment, a porphyrin catalysed epoxidation reaction was chosen as it was also easy to follow the conversion process using gas chromatography. The experiment was carried out in DCM under a nitrogen atmosphere, in the presence of the substrate 1-octene (alkene), with iodosylbenzene as the oxygen donor, and an iron functionalised porphyrin cored HBP. The result revealed that the encapsulated porphyrin was more effective than the non-encapsulated porphyrin. HBPs of different molecular weights corresponding, to the pseudo 2nd, 3rd, and 4th generation dendrimers (5000, 10,000 and 16,000Da) were investigated.⁷² The rate of the reaction increased by ~20% moving from the lowest molecular weight to the highest (**Figure 2.1**). These capabilities of the oxidation catalyst were a result of the branched repeating units around the porphyrin core, controlling both the electronic and steric environments of the binding site. However, a major problem with this type of cored hyperbranched polyester was the lack of solubility in polar and non-polar solvents, rendering further studies impossible.

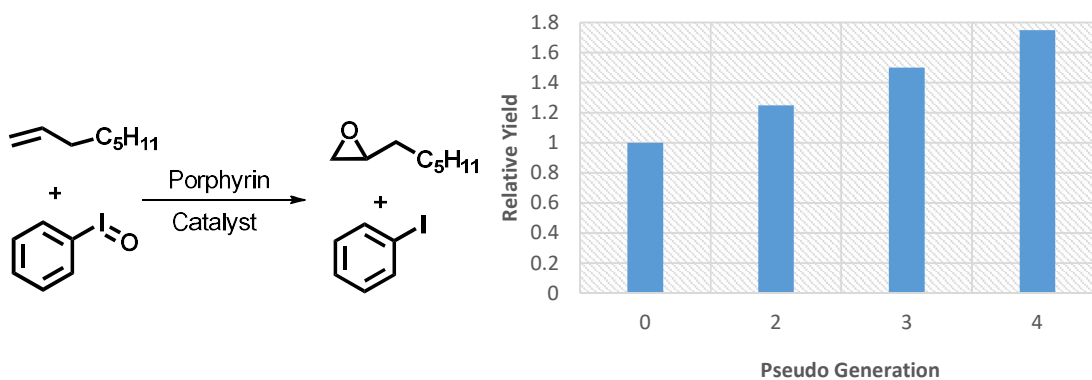
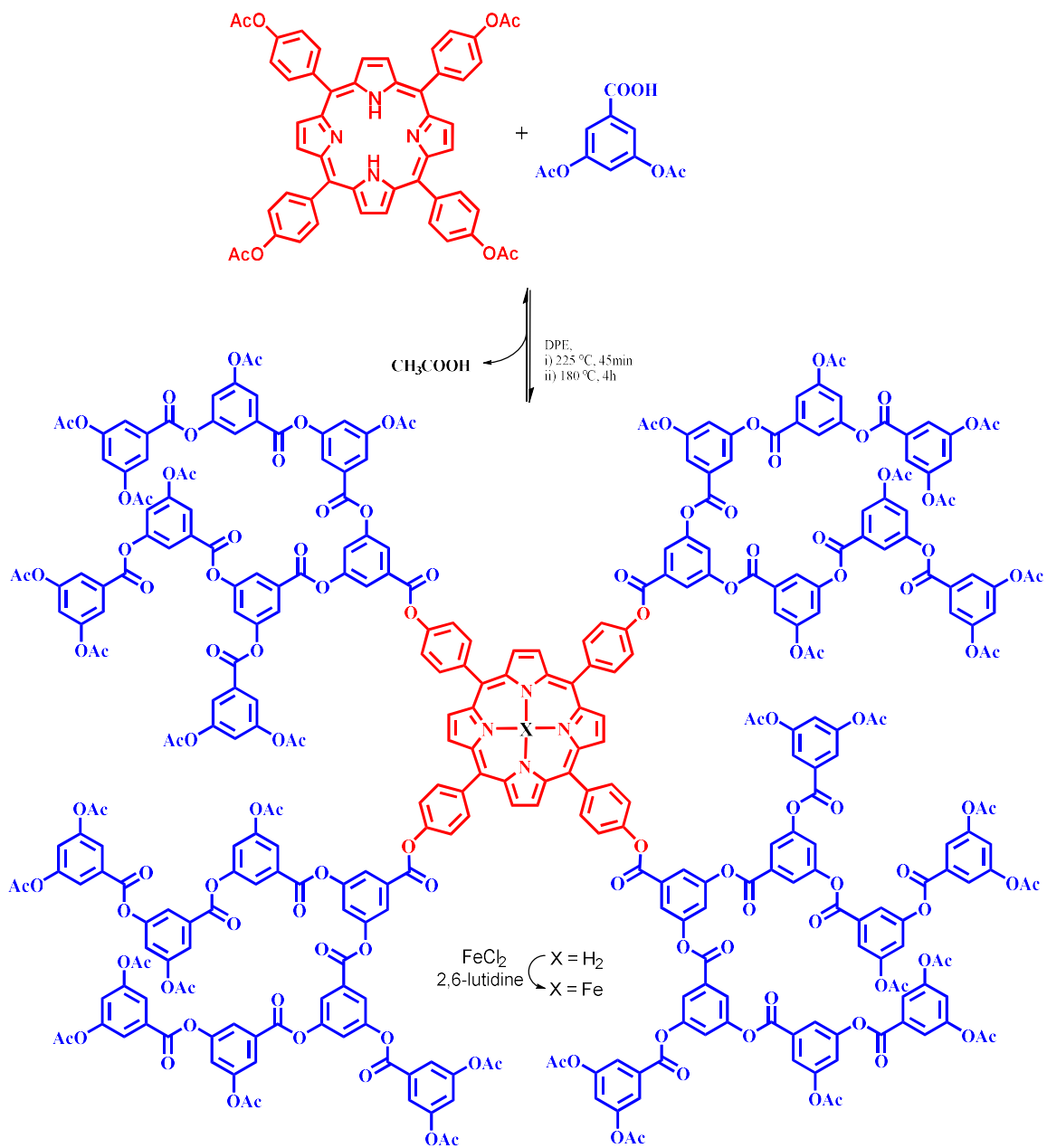


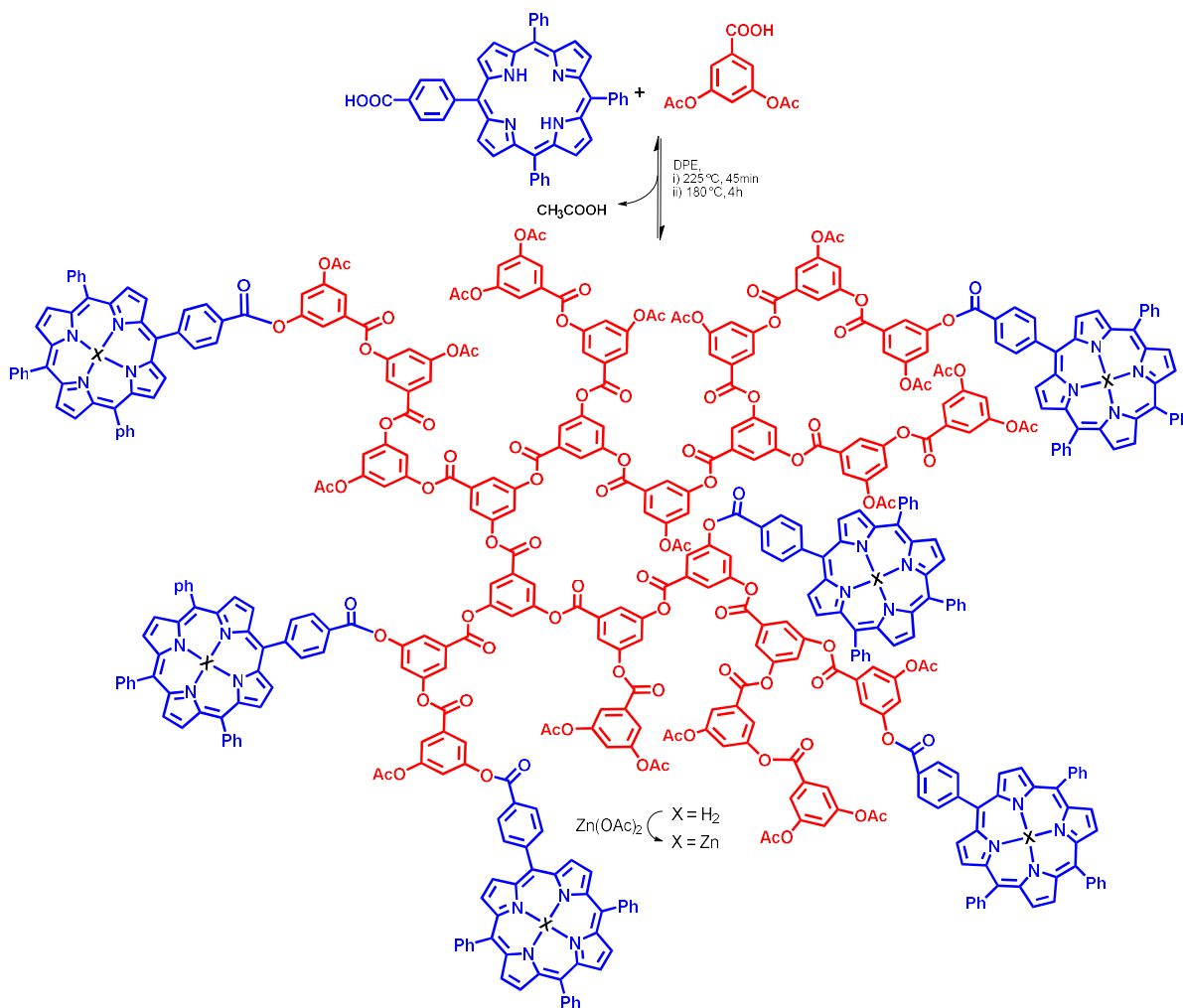
Figure 2-1. Epoxidation reaction of alkene and relative yield results of different molecular weight of cored hyperbranched polymer including free porphyrin.



Scheme 2-1. Synthesis of single cored hyperbranched polymer.

2.1.2. High Loading Peripheral Hyperbranched Copolymers:

In addition, the Twyman group developed a different approach by modifying the functional groups of the porphyrin comonomer from tetra-acetoxy functionalised to mono-acid functionalised.⁷³ Any exotic molecule that has only one carboxyl functional group would enable large numbers of this molecule to be attached along the periphery of the polymer. Monocarboxylic acid porphyrin, A unit, was copolymerised with AB₂ unit, 3,5-diacetoxybenzoic acid monomer to offer high loading metalloporphyrin HBP. The process is shown schematically in **Scheme 2.2**.



Scheme 2-2. Synthesis of high loading peripheral porphyrin hyperbranched copolymer.

This globular macromolecule host system acted as a bimolecular catalyst by binding two reactant groups simultaneously. This was possible because the dynamic flexibility of the HBP helped the reactants get sufficiently close to each other, therefore allowing the reaction to proceed faster. Several catalytic esterification experiments were performed in chloroform between an activated ester and an alcohol using 5% mol of the zinc-metallated porphyrin HBP copolymer or zinc-tetraphenylporphyrin. The results showed a yield of 70% from the reaction catalysed by the copolymer, whereas the yield was 25% and 13% for the control and uncatalysed reactions respectively (**Figure 2.2**). Again, further studies on this copolymer system in different media was restricted because this polyarylester is only soluble in a limited number of solvents.

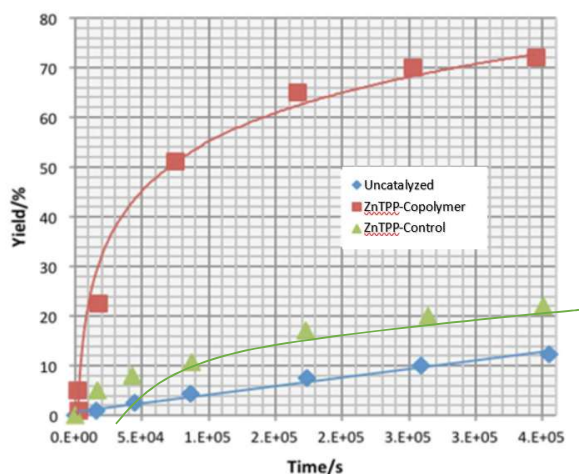
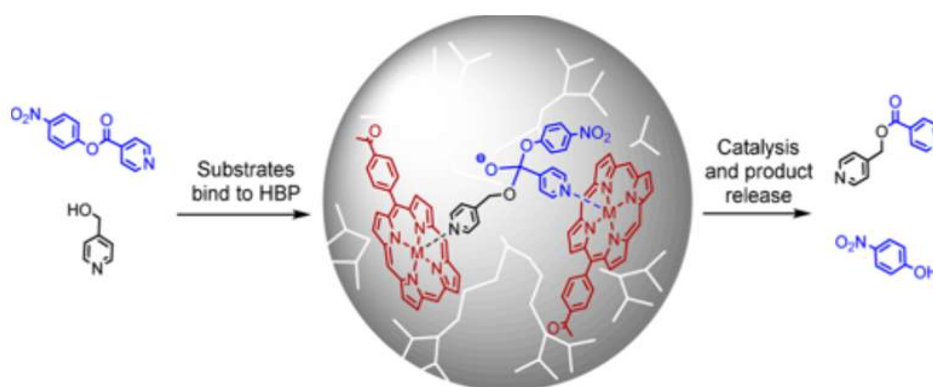


Figure 2-2. Schematic of bimolecular reaction within the hyperbranched copolymer and relative yield results of catalysed reactions.⁷³

2.1.3. Probing Effect of Comonomers on Hyperbranched Copolymer

Properties:

Most studies of highly incorporated comonomers of HBPs surface have involved only a small ratio of comonomer to monomer. However, an important consideration for future projects concerns increasing the molar ratio of the A functionality comonomer to the AB_2 monomer. Incorporating the comonomer within the HBP framework by altering the comonomer/monomer ratios usually affects other properties of HBP systems in addition to their application and structure.

The problem is, that incorporating comonomers would reduce the degree of branching, which in turn leads to an increase in viscosity in the HBP and loss of dendritic properties. For example, typical homopolymerisation of the AB_2 monomer generates HBPs with a 50% degree of branching (DB) and with a viscosity less than that of their linear analogues.⁷⁴ However, if the ratio of comonomer increases by 20%, the degree of branching will be less than 50% leading to an increase in linear points and an increased viscosity. Thus, any synthesised copolymer will possess a lower degree of branching and high viscosity, as most of the branched points were removed and replaced with linear and/or terminal units (**Figure 2.3**). More branching points imply a comonomer that is less incorporated and vice versa. Therefore, the degree of comonomer incorporation is directly related to the degree of branching.

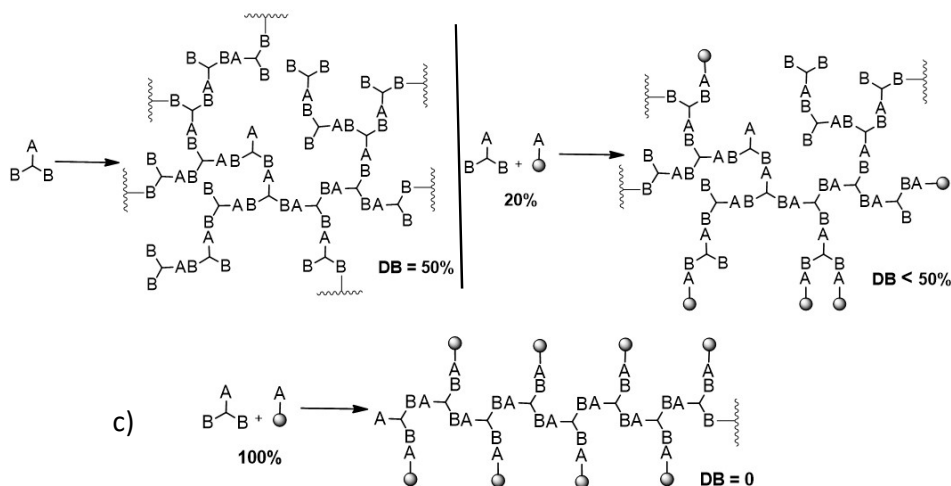
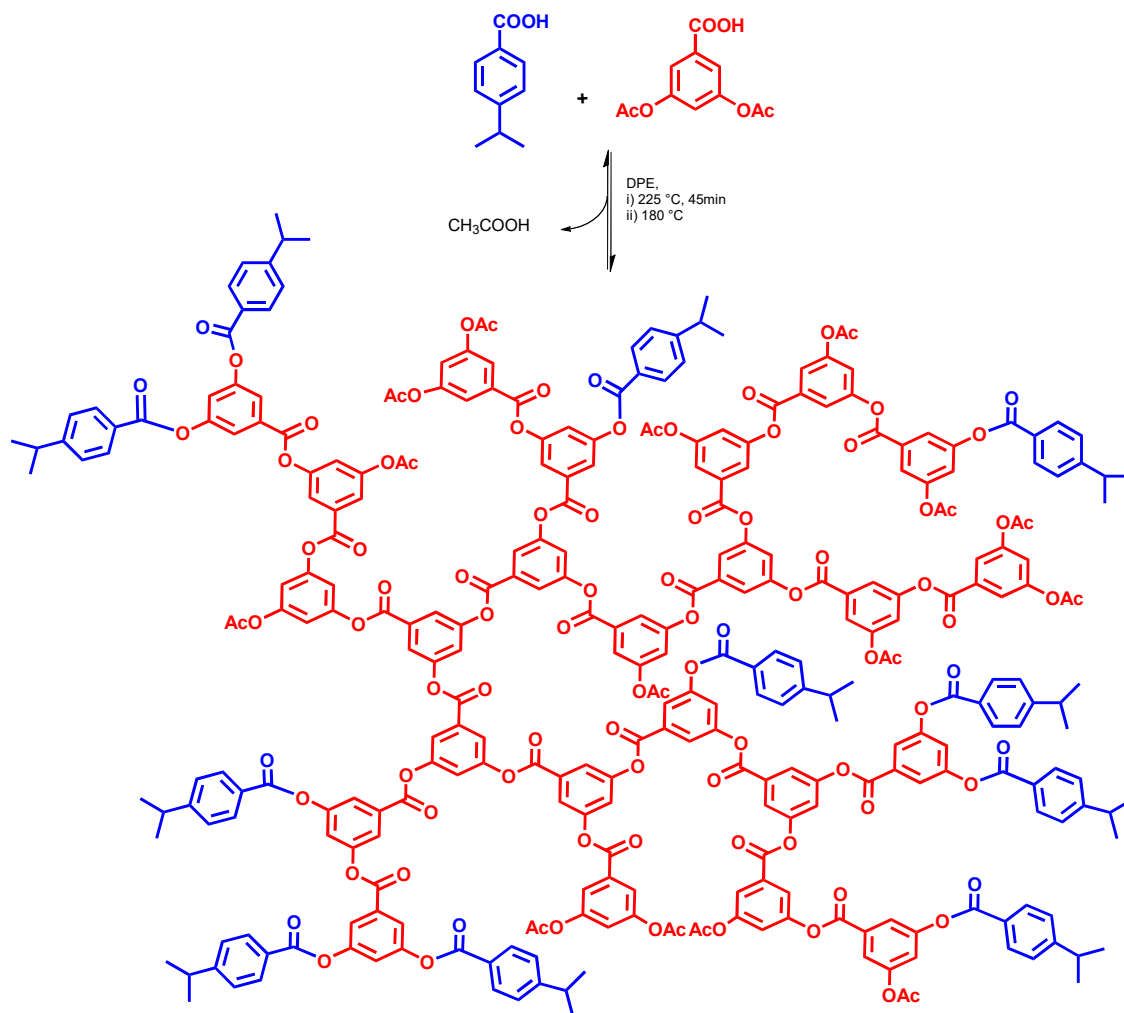


Figure 2-3. Potential structure of different equivalent of monomer/comonomer. Increasing molar ratio of the comonomer will reduce the branching points and increase the linear points, therefore the viscosity of the copolymer will increase. a) Polymerisation of AB_2 monomer usually formed a HBP with 50% degree of branching. b) Adding a comonomer of 20% will reduce the degree of branching with relative increase in viscosity. c) Increasing the ratio of comonomer up to 1:1 compare to monomer, leads to generate virtual linear polymer with no branching points.

To assess these effects in more detail, a subsequent investigation involved preparing a series of hyperbranched copolymers with different molar ratios. The aim was to assess the effect of level of comonomer incorporation on polymer behaviour in relation to the degree of branching and viscosity. The investigation also aimed to determine the maximum possible molar ratio (loading limit) of comonomer functionality while maintaining the characteristics of the HBPs. Twyman et al. aimed to do this by copolymerising 3,5-diacetoxybenzoic acid molar ratios of 0%, 5%, 10%, 20%, 33% and 40% of the comonomer, 4-isopropylbenzoic acid (**Scheme 2.3**).⁷⁵ The ¹H NMR spectrum proved the full comonomer incorporation for each copolymer and GPC analysis (after fractionation) gave HBPs with M_n values of 9,300 (± 400) Da and the same polydispersity of 3.8 (± 0.3). Although ¹H NMR could provide information about comonomer loading, it could not differentiate between the different environments of the protons of the comonomer and AB₂ monomer in the aromatic region. Specifically, ¹H NMR could not distinguish between the different terminal units with comonomers and the linear units (**Figure 2.4**). As such, the degree of branching could not be calculated. However, if we accept that the comonomer loading is directly related to the DB, then we can get useful information regarding changes in physical properties with respect to branching, by comparing the physical property with comonomer loading.

For the copolymer synthesized, the actual levels of incorporation were calculated as, of 5%, 15%, 25%, 45% and 60% which matched precisely the molar ratio used, confirming the excellent level of control available within this AB₂ system. The ¹H NMR spectrum clearly showed that, as the intensity of the propyl peaks increased in the copolymers, the acetate peak became less intense. Thus, the results showed that as the level of incorporation increased, the terminal acetate groups were replaced by propyl groups, which confirms the addition of comonomer results in an increase of the number of linear/terminal units and reduction of the number of dendritic units. Losing dendritic units and increasing the linear/terminal units leads to an open structure with reduced branching. To gain more accurate data on the effect of increasing the level of incorporation on the behaviour of hyperbranched copolymers, the viscosity of these copolymers was examined.



Scheme 2-3. Synthesis of peripheral many-comonomers hyperbranched copolymer.

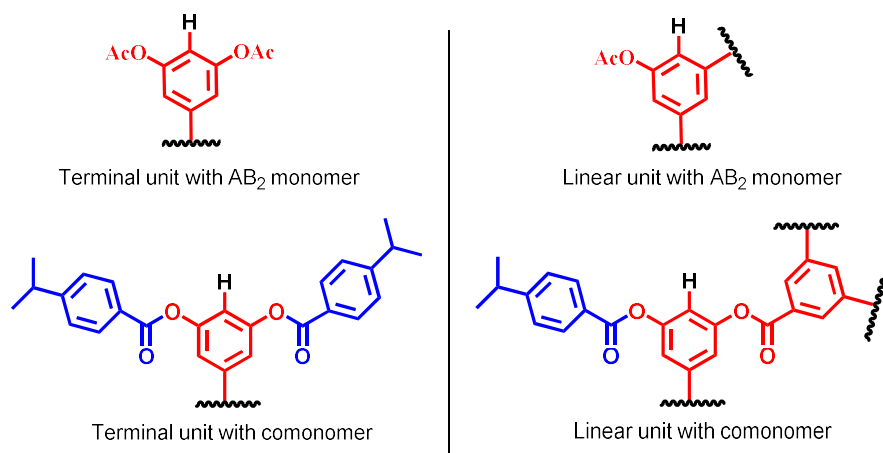


Figure 2-4. Two complicated environment units resulted from the comonomers (below), normal linear and terminal resulted from the AB_2 monomer polymerisation (top).

2.1.4. Effect of Branching on Viscosity:

Series of copolymers were synthesised with different levels of incorporation; but identical molecular weights and polydispersity. It was predicted that as the level of comonomer incorporation increases the viscosity will also increase.

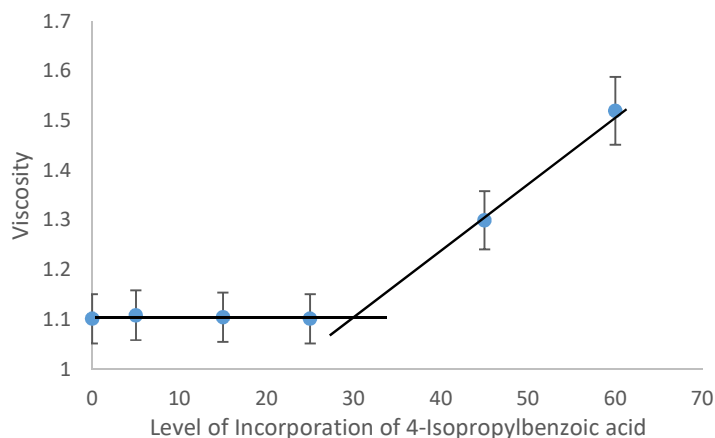


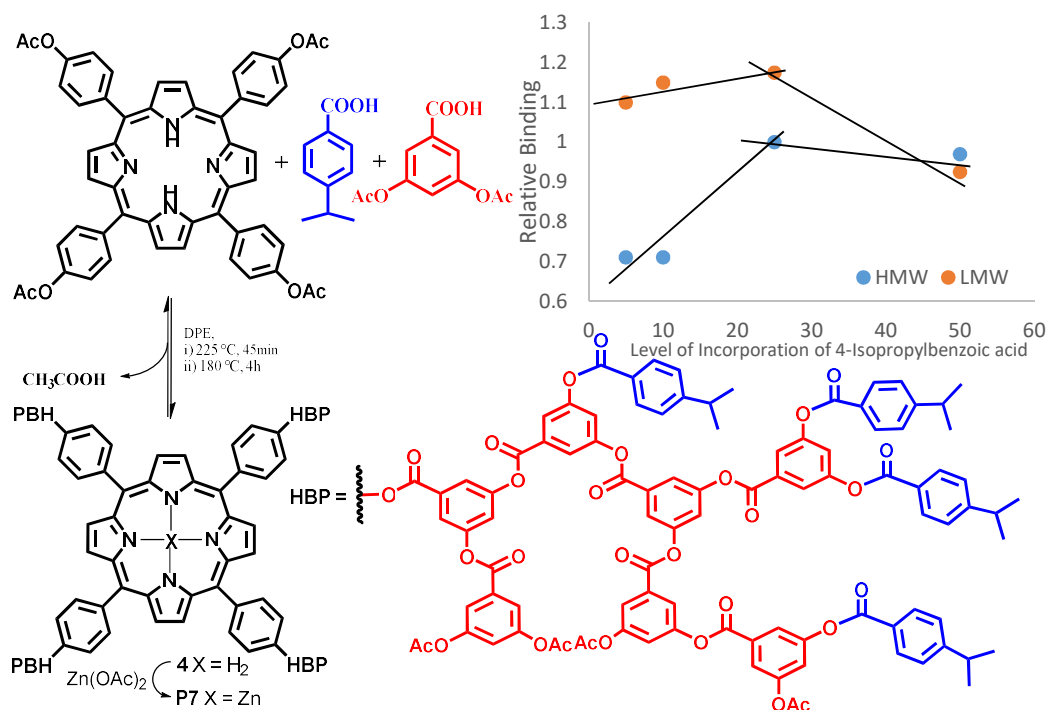
Figure 2-5. Represents the relationship of level of incorporation of hyperbranched copolymer with relative viscosity.

Viscosity experiments were conducted on each sample and the viscosity values were plotted against the level of comonomer incorporation, as shown in **Figure 2.5**. The graph shows that, as the incorporation of comonomers increased, a significant change in viscosity occurred between 25% and 45% incorporation, with a cut-off around 30%. Viscosity values of copolymers with less than 30% incorporation remained low. Viscosities beyond that point increased rapidly. This confirms that the hyperbranched copolymers develop a new open conformation, capable of interacting with other copolymer (and increasing viscosity). The addition of comonomer reduced the number of dendritic units and increased the number of linear units. Therefore, a non-globular architecture formed; interaction between the molecules increased; and the viscosity also increased. However, the presence of a large number of dendritic units below 30% incorporation enables the copolymers to maintain their globular structure, which minimises the interaction of these molecules in solution. Therefore, the viscosity values for copolymers below 30% incorporation were close to those for HBPs, which have a 50% degree of branching. These measurements and viscosity values might be considered to be principle data for copolymers with M_n around 10,000Da, which implies that different results could be obtained with other molecular weights because viscosity is dependent on molecular weight.

2.1.5. Effect of Branching of the Packed Limits within a Hyperbranched Copolymer via Ligand Binding:

Further studies were carried out to understand the possible cause of this behaviour at different M_n values by determining the dense packing within these copolymers. A binding experiment was used to investigate the internal microenvironment of a series of copolymer system by using three different sized pyridine ligands with a metal-functionalised molecule at the focal point of the hyperbranched copolymers. A previous study found that, as the molecular weight of the polymer increased, the steric hindrance around the core also increased. As such dense packing was found to occur around 7,000 Da.⁷¹ Thus, the experiments required metalloporphyrin-cored hyperbranched copolymers with two M_n values, one above and one below this dense packed limit ($M_n \approx 7000$ Da).

Copolymerisation reactions were conducted by using 3,5-diacetoxybenzoic acid with different molar ratios of 4-Isopropylbenzoic acid in the presence of constant molar ratio of tetra(4-acetoxyphenyl) porphyrin (TAPP) as core (**Scheme 2.4**). Reddish brown solid was collected after being isolated from methanol; ¹H NMR indicated sharp peaks corresponding to free porphyrin. Therefore, further purification was done using Biobeads column to remove all unreacted molecules. ¹H NMR analyses confirmed that all fractionated copolymers possessed cored metallated-porphyrin. GPC analysis revealed that the required molecular weights and PD were obtained. Specifically, two porphyrin cored copolymer groups were synthesised. Each group contained four copolymers with 5%, 10%, 25%, and 50% levels of incorporation. The 1st group had M_n value of 15,000±500 Da (PD = 3.2±0.1) and the 2nd group had M_n value of 5000±1000 (PD = 3.1±0.3).



Scheme 2-4. Synthesis of metalloporphyrin cored hyperbranched copolymer and binding results for pyridine ligand with two different molecular weights.

Scheme 2.4 shows the relationship between the level of incorporation of 4-isopropylbenzoic acid and the association constant in the pyridine ligand: there is a cut-off around 25% incorporation for both the low and high molecular weight copolymers. This indicates that the hyperbranched copolymer system maintains their dendritic properties (controlled globular environment) and structure below 25% incorporation for both molecular weights. It was noticed that as the level of incorporation increases, the steric hindrance around the binding sites increased, resulting in poor binding. This study confirmed the viscosity result, that increasing comonomer incorporation (above 25%) results in a macromolecular structure that is extremely open with loss of dendritic properties. Therefore, if we want to use copolymers that possess dendritic properties, the level of comonomer incorporation should not exceed 25%. Future projects should ensure that a maximum molar ratio of 25% or less is used relative to the AB₂ monomer. This will ensure the structure of the hyperbranched copolymers has sufficient branching and can provide an appropriate steric and electronic interior environment.

2.2. Aims:

For a number of potential applications the problem of poor solubility needs to be overcome. To solve this problem, it was proposed to add a solubilising group as the comonomer. The purpose of this study is therefore to develop a new HBP system with a high loading of comonomer functionality to increase solubility. To demonstrate the usefulness of this we also proposed to carry out further work on catalyst applications and study the behaviour and efficiency with different solvents. This can be done by combining core functionalization and comonomer incorporation within one HBP system. As such, the new HBP will contain a catalyst at the core and solubilizing comonomers at or near the surface (**Figure 2.6**).

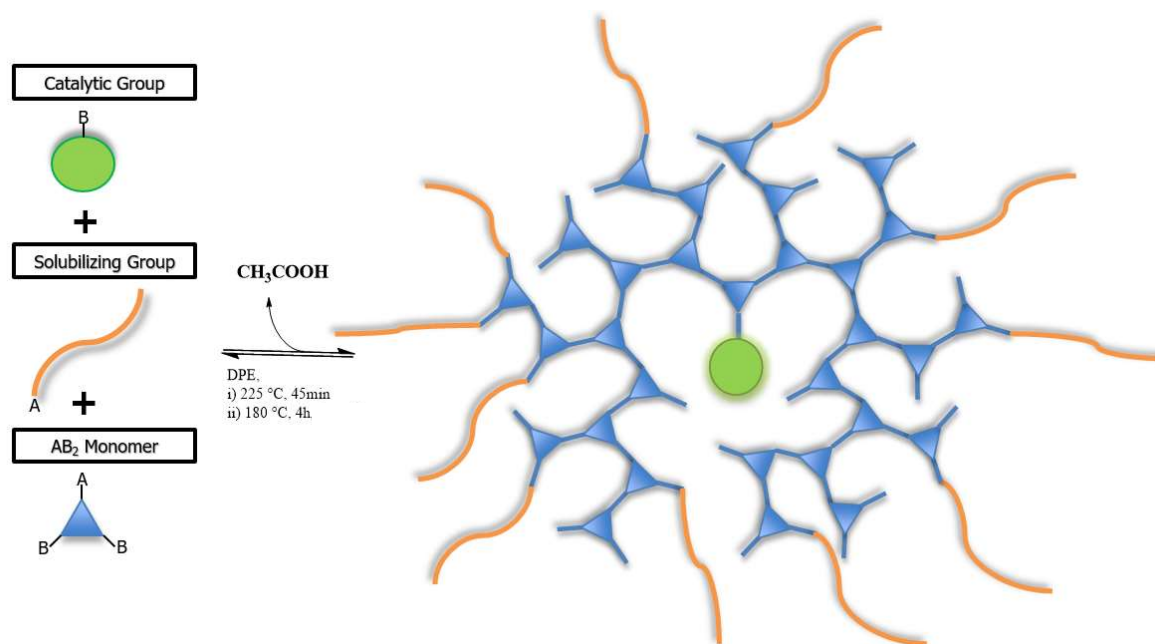
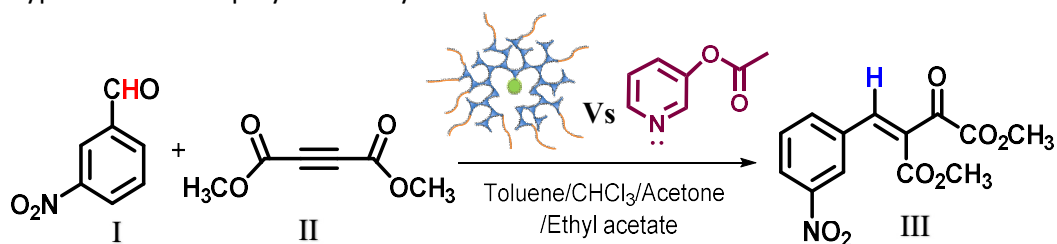


Figure 2-6. Proposed hyperbranched copolymer with high loading comonomers and single cored molecule.

Stearic acid is an alkane with a terminal carboxylic acid. This was selected as comonomer, as this would increase the solubility of HBPs in less polar solvents, such as toluene, diethyl ether and n-hexane. Pyridine was chosen as the core unit because it is a nucleophilic catalyst for a number of reactions. To encapsulate pyridine within our polymer we require an acetoxy functionality.

The catalysed reaction selected is shown in **Scheme 2.5**, and involves an alkyne molecule I and an aldehyde II, which can be reacted together using pyridine as the catalyst. The investigation was conducted using ^1H NMR to study the conversion of alkyne I to alkene III by measuring the appearance of the new of alkene's peak at 7.14 ppm and the disappearance of the aldehyde's peak at 10.30 ppm.⁷⁶ The performance of the hyperbranched copolymer will be examined using different solvents, such as toluene, chloroform, and ethyl acetate. The control reactions using just pyridine (free acetoxy pyridine) will be analysed individually in each solvent and the extent of conversion (yield) of each catalyst will be compared to that obtained using the hyperbranched copolymer catalysts.



Scheme 2-5. Reaction of alkyne with aldehyde used as model to test the efficiency of catalytic systems. Reaction tracked by Monitoring the Intensities of Protons *H* and *H* using NMR technique.

Previous studies using a different HBP (catalysing a different reaction), demonstrated that the HBP systems were significantly better as catalysts than those of the control reactions (no HBP). The work postulated the reaction took place inside the HBPs which possess a favourable electronic environment for encapsulating small molecules, as well as providing a good electronic environment, that can stabilise any intermediate. If this is controlling factor, then these HBP catalysed reactions should be significantly less sensitive to solvent when compared to the control reactions. More investigation may be needed to determine whether changing the solvent can affect the performance of the HBPs. Therefore, one of the aims in this research is to examine the efficiency of the HBPs as catalysts in different solvents.

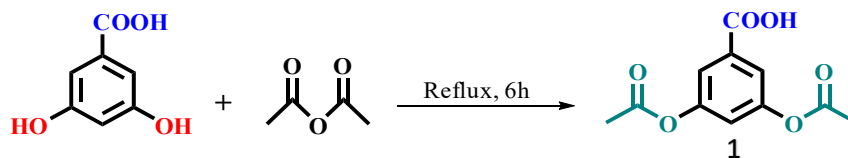
2.3. Synthesis:

2.3.1. Summary:

Polycondensation was selected to polymerise the 3,5-diacetoxybenzoic acid monomer as the model system. Removing the generated by-product, acetic acid, alters the equilibrium to produce hyperbranched polyarylester with a 50% degree of branching along with higher molecular weight of polymers. The polymerisation procedure was adapted from previous research conducted by Turner and his colleagues.⁷⁷ After selecting a comonomer and the core molecules, it was assumed that a functionalised carboxylic acid and ester would be the preferred substances used in the reaction as the required reversibility would be maintained due to the mechanism of this reaction which involves a reversible transesterification. This research's objective is to explore the catalysis in a variety of solvents; the solubilisation group stearic acid and the catalyst 3-acetoxypyridine were selected as they can be easily implemented in the hyperbranched copolymer. The alkane chain from the stearic acid evidently ranges from 0.89-2.60 ppm in the ¹H NMR spectrum of the copolymer, whereas the α and β aromatic protons of the pyridine molecule resonate at 8.58 ppm. Overall, the synthetic technique is uncomplicated, especially as unwanted by-products (such as acetic acid) can be removed via simple filtration making the product is easy to purify.

2.3.2. Polymerisation of 3,5-Diacetoxybenzoic acid, **2HBP**:

The AB₂ monomer, 3,5-diacetoxybenzoic acid, was polymerised without a core or comonomer in order to understand the process involved in step-growth polycondensation as well as to obtain information relating to the synthetic method and characterisation of the hyperbranched polyarylester product (HBP). Therefore, 3,5-diacetoxybenzoic acid **1**, was first created from 3,5-dihydroxybenzoic acid in a single step reaction with acetic anhydride (**Scheme 2.6**). Following six hours of refluxing, the excess of acetic anhydride and acetic acid by-product were removed via vacuum. Moreover, in order to avoid the risk of premature oligomerization of the AB₂ monomer, extra care was taken to ensure that the temperature did not rise above 80 °C. The crude product obtained was dissolved in hot chloroform prior to being precipitated into petroleum ether and left at 5 °C overnight. The following day, the pure compound was collected by filtration, which yielded a white powder in 34%. The ¹H NMR revealed a broad singlet at 10.83 ppm from the carboxylate hydrogen, a doublet at 7.72 ppm from *o*-ArH, a triplet at 7.20 ppm from the *p*-ArH, and a singlet at 2.33 ppm from the acetate hydrogens. Mass spectrometry produced a molecular ion of 237 which was consistent with the structure. The IR spectrum also supported the successful synthesis, showing a new intense peak at 1690 cm⁻¹ from the C=O functional group of ArOCOCH₃ group, and an absence of a broad peak at 3195 cm⁻¹ from the OH functional group.



Scheme 2-6. Synthesis of 3,5-diacetoxybenzoic acid.

Following this, the polymerisation was carried out by placing 3,5-diacetoxybenzoic acid **1** monomer and diphenyl ether (as solvent) in a round bottom flask connected with a distillation kit. The mixture was repeatedly evacuated and flashed with nitrogen while the temperature reached 225 °C for 45 minutes under atmospheric pressure; during this stage, the polymerisation process was able to form oligomeric species. The temperature of the system was lowered to 180 °C while the reaction was subjected to a (low) vacuum for 4 hours. The aim of reducing the pressure was to drive the reaction towards the product by removing the acetic acid by-product (**Scheme 2.7**). In regard to

The polymerisation process has produced a number of different proton environments in comparison to the monomer. In the monomer, we observe an intense singlet at 2.30 ppm corresponding to the acetoxy group, which integrates as six protons. During the polymerisation process, each propagation step consumes one acetoxy group and adds a new monomer containing two acetoxy groups to the growing polymer. As the polymer increases in size, the integration value for this peak is reduced until it reaches a relative value of three when compared to the aromatic protons. In the aromatic region we witness a number of peaks between 7.23 ppm to 8.10 ppm. The HBP possesses three types of monomer environments which are referred to as dendritic unit, linear unit, and terminal unit; they are highlighted in **Figure 2.7**.

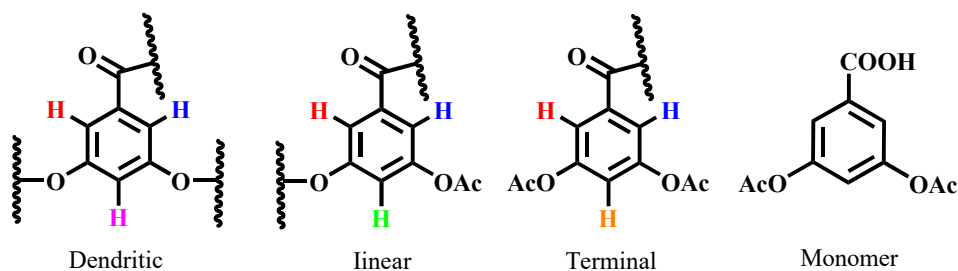


Figure 2-7. Structural units present in hyperbranched polymer of meta-protons and para-protons.

The protons *Ortho* to the carboxylate group were equivalent in the monomer. As a result of the polymerisation, these protons (next to carbonyl) are no longer equivalent. The resonances from these protons exist as very broad peaks between 7.70-8.10 ppm (**Figure 2.8**).

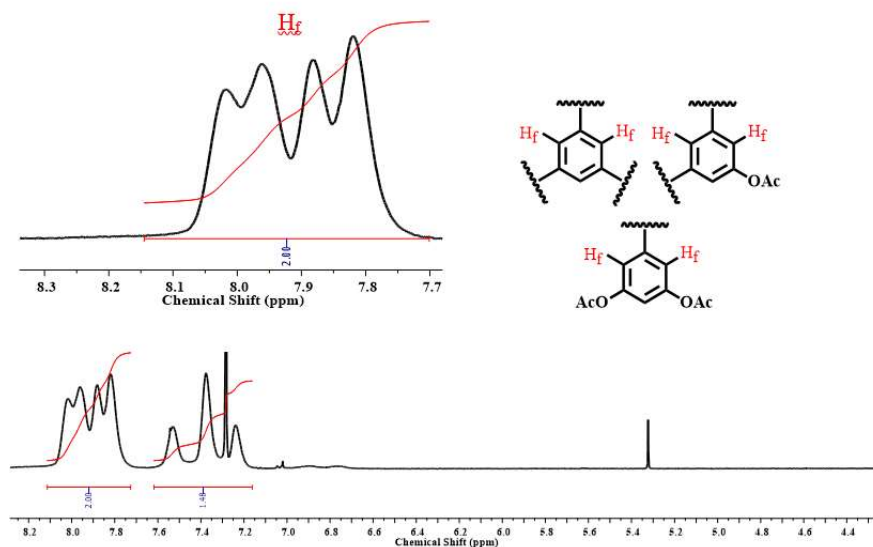


Figure 2-8. The ^1H NMR spectrum of meta-proton of poly(3,5-diacetoxybenzoic acid).

Moreover, in the monomer there is a triplet signal at 7.20 ppm which is attributed to the proton *para* to the carboxyl function. However, during polymerisation this proton can be seen as three well defined peaks. These peaks appeared at 7.23 ppm, 7.38 ppm, and 7.55 ppm, and are recognised as being the dendritic, linear, and terminal protons (para to the carbonyl), as is illustrated in **Figure 2.9**. Furthermore using ^1H NMR, the relative integration ratios of these units dendritic (D), linear (L), and terminal (T) can be used to calculate the degree of branching by utilising **Equation 1**.

$$DB = \frac{D + T}{D + L + T} = \frac{0.24 + 0.26}{0.24 + 0.50 + 0.26} = 50\%$$

Applying the integration values of 0.24, 0.50, and 0.26 obtained from the polymer (see **Figure 2.9**) provided a DB around 50%, which is consistent with this type of AB_2 polymerisation.⁷⁸

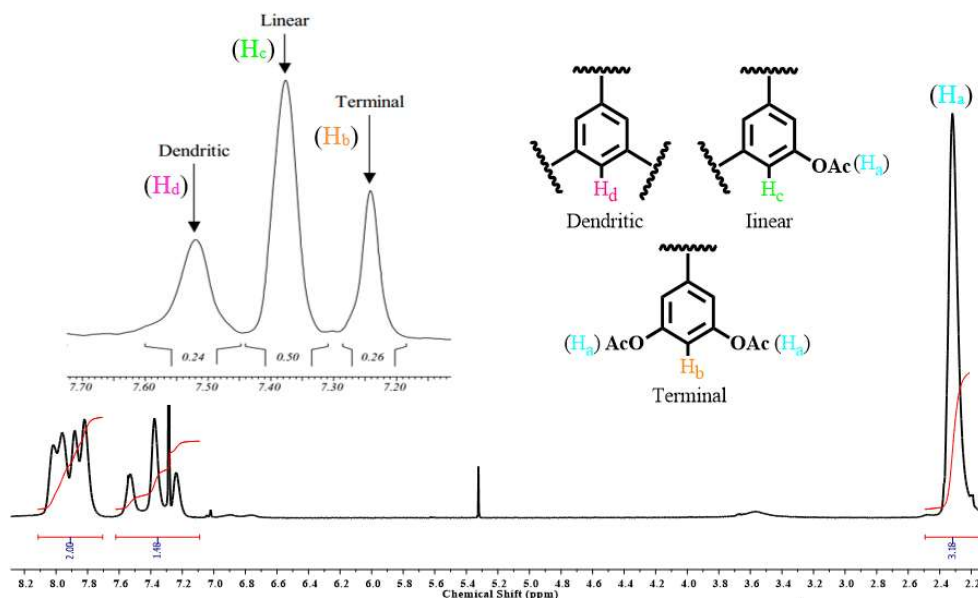


Figure 2.9. The ^1H NMR spectrum of *para*-proton of poly(3,5-diacetoxybenzoic acid) and assigning the values of dendritic (D) unit, linear (L) unit, and terminal (T) unit.

Generally, the structural conformation of AB_2 hyperbranched polymers is such that dendritic growth of the polymer controls the number of terminal units. On the contrary, reacting a terminal unit with a new AB_2 monomer results in linear growth that leads to no net increase of terminal units. Dendritic growth generates a dendritic unit from a linear unit and in doing so adds a new terminal unit. Therefore, the number of

dendritic units is always smaller in comparison to the number of terminal units; in addition, at higher degrees of polymerisation, and with a DB equal to 50%, the number of dendritic (D) units and terminal (T) units is almost equivalent. This allows the identification of ^1H NMR resonances of linear (L) units to be relatively straightforward. Consequently, the peaks at 7.23 ppm and 7.55 ppm are approximately equal and correspond to terminal units and dendritic units respectively. Therefore, the larger peak at 7.38 ppm can be attributed to the linear (L) units. Nevertheless, the hyperbranched polyarylester **2HBP** was synthesised successfully with a 50% degree of branching. The same procedure will be applied in the following step in order to synthesise a copolymerisation.

This therefore led to an investigation that involved preparing a copolymer with a solubilising group via a one pot synthesis procedure. Solubility will be explored using a series of copolymers in order to evaluate their efficiency in respect to solubilising; however, level of comonomer incorporation would always be kept below 25%. Therefore, the copolymer would be synthesised by applying different molar ratios of monomer to comonomer. This would present us with the opportunity to investigate the effect of comonomer loading on solubility. To achieve these objectives, specific functional groups are required to enable the comonomer to be incorporated; in particular, the use of a carboxylate group on the alkyl chain. A decision was made to use stearic acid **3** (SA) as the comonomer since it was commercially available and inexpensive. By employing the same producer discussed in the previous section, the copolymerisation experiment was conducted using three different molar ratios of 3,5-diacetoxybenzoic acid **1** /stearic acid **3** (**4HBP-SA**) with 2.5:1 (40%), 5:1 (20%), and 10:1 (10%). These copolymers are referred to as 4HBP-SA40, 4HBP-SA20, and 4HBP-SA10 (**Scheme 2.8**). Each mixture was individually run by heating them with an equal mass of diphenyl ether. After four hours under vacuum, the polymers were precipitated from hot THF into cold methanol and washed repeatedly with methanol to remove any impurities. The presence of the stearic acid molecules was evident from the ^1H NMR spectrum, which revealed a number of broad peaks in the alkyl region (**Figure 2.10**).

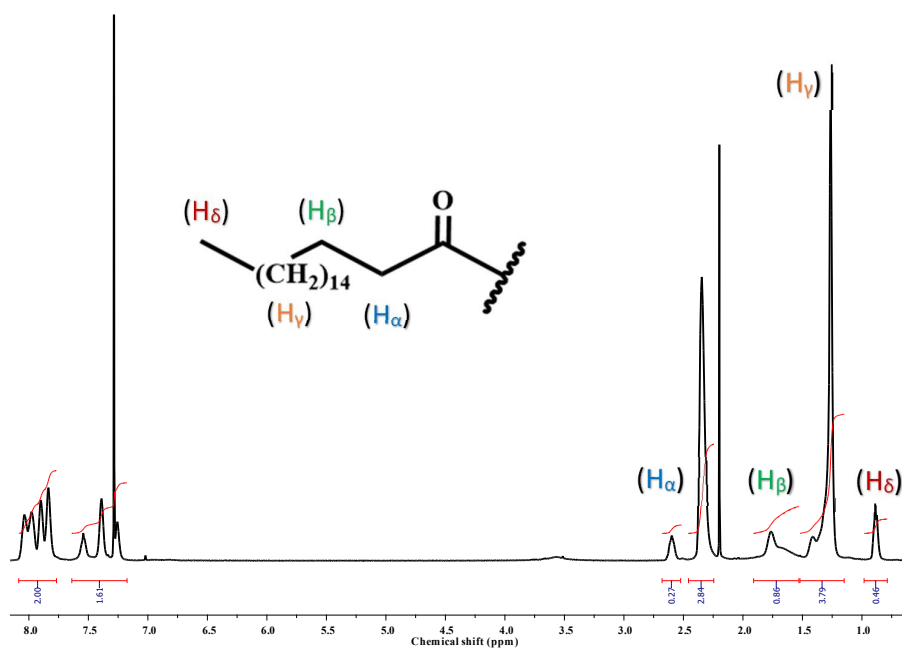


Figure 2-10. The ^1H NMR spectrum of hyperbranched copolymer (4HBP-SA20).

The alkane's protons provided four broad peaks. The peaks at 2.60 ppm and 1.77 ppm were assigned as the protons α and β for each carbonyl group respectively. The peak at 1.27 ppm corresponds to the central 28 protons, with the terminal methyl group seen at 0.89 ppm. The molecular weight of each copolymer was estimated by GPC and ranged from 3,000 to 27,000 Da, with a PD from 1.9 to 5. The level of incorporation of stearic acid was identified from the ^1H NMR spectrum which provided the following values: 41% for 4HBP-SA40, 22% for 4HBP-SA20, and 15% for 4HBP-SA10. These results suggest that the molecular weights and PDIs are difficult to control; however, the level of the comonomer incorporation could be controlled.

Once synthesis of the hyperbranched copolymer was confirmed, with different levels of comonomer incorporation, an estimate of the solubility was tested by dissolving 1 mg in 1 mL of various solvents, and placed in the shaker machine for 1 hour, so as to ensure that all of the samples were given sufficient time to dissolve. The data is shown in **Table 2.1**.

Polymers Solvents	HBP	4HBP:SA10	4HBP:SA20	4HBP:SA40
	100% of AB ₂ 0%Stearic acid	2.5:1 10%Stearic acid	5:1 20%Stearic acid	10:1 40%Stearic acid
Level of Incorporation	0%	15%	22%	41%
DMSO	100%	0%	0%	0%
Acetone	100%	100%	100%	100%
Ethyl acetate	100%	100%	100%	100%
Chloroform	100%	100%	100%	100%
Diethyl ether	0%	30%	50%	100%
Toluene	0%	70%	100%	100%
n-Hexane	0%	0%	30%	50%
M _n	9150	7550	27600	3100
PD	11	2.5	5.1	1.9

Table 2-1. Solubility estimation of hyperbranched copolymer in range of solvents.

The unmodified polymer (0% stearic acid) was completely insoluble in toluene, diethyl ether, and hexane, while the solubility measurements confirmed that stearic acid incorporation improved the solubility. The level of solubility depends on the level of comonomer incorporation; for example, it was observed that the solubility trend increased alongside diethyl ether, recorded as being 30% and 50%, until it reached 100% as the level of stearic acid within the copolymer increased as 15%, 22%, and 41% respectively. Similar observation was made in regard to hexane although it only reached a maximum of 50% for 41% level of incorporation, while toluene resulted in 100% solubility for both 22% and 41% levels of comonomer incorporations.

Generally, the 4HBP-SA10 containing a 15% level of incorporation show poor solubility in diethyl ether and hexane, while it was recorded as being 70% in toluene. In addition, the 4HBP:SA20 with a 22% level of incorporation offered more effective solubility in toluene (that was 100%) along with the unexpected results of diethyl ether (50%). However, the solubility of the copolymer reached 100% in diethyl ether when the level of incorporation consisted of 41% of 4HBP-SA40. Nevertheless, this is above our self-proposed limit of 25% incorporation and hexane and diethyl ether were excluded from further experiment.

Furthermore, in mild polar solvents such as acetone, chloroform, and ethyl acetate, the copolymers were 100% soluble; however, the fact that there was such a significant difference in polarity indicated that modified copolymers were not soluble in DMSO. Overall, this methodology consisting of high loading comonomer has provided the polyarylester with good solubility characteristics, which has overcome the issue concerning limited solubility in a range of solvents. To summarise, 5:1 (20%) molar ratio of monomer/comonomer was selected to conduct further experiments within this project due to the fact that it provides reasonable solubility while maintaining the dendritic property of the hyperbranched copolymer. Moreover, since it was not possible to control the molecular weight of the product, it was necessary to study the effect of adding a core molecule to determine whether or not this would help to control/influence the molecular weight.

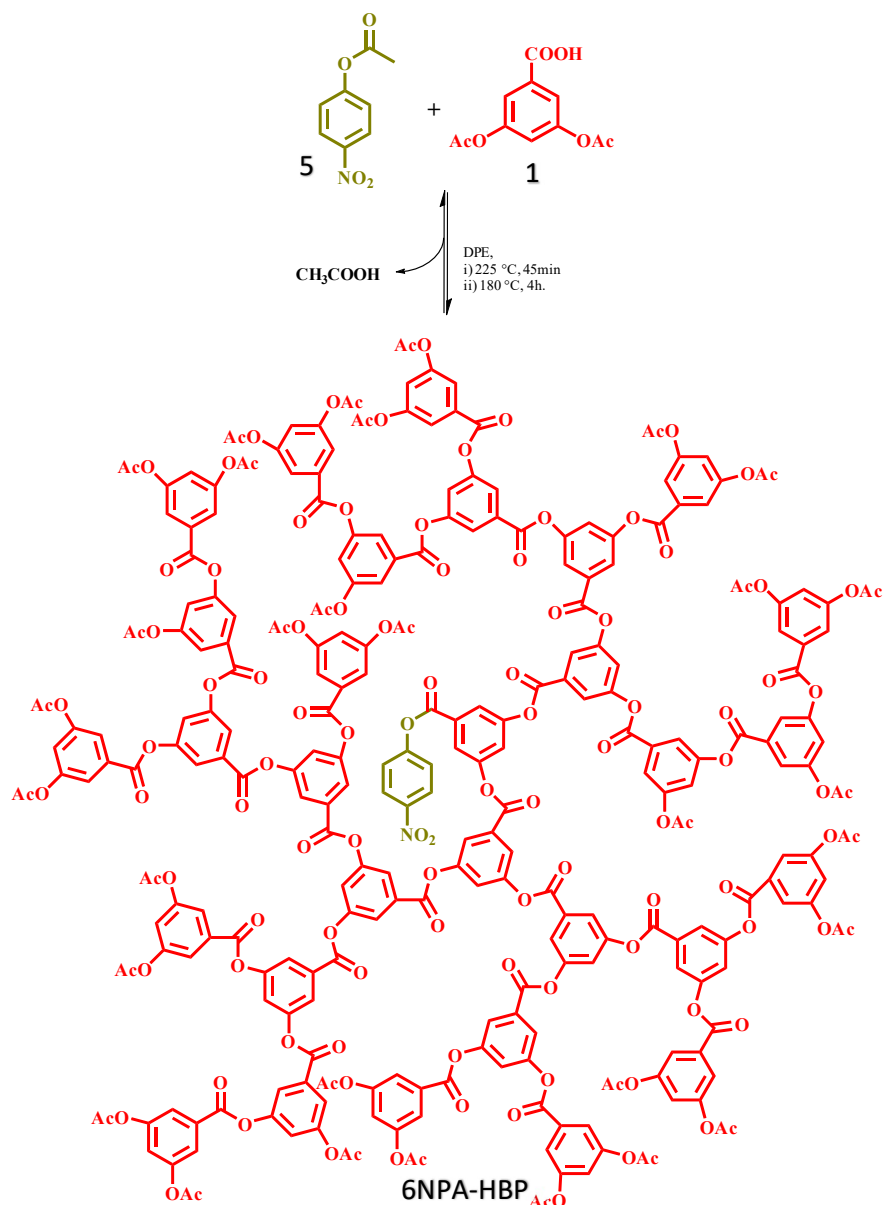
2.3.4. Controlling the Molecular Weight of the Hyperbranched Copolymer by Adding 4-Nitrophenyl Acetate as Core, **7NPA-HBP-SA**:

The previous section revealed how copolymerisation of the monomer and the comonomer with different molar ratios generated a control of the level of incorporation, but led to an irregular trend of molecular weights. Taking this into consideration, it was decided to add a core molecule into the copolymerisation system. This decision was made according to previous research that successfully reacted core molecules with various ratios of monomer in order to control the molecular weight.⁷⁹ Therefore, adding a core molecule to the copolymerisation process may help to control or limit the molecular weight of the copolymers. The initial step was to polymerise the core unit 4-nitrophenyl acetate **5** (NPA) molecule as a core with 3,5-diacetoxybenzoic acid **1** at different molar ratios (**6NPA-HBP**). Specifically, three different ratios of core **5** /monomer **1** were studied 1:40 (2.5%), 1:20 (5%), and 1:10 (10%). The polymerisation reactions were carried out by heating them to 225 °C so as to begin the oligomerisation, before reducing the temperature to 180 °C and applying the vacuum for a period of 4 hours (**Scheme 2.9**). The product was then dissolved in the minimum amount of hot THF and precipitated in cold methanol. The ¹H NMR spectrum confirmed the incorporation of the core molecule within the homopolymers, by showing a peak at 8.35 ppm, assigned as the protons *meta* to the ester group of 4-nitrophenyl acetate. The GPC analysis revealed that the M_n value of the first polymer 6NPA-HBP2.5% was 22,000 Da, while it was 14,600 Da and 7,600 Da for the second 6NPA-HBP5% and third 6NPA-HBP10% polymers respectively (**Table 2.2**).

The Polymer	M _n	PD
6NPA-HBP2.5	22,000	3.0
6NPA-HBP5	14,600	2.1
6NPA-HBP10	7,600	3.5

Table 2-2. Results of controlled molecular weights of homo-polymerisation of AB₂ monomer with core molecule.

Utilising a core molecule has provided the homo-polymerisation with a number of advantageous such as decreasing the PD of polymer from 11 to around 3. The results also revealed an impact on molecular weights, by producing a well-ordered sequence. This indicates that an increase in the core lowered the molecular weight of polymer. Adding less core leads to increase molecular weight of polymer. Therefore, polymer 6NPA-HBP2.5% has the largest molecular weight, which is almost twice the weight of the second polymer 6NPA-HBP5%, whereas the third polymer 6NPA-HBP10% is only half the weight of the second polymer. Theoretically core can control the molecular weight if the reaction is reversible. Starting ratio should be reflected with final product due to only one core can involve in and every molecule have core. Thus, our reversible transesterification reaction (dominated by thermodynamic) resulted in a statistical distribution of core units, providing the reaction conditions are such that equilibrium lies in favour of the products. Such of this control reaction was intensively investigated within our group.^{79,80}



Scheme 2-9. Polymerisation of 4-nitrophenyl acetate molecule as core with 3,5-diacetoxybenzoic acid monomer (6NPA-HBP).

In regard to the homopolymer results, this reaction was therefore repeated in order to examine its reproducibility with respect to control and/or its ability to influence the molecular weight of the cored hyperbranched copolymer system (7NPA-HBP-SA). Specifically, cored copolymerisations were individually carried out by adopting the same procedure, as previously discussed (Scheme 2.10), using three different ratios of the core 5 / (monomer 1:comonomer 3); 1/(40:8), 1/(20:4), and 1/(10:2). The ratio between the core and the total monomer:comonomer was adjusted to 2% for 1/(40:8), 4% for 1/(20:4), and 8% for 1/(10:2), which was expected to have same control over

molecular weights, as observed for the homopolymer (6NPA-HBP). In addition, the level of comonomer incorporation was maintained at an overall loading of 20%. This would help us gain a better understanding of the general consequences of producing relative/certain molecular weights of cored pyridine copolymer in a catalysis reaction. The presence of the core molecule was verified by the ^1H NMR spectrum, which revealed a distinct peak at 8.34 ppm (**Figure 2.11**). In addition, this resonance occurred at a higher shift than it did in the ^1H NMR of the starting material. The difference in chemical shift indicated that the 4-nitrophenyl acetate molecule had been physically incorporated into the polymer, rather than simple 'mixed' with polymer.

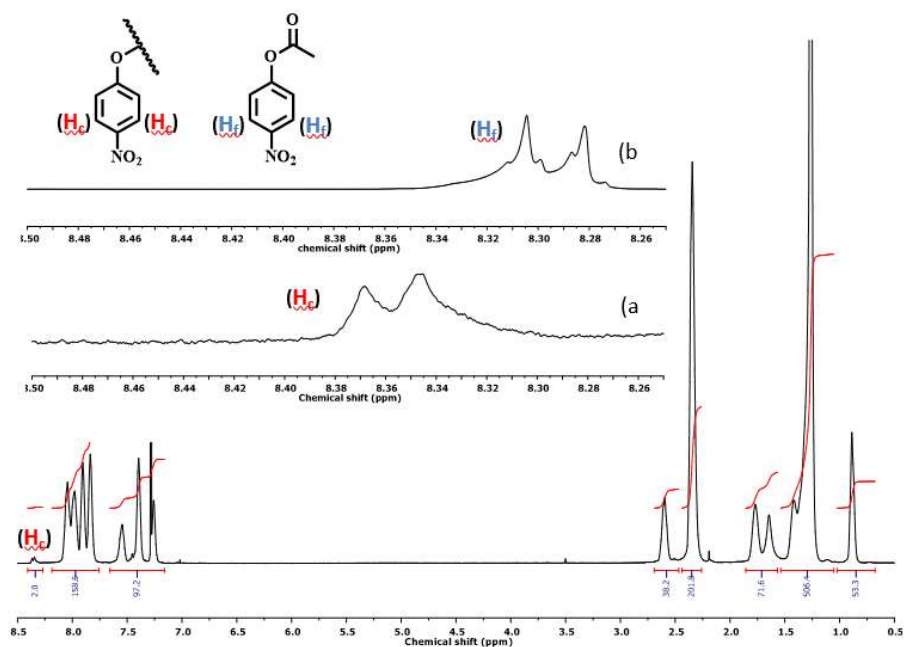
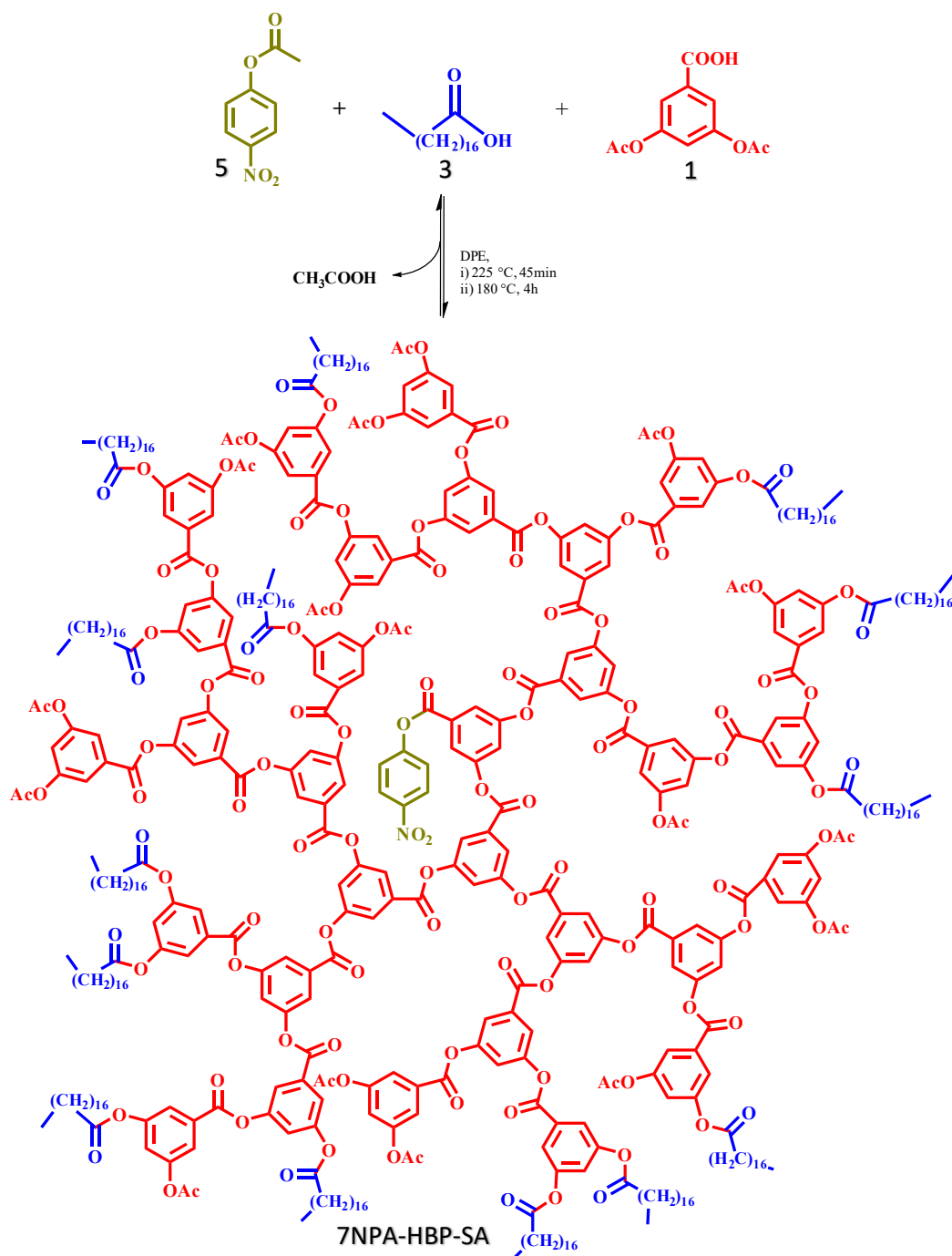


Figure 2-11. The ^1H NMR spectrums of core 7NPA-HBP-SA; a) NPA within the copolymer showing a chemical shift at 8.34 ppm. b) NPA, free molecule indicating lower chemical shift compare to cored one that is at 8.28 ppm.



Scheme 2-10. Synthesis of 4-nitrophenyl acetate cored hyperbranched copolymer of 3,5-diacetoxybenzoic acid with stearic acid (7NPA-HBP-SA).

On this occasion, it was noticed that the molecular weights were not dependant on the core ratio. This suggests that the cored hyperbranched copolymers do not have the same level of influence or control over the molecular weight as the cored homopolymer. This was not expected and the experiment was repeated a number of times; the data is presented in **Table 2.3**. The results confirm that the molecular weight of the polymerisation cannot be controlled. However, the level of the comonomer incorporation does appear to be controlled (around 20%). The reason why the molecular weight was not controlled is still ambiguous, but the polymerisation is sensitive to many factors, including temperature, time, and quality of the vacuum. As these can all vary when the reactions are carried out separately, it was decided to perform all of the reactions at same time, as well as at the same temperature and using the same vacuum line. A multi-position heating block was used and fitted with three round-bottom flasks, each charged with a different ratio. The entire system was then connected to the same vacuum pump via a vacuum line. Surprisingly, the results once again showed that the molecular weights were random. At this stage, we are unaware of the reason for why there is a loss of control. It was therefore decided that we would conduct a number of experiments on pyridine cored hyperbranched copolymer and select the products that produced the targeted molecular weights (discarding the others). Although this is not considered ideal, it was the only possible way to move forward to the next stage.

Ratio of core/(monomer:comonomer), Percentage ratio	M _n and PD of 1 st Run	M _n and PD of 2 nd Run	M _n and PD of 3 rd Run	M _n and PD of unified atmosphere
1/(40:8), 2%	4,500 - 2.0	22850 - 4.0	17,750 - 2.3	2,850 - 3.3
1/(20:4), 4%	16,100 - 2.2	2,850 - 1.3	15,300 - 2.8	17,050 - 2.6
1/(10:2), 8%	12,650 - 3.4	1,850 - 1.3	21,600 - 2.0	14,550 - 2.2

Table 2-3. A core molecule (NPA) had been used in turn to control the molecular weight of the hyperbranched copolymer. The table shows in first column the ratio of core compares to other molecules, each mixture was run individually and the results that obtained from GPC of 7NPA-HBP-SA were expected to be in order and sequence according to their ratios. The experiment was done three times, the results of 2nd run showing the molecular weights were in order but not in sequence as such as homo-polymerisation (table2-2). In contrast, the molecular weights of other two experiments were disordered. Eventual experiment was conducted via unifying the reaction conditions of the three different ratios. Nevertheless, the results indicated the molecular weight could not be controlled, but in general the core helped to reduce the PD of the copolymers.

2.3.5. Synthesis of Pyridine 3-(Acetoxymethyl) Cored Hyperbranched Copoly (3,5-Diacetoxybenzoic acid) and (Stearic acid), **8AMPy-HBP-SA**:

Although 4-nitrophenyl acetate failed to control the molecular weight, it was successfully incorporated into a hyperbranched copolymer. We therefore moved forward with our study examining the catalysis and the effect of a controlled environment. The study carried out an investigation into how the catalysis reacts in different solvents by applying the cored hyperbranched copolymer so as to demonstrate the microenvironment existing around the catalyst (pyridine) in comparison to the bulk solution. Previous studies showed that 4-acetoxypyridine core HBPs could be used as catalysts. However, the pyridine could be cleaved during catalysis or purification.⁸¹ Therefore, 3-(acetoxymethyl) pyridine (AMPy) **9** would be used (**Figure 2.12**). Selecting the pyridine with the methylene group (spacer) between the pyridine and the acetate, would enable the pyridine to be more stable within the copolymer. This stability is generated by preventing conjugation between the ester group and the pyridine.

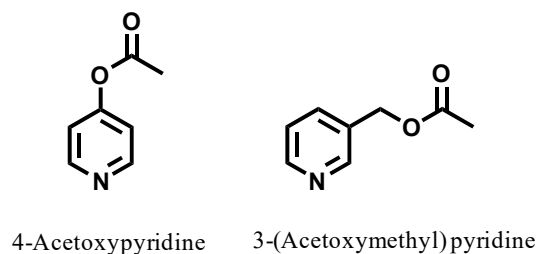
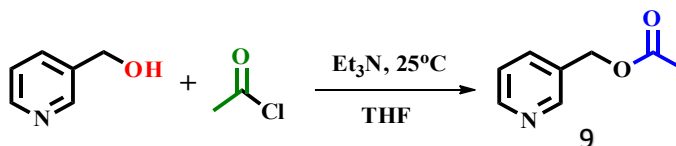


Figure 2-12. Derivatives of pyridine.

The target molecule, 3-(acetoxymethyl) pyridine (**9AMPy**) was synthesised from 3-pyridinemethanol which was acetylated using acetyl chloride in the presence of triethylamine (**Scheme 2.11**).⁸²



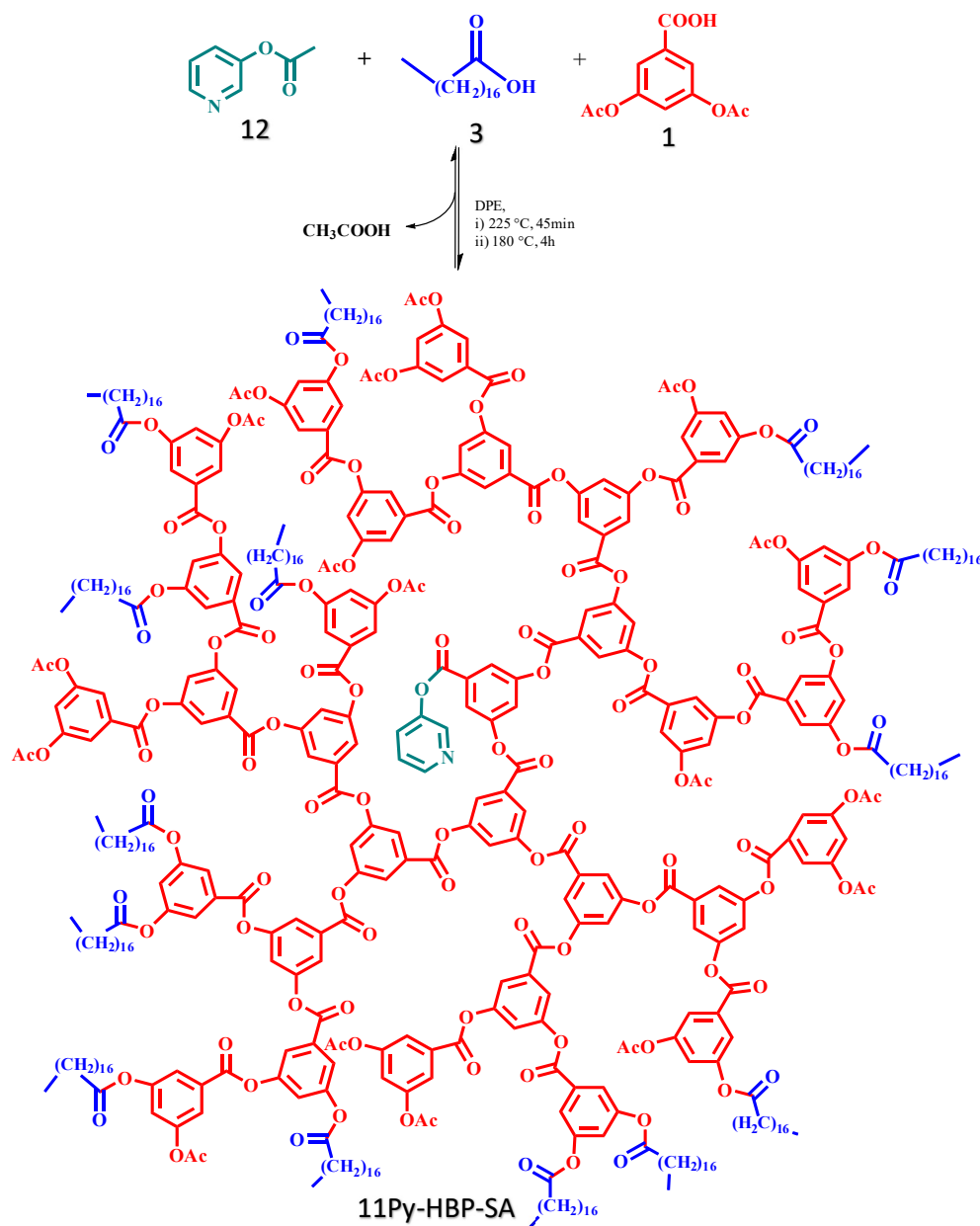
Scheme 2-11. Synthesis of 3-(acetoxymethyl) pyridine.

The reaction was carried out at room temperature; the yield of the product was approximately 65% after being washed with saturated sodium hydrogen carbonate followed by distilled water. Successful synthesis was reinforced by the ^1H NMR spectrum which showed a new large singlet at 2.12 ppm, corresponding to 3 hydrogens on the acetoxy functionality. Mass spectrometry supported this, showing a molecular ion with m/z of 152. Furthermore, the IR spectrum revealed a new intense peak at 1744 cm^{-1} from the $\text{C}=\text{O}$ functional group of $\text{ArCH}_2\text{OCOCH}_3$. In addition, a broad peak around 3220 cm^{-1} from any OH functional groups within the starting material was absent.

Once the 3-(acetoxymethyl) pyridine **9** was synthesised, it was used as a core in a copolymerisation using a 1:40:8 ratio of core **9**/monomer **1**/comonomer **3**. The ^1H NMR spectrum of the product indicated that a copolymer had been synthesised, although there was no indication that pyridine had been incorporated during the reaction. This process was repeated multiple times with different ratios, even increasing the ratio of the core up to 30%, but no evidence for core incorporation could be found. There are two possible reasons, the stearic acid could be inhibiting the incorporation process by causing an unfavourable acid-base interaction with pyridine. However, as 4-acetoxypyridine have successfully reacted with the acidic monomer, this reason therefore was excluded. The second reason may be due to a lack of reactivity. However, the polymerisation was conducted in absence of the comonomer so as to determine whether or not the 3-(acetoxymethyl) pyridine **9** could react with the monomer **1** (**10AMPy-HBP**). Unfortunately, the results confirmed that 3-(acetoxymethyl) pyridine does not have the ability to be incorporated within the hyperbranched copolymer. This had therefore verified that the carbonyl group of the acetoxy functionality is not active enough to be attacked and is an ineffective electrophile.

2.3.6. 3-Acetoxybenzoic acid Cored Hyperbranched Copoly (3,5-Diacetoxybenzoic acid) and (Stearic acid), **11Py-HBP-SA**:

In order to overcome the issue of low reactivity, the CH₂ spacer between the pyridine and the ester group was removed. The 3-acetoxybenzoic acid (Py) was thought to be less susceptible to cleavage but reactive enough to be incorporated within the copolymer. Therefore, 3,5-diacetoxybenzoic acid, stearic acid, and 3-acetoxybenzoic acid were copolymerised by adopting the same procedure (**Scheme 2.12**).



Scheme 2-12. Copolymerisation with 3-acetoxybenzoic acid.

The ^1H NMR spectrum of the product confirmed incorporation by showing a new distinct peak at 8.58 ppm. This peak was attributed to the 3-acetoxypyridine aromatic α and β protons, as highlighted in **Figure 2.13**. Moreover, GPC analysis confirmed copolymerisation, generating an M_n value of 10,000 Da and PD = 2.4.

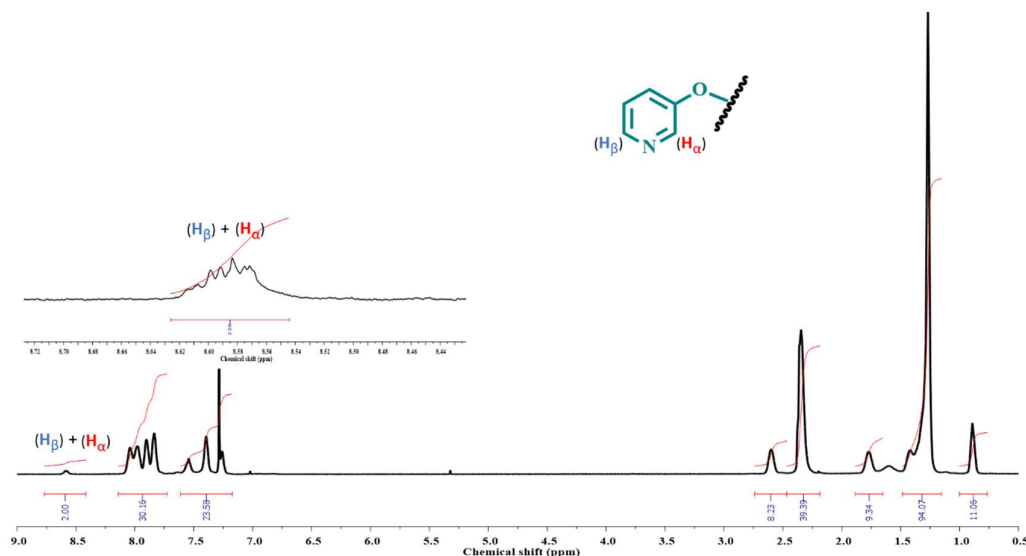


Figure 2-13. The ^1H NMR spectra of pyridine cored hyperbranched copolymer.

Having successfully synthesised a pyridine cored copolymer, we now wished to synthesise a series of polymers with a range of molecular weights but a single pyridine core and identical level of stearic acid incorporation. It was decided that the copolymerisation would be conducted with ratios of monomer/comonomer/core equal to 1:40:8, 1:20:4, and 1:10:2. Each of these reactions were repeated several times in an attempt to generate a copolymer with a reasonable spread of molecular weights as well as a consistent level of pyridine and steric acid. Furthermore, conditions were modified, such as increasing the reaction time and employing different vacuum pumps. In addition, the reactions were scaled up in order to produce sufficient polymer to carry out multiple comparable catalysis reactions; for example, 10 g of 3,5-diacetoxybenzoic acid was copolymerised during the solution phase utilising 10 g of diphenyl ether, with 1 mL of 3-acetoxypyridine and 2.40 g of stearic acid. These reactions yielded between 8-9 g of copolymer after purification. In all cases, ^1H NMR confirmed the incorporation of the core molecule, as well as the level of comonomer incorporation, which was 20% in all cases. Despite the fact that we were unable to control the molecular weight by

core incorporation, we were one again able to control the level of comonomer incorporation. The molecular weights of the copolymers obtained are presented in **Table 2.4.**

Copolymer termed	11Py-HBP-SA.1	11Py-HBP-SA.2	11Py-HBP-SA.3	11Py-HBP-SA.4
Ratio of core:monomer:comonomer	1:40:8	1:10:2	1:10:2	1:5:1
Total ratio of core:monomer	1:48	1:12	1:12	1:6
M_n by GPC	10,000	6,000	5,000	5,000
PD	2.4	3.7	2.8	2.5
M_n by NMR	18000	8500	5500	5400
Level of core incorporation	55%	70%	90%	92%
Level of comonomer incorporation	20%	22%	22%	22%
Concentration of pyridine in 100 mg of the copolymer in 1 mL of the solvent^(a)	5x10 ⁻³ M	0.016M	0.02M	0.024M

Table 2-4. Pyridine concentration data within the copolymers and M_n calculated using NMR technique. (a) Calculated using ¹H NMR and benzaldehyde as an internal standard.

The concentration of pyridine within the copolymers can be determined by dissolving a certain amount of the copolymers with a known concentration of benzaldehyde. The benzaldehyde and pyridine peaks in the ¹H NMR spectrum could be integrated and used to calculate the pyridine concentration. In addition, ¹H NMR can also be used to calculate M_n by comparing the intensities of the core (pyridine) to aromatic peaks; the data is presented in Table 2.4. In general, the M_n values calculated by NMR were higher in comparison to those calculated by GPC. Typically, the GPC is calibrated against linear polystyrene which result in the molecular weight of branched polymers being underestimated.⁸³ This is due to the structure of the hyperbranched molecule which adopts compact conformations in solution, whereas classical linear polymers adopt a more open conformation (i.e. the calibration standards). However, molecular weights calculated by NMR assumes that every copolymer possesses a core unit, which can lead to an over estimation of M_n.⁸⁰ For example, the 11Py-HBP-SA.4 copolymer had an M_n

of 5400 while the 11Py-HBP-SA.1 copolymer had an M_n of 18000. If we compare the molecular weights from GPC with those calculated with NMR, we can estimate the level of core incorporation. These were calculated as 92% and 55% for 11Py-HBP-SA.4 and 11Py-HBP-SA.1 respectively.

In principle, any of 11py-HBP-SA.3 and 11py-HBP-SA.4 can be used in the catalyst reactions in the following steps. Because they are best candidate offered a cut off in term of the molecular weights by NMR and GPC, high level of core incorporation and low PD. In addition, a quick experiment was conducted to estimate the solubility of these copolymers (11py-HBP-SA.3) in different solvents. The data is shown in **Table 2.5**. The maximum value was 1.450 g in 1 mL of acetone whereas the minimum value was 0.900 g in 1 mL of toluene. Therefore, it was decided to utilise 0.600 g of the copolymer per 1 mL so as to ensure complete solubility; this amount is equal to 0.14 M of pyridine concentration.

Solvent	Estimated solubility
Acetone	1.450g
Ethyl acetate	1.330g
Chloroform	1.250g
Toluene	0.900g

Table 2-5. Solubility test of 11py-HBP-SA.3.

2.4. UV/Vis Study:

2.4.1. Preface:

like dendrimers, HBPs have unique internal environments which can be applied to a range of applications including targeted drug delivery, site isolation, and encapsulation.^{64,84–86} The study of the electronic and steric factors affecting the internal environment of HBPs, demonstrated HBPs are indeed capable of being applied as genuine alternatives to dendrimers involving controlled and selective environments.⁷¹

A pseudo-generational series of HBPs possessing a catalytic/ binding core was required to investigate the internal environment. This was achieved by polymerising the 3,5-diacetoxybenzoic acid with a metalloporphyrin as core. The steric properties of a series HBP were assessed by studying ligand binding of three different sized ligands to the central core. The outcome suggests the HBPs display certain dense packing values, whilst catalytic experiments exhibit steric hindrance around the metalloporphyrin core. This gives rise to polymers which possess shape selective catalytic properties. The results also show the chemoselectivity was shifted 3.5-times towards a small linear alkene, which is less reactive compared to large cyclic and electrophilic alkenes.⁷¹

Subsequently, UV/Vis titration analysis was used to probe the microenvironment of the hyperbranched copolymer in toluene and chloroform. The investigation utilised a zinc functionalised 4-acetoxyphenyl porphyrin (ZnTAPP) as a probing molecule to calculate the binding affinity to the pyridine core of the hyperbranched copolymer. A free pyridine molecule was used as a control for comparison (**Figure 2.14**). The binding constant reflects the capability of ZnTAPP to access the core of the HBP to bind with the pyridine ligand. This study will yield valuable data showing the effects of different solvents on the behaviour of HBPs. From observing previous literature, it is known that bulky hyperbranched copolymers can provide unique microenvironments within solvent media. Since this is where the binding or catalysis reaction takes place, the copolymer will remain intact. Toluene and chloroform were chosen to investigate any solvent effects on the microenvironment of the HBP, as toluene has a similar aromatic structure to the hyperbranched copolymer, whereas the structure of chloroform is very

different. The similarity between the structures of bulk hyperbranched copolymers and toluene may cause the solvation of the copolymer. In this case, binding should prove more efficient than chloroform due to the ease of access of the substrate to the core of the hyperbranched copolymer. This is similar to the chemistry shown by a porphyrin core star polymer demonstrated by Fréchet et al.⁸⁷ Conducting these experiments may allow predictions to be made regarding the progress and mechanism of the catalysis reaction. In the next section, we will discuss the use of a pyridine core hyperbranched copolymer and pyridine control as catalyst.

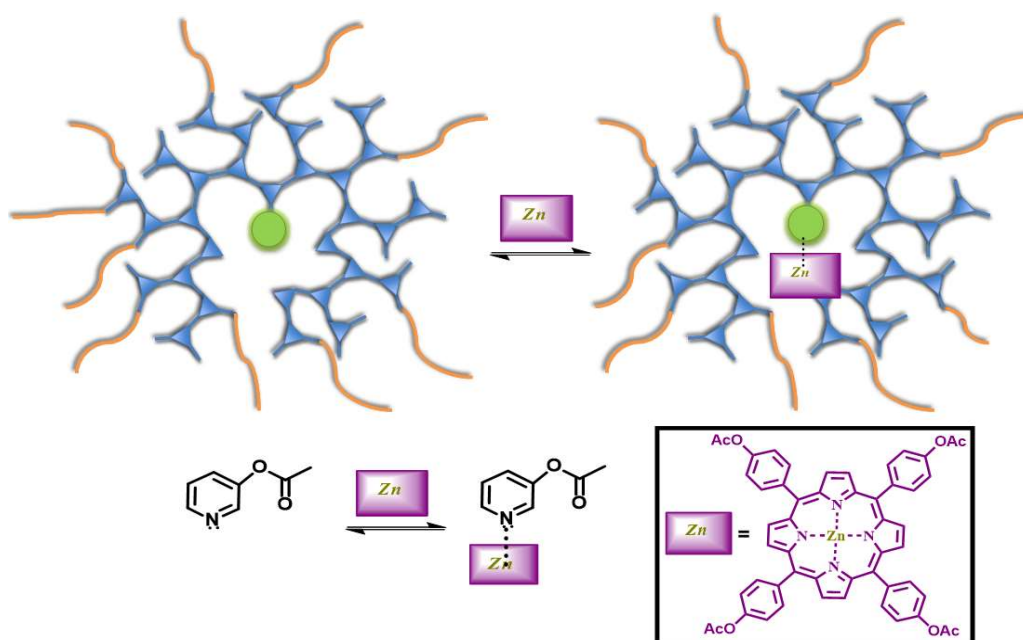
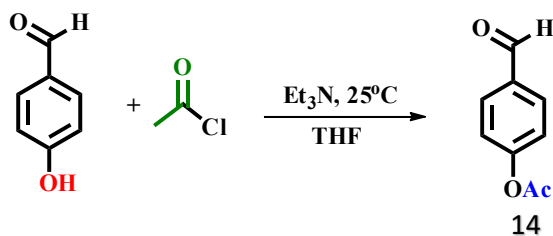


Figure 2-14. Top: UV studies to explore steric and electronic microenvironments within the pyridine core hyperbranched copolymer in different media. Bottom: Controlled pyridine reaction using 3-acetoxypyridine.

In the previous section, cored pyridine hyperbranched copolymers were prepared, thus the copolymer which had been used in this study was 11Py-HBP-SA.2. On the other hand, 4-acetoxyphenyl porphyrin (TAPP) needs to be synthesised first. To provide UV/Vis titration analysis, zinc was inserted into pre-prepared 4-acetoxyphenyl porphyrin (TAPP). Upon zinc insertion, a coordination complex was formed by loss of inner protons of the porphyrin, allowing the remaining coordination site to bind with pyridine ligand. The progress of the titration experiments can be followed via gradual shifts in the Soret band to the right with each addition of ligand around 8 nm, from 420 nm to 428 nm.

2.4.2. Synthesis of 4-Acetoxyphenyl Porphyrin, **15TAPP**:

The preparation of 4-acetoxyphenyl porphyrin (TAPP) utilised pyrrole and 4-acetoxybenzaldehyde^{88,89} in a two-step process using readily available laboratory reagents. Though commercially obtainable, 4-acetoxybenzaldehyde **14** was prepared simply from the 4-hydroxybenzaldehyde. The acetylation reaction was conducted in the presence of acetyl chloride and with triethylamine acting as a catalyst (**Scheme 2.13**).⁸² The reaction was completed in 30 mins using dry conditions at room temperature with a good yield (60%).

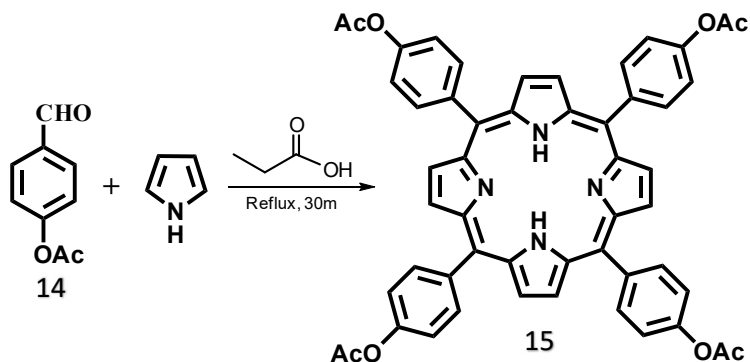


Scheme 2-13. Synthesis of 4-acetoxybenzaldehyde.

The product was washed with saturated sodium hydrogen carbonate solution followed by distilled water to remove any impurities. The success of the reaction was confirmed by the appearance of a singlet at 2.31 ppm by ¹H NMR, corresponding to the acetoxy functionality. The OH group resonance at 10.63 ppm present in the starting material was no longer present in the ¹H NMR spectrum of the product.

Now with a sufficient quantity of benzaldehyde precursor, the subsequent step was to synthesise TAPP. The procedure was conducted by refluxing equal molar quantities of distilled pyrrole and 4-acetoxybenzaldehyde **14** in the presence of propionic acid (**Scheme 2.14**). The resulting black slurry was a mixture of the desired crystalline porphyrin, and other soluble by-products. The desired product was collected by simple filtration and washed with methanol to reveal purple crystals (yield: 24%). Reaction completion was confirmed via ¹H NMR, revealing a characteristic peak at minus (-) 2.78 ppm corresponding to the two internal highly shielded N-H protons. A large singlet at 2.52 ppm corresponding to 12 hydrogens from the methyl protons on the acetoxy group was also present, along with resonances attributed to the phenyl ring as doublets at 7.54 ppm and 8.26 ppm (for *meta* and *ortho* protons respectively). A singlet at 8.91 ppm from the pyrrole hydrogens on the porphyrin was also visible. Further supporting

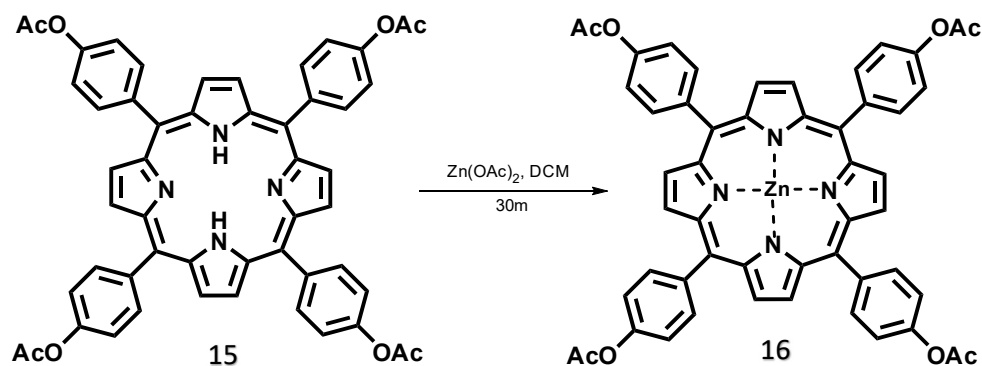
confirmation was provided by mass spectrometry, showing a molecular ion peak of 847. UV/Vis spectrophotometry revealed four distinctive Q-bands at 515 nm, 551 nm, 591.5 nm, 648.5 nm and an intense absorption corresponding to the Soret band at 420 nm (λ_{\max}).



Scheme 2-14. Synthesis of 4-Acetoxyphenyl Porphyrin (TAPP).

2.4.3. Porphyrin Zinc Complex, **16ZnTAPP**:

Metalation of the porphyrin was required before binding could be studied. TAPP **15** was dissolved in DCM and an excess of zinc acetate dihydrate was added. The solution was then refluxed for 30 mins (**Scheme 2.15**). Any excess zinc acetate and solvent was removed *via* filtration and rotary evaporation. Metalation success was proved through UV/Vis spectrum; the zinc-porphyrin complex now showed two peaks at 547.5 nm, and 586 nm (**Figure 2.14**) in addition to the Sort band at 420 nm. Further evidence supporting the structure came from ^1H NMR. The spectrum showed an absence of inner N-H signals at -2.78 ppm. Moreover, mass spectrometry confirmed the insertion by showing a molecular ion peak of 909.



Scheme 2-15. Synthesis of tetraacetoxypheyl porphyrin zinc complex.

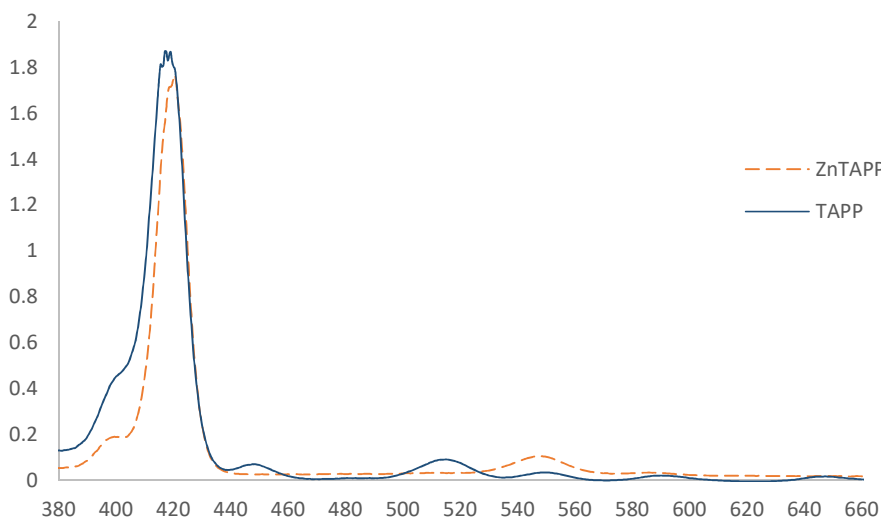


Figure 2-15. UV-Vis spectrum of free porphyrin (black), and zinc porphyrin complex (red).

2.4.4. Binding study:

Having successfully prepared and characterised ZnTAPP **16**, investigations were carried out to evaluate the interaction between the pyridyl unit and ZnTAPP. The results were used as a control when studying the same interaction using the pyridine core hyperbranched copolymer and ZnTAPP in chloroform and toluene. This titration was conducted by preparing the appropriate concentration to monitor the binding as it is a 1:1 binding reaction. Therefore, solutions of ZnTAPP (10^{-6} M), and 3-acetoxypyridine **12**/pyridyl hyperbranched copolymer (10^{-2} M) were prepared which were adopted from a previous study in our group.⁹⁰ To maintain the same concentration of ZnTAPP during the titration experiment, a ZnTAPP stock solution was used to prepare all other pyridine solutions. The solution of pyridine core hyperbranched copolymer was prepared by dissolving 62.5 mg in 1 mL of the stock solution. Measurements in previous sections (2.3.6) have shown the copolymer (11Py-HBP-SA.2) has a pyridine concentration of 0.016 M per 100 mg in 1 mL of solvent. The titration experiments were performed by placing 3 mL of the stock solution in a UV cuvette and titrating with 10 – 20 μ l of the pyridyl ligand then recording UV/Vis spectra after each addition to monitor the shift of the Soret band (**Figure 2.16**).

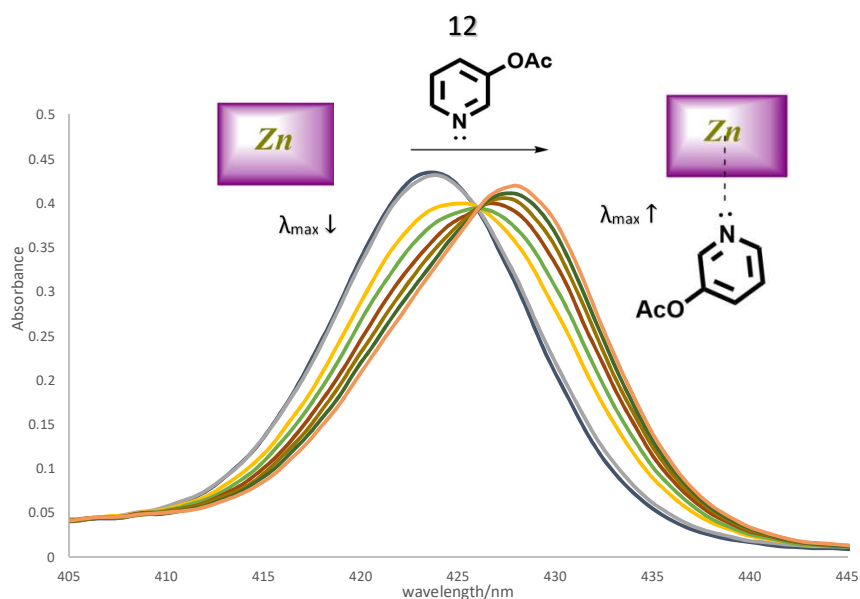


Figure 2-16. Plotting the wavelength of the ZnTAPP against the absorbance, indicating once the ligand **12** (3-acetoxypyridine) concentration increase by adding each time the Soret band started shifting in toluene.

The binding/association constant (K_a) could be determined by plotting the concentration of added ligand versus the change in the ZnTAPP absorbance at λ_{\max} (Figure 2.17) and fitting the data to a 1:1 binding model using GraphPad. The experiment was repeated with each solvent and ligand at least two times and the average from these values was calculated.

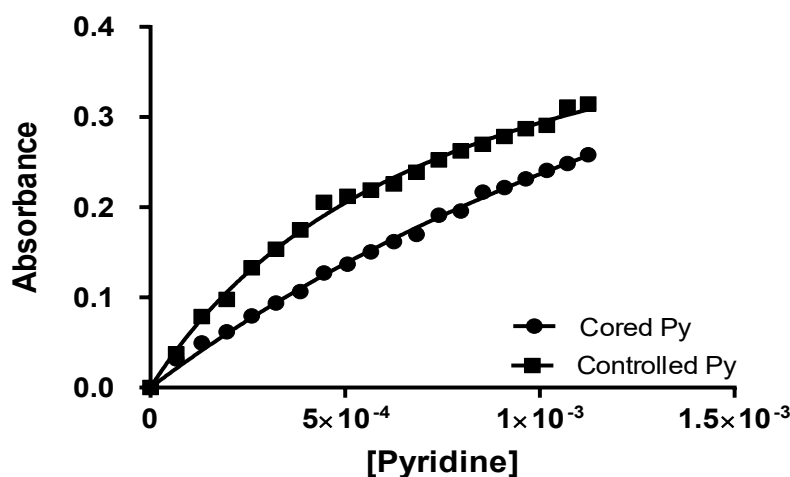


Figure 2-17. Pyridine concentration vs. absorbance of cored and controlled pyridine with TAPP in chloroform.

These experiments indicate the binding constant for the control interaction using pyridine was unaffected by solvent, showing K_a values of $1.6 \times 10^3 \text{ M}^{-1}$ in chloroform and $1.65 \times 10^3 \text{ M}^{-1}$ in toluene. However, when the copolymer was used, the K_a in toluene was 330 M^{-1} and 175 M^{-1} for chloroform (Figure 2.18).

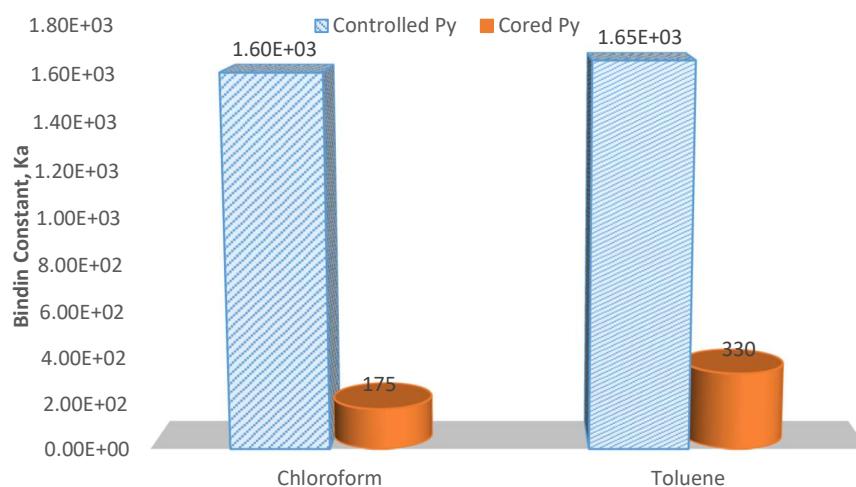


Figure 2-18. Binding indicates that binding is almost equal in both solvents in term of controlled pyridine reaction (box shape). However, within the macromolecules, binding is twice as strong in toluene, indicating a controlled microenvironment within the macromolecules (cylinder shape).

The K_a values for the copolymer were significantly reduced in both solvents with the binding constants in toluene double the value obtained in chloroform. This is due to the solvent effecting the polymer structure and/or solvation of ZnTAPP. That is, the polymer may be providing a significant steric barrier towards binding and the extent of this barrier would depend on the solvents' ability to solvate the interior of the polymer (i.e. to "swell" the polymer). If the internal regions of the polymer are not well solvated, the polymer may be 'compressed' which will increase the steric barrier. However, if the polymer is well solvated, then the polymer will be 'more open' and the ZnTAPP will have easier access to the pyridine core. This is consistent with Fréchet's work, which showed that porphyrin core poly(caprolactone) stars formed a more extended conformation in a good solvent (toluene), yet in the presence of a poor solvent such as DMSO it collapses.⁸⁷

Alternatively, differences in K_a could be due to the solvation preference of the ZnTAPP. For example, the lower K_a observed for chloroform could be due to the excellent solvation of ZnTAPP and poor solvation of the polymer interior (**Figure 2.19**). If this were the case, then the ZnTAPP would have no electronic driving force to integrate into the polymer. Put simply, the big difference in K_a for toluene and chloroform is due to a combination of steric and electronic effects.

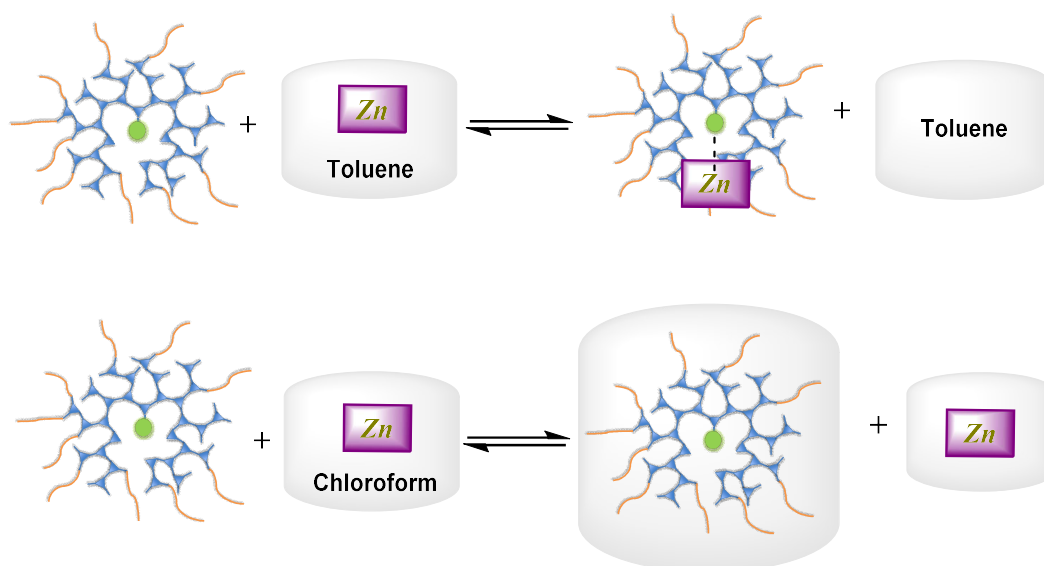


Figure 2-19. Bottom: possible explanation that ZnTAPP (porphyrin) prefers to be solvated in the chloroform, this could inhibit the interaction with the centre of the copolymer to generate weaker binding. Top, toluene represents poor solubility for the ZnTAPP, hence, the copolymer provides a better environment for the ZnTAPP to be solvated within it. This would enhance the interaction between them to obtain a very large binding constant compared to chloroform.

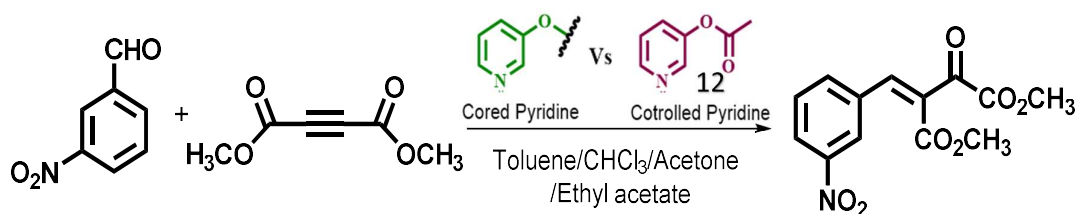
The binding results should allow us to make a prediction about the success or failure of any homogenous catalysis experiments using either chloroform or toluene as the solvent. Specifically, we might expect a slower reaction in chloroform due to limited internal access/solvation. Limiting or encouraging access to the catalytic unit is important as it adds an additional component that may enhance or limit the catalytic process.

In addition, “compartmentalisation” may also provide an alternative pathway for the catalysed reaction. For example, if the reaction involves a charged intermediate, then the rate of the reaction can be increased if the charges are stabilised using a polar solvent. The rate of a reaction involving a charged TS or intermediate is dependent on the solvent, however, if the reaction takes place within an isolated “compartment”, then the rate will be independent of the solvent. This may be the case even if the “compartment” can stabilise charge, as it will stabilise charge independent of external solvent. The expanded structure of copolymer in toluene would enable it to stabilise the intermediate charge within its entity. Therefore, this might lead to a similar result in terms of using pyridine control and pyridine core as a catalyst. Also, we predict a big difference between both catalysts towards the pyridine control due to the copolymer adopting a more compressed conformation in chloroform.

2.5. Catalysis:

2.5.1. Catalysis Reaction of an Alkyne with an Aromatic Aldehyde, Monitored by GC:

In this step of the project, the catalysis reaction was reacted using both type of catalysts; the pyridine cored hyperbranched copolymer and the control pyridine (free pyridine). The reactions with both catalysts were run in the same pyridine concentrations and conditions and comparisons were made to understand the effect of the branched structure on 'compartmentalisation' and catalysis efficiency. The reaction has been chosen to exhibit the possible effect of a pyridine core compared to the control. The reaction shown in **Scheme 2.16** was adopted from Nair's published work. The experiment was conducted in different media to investigate the impact of the solvent on rate of the reaction, and to study the effect of the branched structure on the progress of the reaction.



Scheme 2-16. Schematic showing general reaction of alkyne with aldehyde, that was used in the project to study the progress of the reaction towards the product (alkene) by using two different catalysts. The experiment was conducted in different media to investigate the impact of the solvent on rate of the reaction, and to study the effect of the branched structure on the progress of the reaction.

The reaction initiation involved the attack of pyridine on the alkyne (dimethyl acetylene dicarboxylate) to produce a charged intermediate. In turn, this charged intermediate then reacted with the aldehyde (3-nitrobenzaldehyde) to form the product (2-oxo-3-benzylidenesuccinate) (**Scheme 2.17**). Generally, such a reaction that includes several charged intermediates is expected to be solvent dependent, therefore, conducting the reaction in range of solvents (**Table 2.6**) would enable the solvent with higher polarity to stabilise this charge better. The ability of the solvent to solvate reagents and stabilise the intermediate accelerates the rate of the reaction. The relative rates of the pyridine control reaction in different solvents is anticipated in the following order:

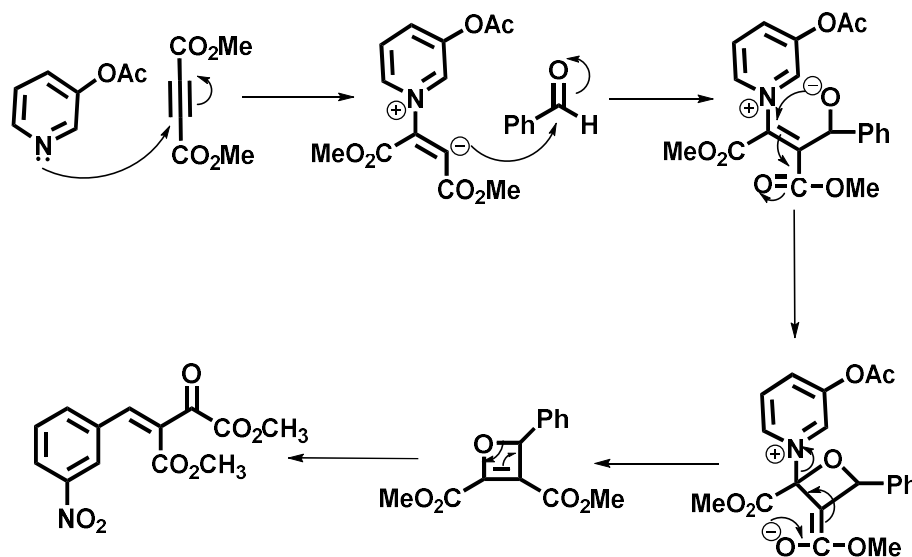


Solvent	Toluene	CHCl ₃	DCM	Acetone	Ethyl OAc	DMSO	DMF
Polarity (δ_p)	1.4	3.1	6.8	10.4	5.3	16.4	13.7

Table 2-6. Polarity for some solvents at 25 °C, which adopted from Hansen Parameters.⁹¹

The progress of this catalysis reaction can be followed accurately using ¹H NMR but is considered expensive and the use of specific solvents is limited. Thus, gas chromatography (GC) was chosen due to the ease of use, reduction of costs and availability of solvents.

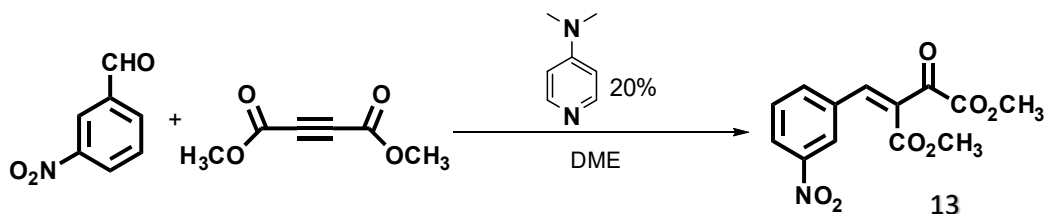
The pyridine core hyperbranched copolymer was characterised, showing a molecular weight of 5000 Da and maintaining a level of comonomer incorporation of less than 25%. The catalysis reactions using pyridine core hyperbranched copolymer was performed using a pyridine control catalyst first, to obtain information and observations to consider in the main reaction synthesis. Nair et al. suggested the molar equivalent of the catalyst to be a 20% molar ratio according to the reactants.⁷⁶



Scheme 2-17. Catalysis reaction mechanism.

However, calibrating the GC machine was required first to determine the peaks of each component of the reaction including reactants, which were purchased from Sigma Aldrich. The product, 2-oxo-3-benzylidenesuccinate, was not available commercially, therefore it was synthesised by mixing dimethyl acetylene dicarboxylate (DMAD) with 3-nitrobenzaldehyde in the presence of 4-dimethylaminopyridine (DMAP; 20 mol %)

(Scheme 2.18). The ^1H NMR spectrum confirmed the presence of the desired product; the two methoxy groups were seen at 3.71 ppm and 3.83 ppm as two singlets. Moreover, the alkene proton resonated at 7.14 ppm with the absence of aldehyde proton from 10.30 ppm, ^1H NMR is showing in Figure 2.22.



Scheme 2-18. Synthesis of 2-oxo-3-benzylidenesuccinate with 4-dimethylaminopyridine (DMAP) as catalyst.

For calibration, neat samples of 3-nitrobenzaldehyde and DAMD (starting materials), the 2-oxo-3-benzylidenesuccinate (products) and naphthalene (the internal standard) were injected into the GC machine. Signals for DAMD and the product appeared after 1 and 15 minutes respectively, whereas the signal of 3-nitrobenzaldehyde appeared after 9 minutes at a temperature of 170 °C. The signal for DAMD was weak and very close to the other peaks (overlapped). Furthermore, the product signal was broad (i.e. multimodal peaks) and poorly resolved, and therefore, the decision was made to monitor the progress of the reaction depending on the consumption of the 3-nitrobenzaldehyde which was identical with good resolution. The system was calibrated again with seven appropriate concentrations of 3-nitrobenzaldehyde ranging between 0.1 M-0.7 M. This allowed a calibration curve to be plotted of peak area vs. concentration.

The pyridine control reaction was run with a number of solvents including toluene, chloroform, DMF, ethyl acetate, and DME. The reaction system was charged with mixture of equivalent molar ratio equated to 0.7 M of 3-nitrobenzaldehyde (528 mg, 3.5 mmol), DAMD (497 mg, 3.5 mmol), and naphthalene (448 mg, 3.5 mmol). Then the system was evacuated and flushed with nitrogen and 5 mL of the solvent was added. Once the 20 mol % of 3-acetoxypyridine **12** (95 mg, 0.7 mmol) was injected (equal 0.14 M) to a sealed reaction flask, the reaction turned reddish in colour, signalling reaction completion. Samples were taken after 30 minutes, followed by a sample every 24 hours

for three days. Each reaction was repeated twice and results for toluene and chloroform are shown in **Figure 2.20**.

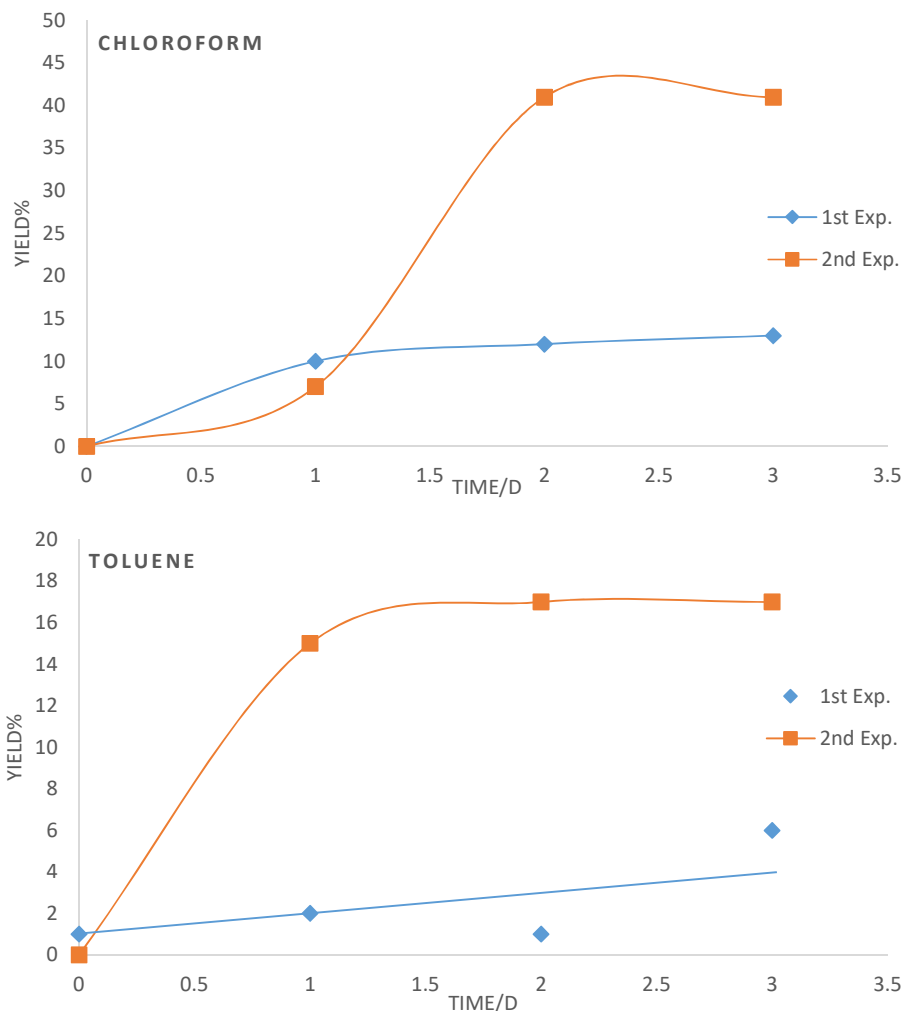


Figure 2-20. The controlled pyridine catalysis reaction for toluene and chloroform are presented. The yield progress of the reaction was monitored via GC. The graphs show the trend of the yield of 1st and 2nd experiments are not reproducible in both solvents.

The analysis of the 3-nitrobenzaldehyde showed the reaction which was catalysed using free pyridine was not reproducible from the first and second run in all solvents. This is obvious from the graphs of chloroform and toluene. The yield of the first experiment in chloroform reached 41% yet it was only 13% in the second experiment. Whereas, the yield in toluene ranged from 6% to 17% for the first and second experiments respectively. Such very high differences between the first and second experiment was obtained, which was expected due to physical and technical problems regarding the withdrawal of the samples from the reactors and injecting them into the machine.

In this investigation, there are several sources for error, one of which occurred in the percentage yield calculations. The values obtained may be inaccurate as they were calculated using only one component of the reaction: 3-nitrobenzaldehyde. Also, degradation or interaction with other parts of the molecule could have led to unreliable results. Ideally, we wanted to see the disappearance of starting materials and the appearance of product (with the same concentration as the starting material). Further data is required to determine the exact mechanism of how the starting materials is converted into product. However, it was not possible to investigate the significant relationship of the 3-nitrobenzaldehyde and 2-oxo-3-benzylidenesuccinate further, due to the broadness and overlapping of the peak sizes of the product.

Other techniques must be used to monitor the reaction and yields over time. The ^1H NMR can exhibit noticeable peaks for starting materials and products without overlapping. This would allow us to monitor the conversion of starting materials to product easily. Therefore, free pyridine will be investigated again in the following section, followed by NMR to obtain reproducible valid results.

2.5.2. Catalysis Reaction in Standard Solvent, Monitored by NMR:

Catalysis reaction were previously studied using pyridine in chloroform and toluene. The results showed there was a big error between individual experiments for all solvents studied. This led us to look at alternative techniques to improve the analysis of the reaction and to measure the conversion. For the NMR analysis of the reaction, a number of choices of experimental methods were possible. The reaction could be carried out in deuterated solvents, but this would be expensive and would limit the choice and reduce the pool of possible of solvents. Alternatively, the reaction could be carried out in standard solvents. We could then remove samples, evaporate the solvent and redissolve in deuterated chloroform (for analysis). However, for high boiling solvents such as toluene or DMF gentle heating would be required to speed up evaporation, which may be a problem.

The first experiments were, therefore, carried out in non-deuterated toluene, chloroform, DMF, ethyl acetate, and DME. The reaction progress in toluene gradually reaches 10% on the second day. The yield kept going up gradually, but suddenly increased to 60% on the third day. Furthermore, the progress in DME indicated a shaky, by slow increase in yield up to 12% by day three (**Figure 2.21**).

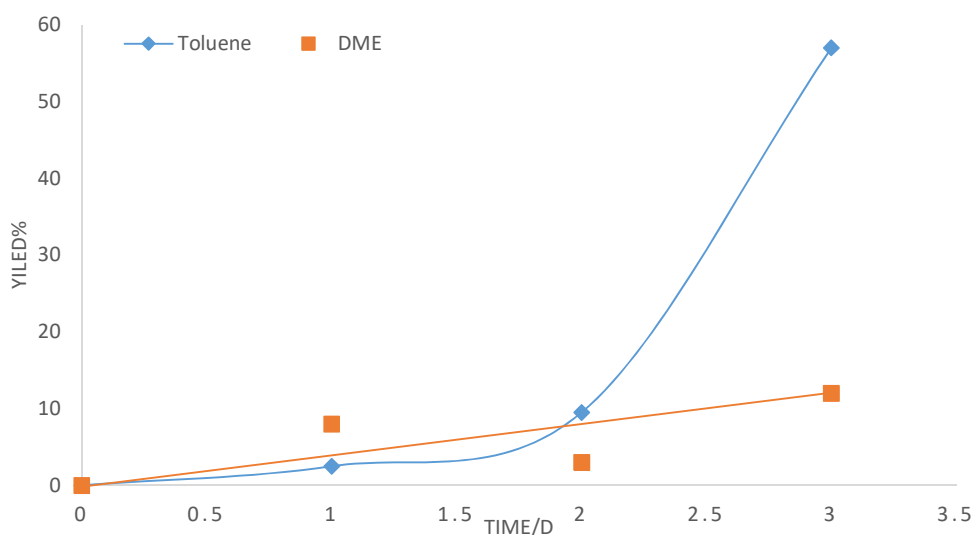


Figure 2-21. The ^1H NMR was used to monitor the progress of controlled reaction that run in previous section simultaneously with GC analysis. The solvent of the samples was removed under nitrogen and some of them required a bit of heat at 25°C , then dissolved again in deuterated chloroform in order to continue the analysis. The blue graph represents the yield of toluene which showed dramatic increase after the second day reaching up to 60% after it was 10%. On the other hand, the progress of the reaction in DME was unstable by increasing the yield to 10% then went down in the next day. The following day the yield devolved again reaching 12%. Therefore, a decision was made to improve the reaction condition as well as avoiding the evaporation process which expected to be one of the factors behind such these results.

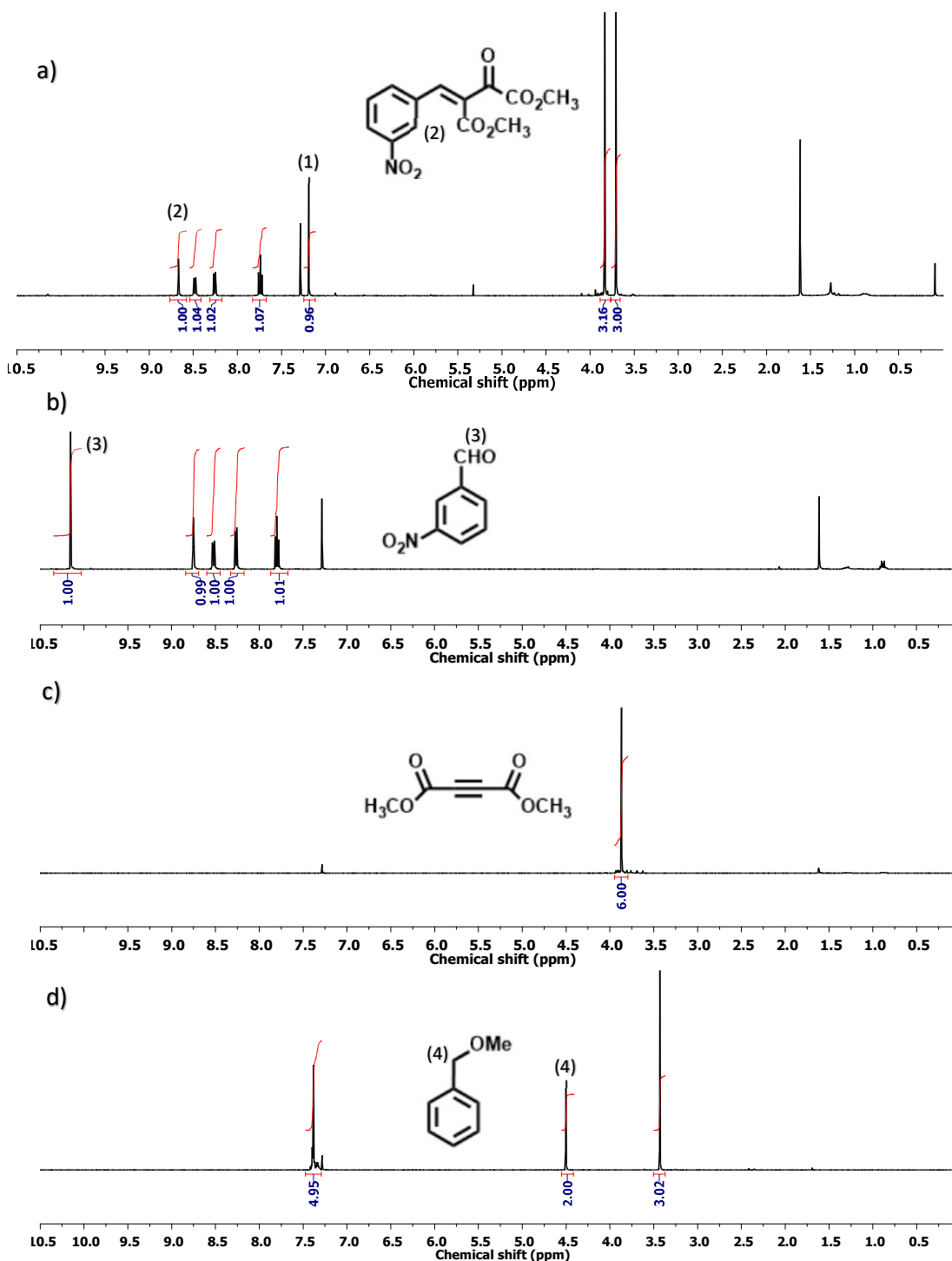
Many factors may have affected these results. This could be the long-time process required to evaporate the solvent which includes heating then transferring from one vial to another. This is a major source of uncertainty, as the method used to remove the solvent could be the reason for the sudden increase the rate of the toluene reaction. This could occur as evaporation is slow, resulting in concentration increases (speeding up reaction). As well as, heating will also speed up the reaction. A final source of uncertainty could be sample loss during all the transfers. These undesirable results led us to rethink for new procedure to monitor the reaction.

2.5.3. Direct NMR Analysis for Catalysis Reaction, using Deuterated Solvents:

In this section, the same catalysis reaction using pyridine was run in deuterated solvent and the data analysed directly within the NMR tube. This preserves the reaction conditions and avoids contamination, sample loss and errors due to heating, delivering more robust data. Moreover, NMR allows yield calculation by studying both consumption of the aldehyde (peak at 10.30 ppm) and formation of product (alkene peak at 7.14 ppm), and by following the proton resonating at 8.73 ppm that corresponds to the phenyl ring of the product (2-oxo-3-benzylidenesuccinate) (**Figure 2.22**). As a result, we expect to obtain reliable and repeatable data with a low margin of error. Due to the specific nature of some deuterated solvents, cost and/or limited availability some were excluded, including DMF, DMSO, and DME. Hence, the initial control reaction was studied in chloroform and toluene, and later followed by acetone and ethyl acetate.

Using 1 mL of solvent an NMR sample was prepared at 0.7 mmol of starting materials (3-nitrobenzaldehyde, and DMAD), 0.14 mmol of catalyst (3-acetoxypyridine), and 0.35 mmol of benzyl methyl ether (the internal standard). The NMR tube was gently shaken and spectra recorded at various time intervals. Changes in the spectra confirmed that the reaction was progressing, these are shown in **Figure 2.23**.

Figure 2-22. Four different ^1H NMR spectra that clarify the peaks utilised to calculate the yield progress of controlled pyridine catalysis reaction. a) the spectrum of 2-oxo-3-benzylidenesuccinate (product) indicating the proton (1) of alkene at 7.20 ppm that was used to monitor the progress of the reaction. Proton (2) at 8.67 ppm can be used to monitor the reaction in the same way as proton (1), while the remaining the peaks in aromatic region cannot be followed due to overlapping with 3-nitrobenzaldehyde's peaks. b) consumption of aldehyde (3) at 10.30 ppm of 3-nitrobenzaldehyde was monitored to measure the progress of the yield compare to the alkene's peak. c) DAMD shows six protons at 4.80 ppm that overlap with methyl groups of 2-oxo-3-benzylidenesuccinate and cannot be used to calculate yield. d) benzyl methyl ether was used as internal standard to overcome issues due to inability to monitor the alkene's peak in some cases. Using 0.35 M of the standard during the catalysis reaction, the peak (4) protons of benzyl methyl ether at 4.50 ppm may be used to compare to aldehyde's peak.



The stacked plots below of the ^1H NMR spectra show the catalysis reaction progression in deuterated toluene. A singlet peak at 8.73 ppm begins to appear which is attributed to the new phenyl proton (2) in of the product (2-oxo-3-benzylidenesuccinate). In toluene the peak corresponding to the alkene at 7.14 ppm could not be observed as it overlapped with the solvent peaks. However, this was only a problem in toluene and the peak was detected in all other solvents. The peak for the aldehyde (10.30 ppm) decreased as the reaction progressed. To follow the reaction and allow changes in concentration to be calculated, a known amount of benzyl methyl ether was added, and the methyl peak integrated and used to monitor the reaction progress by comparison to the aldehyde. The reaction was conducted twice in each solvent and the results were averaged.

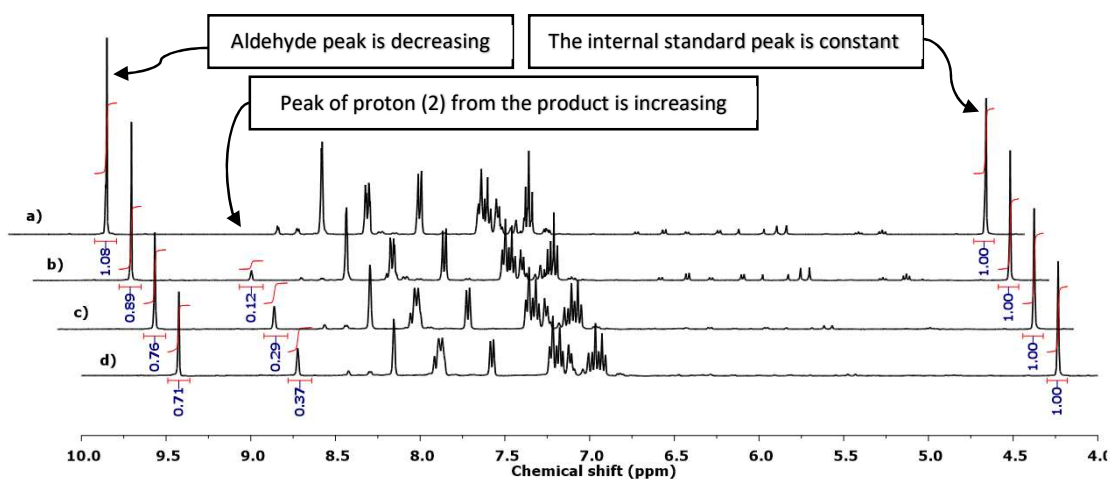


Figure 2-23. The ^1H NMR spectra demonstrates the progress of 2nd controlled pyridine catalysis experiment in deuterated toluene. a) one hour from the start; the standard's peak at 4.55 ppm was integrated in order to monitor the progress of the reaction. b) 24 h the spectrum shows reaction progress by the appearance the signal of proton (2) from the aromatic group of the product at 8.73 ppm. c) at 48 h the alkene peak at 7.20 ppm is no longer detected, enabling the yield of the reaction to be calculated based on increase of the peak of proton (2) of phenyl ring and decrease of the peak of aldehyde at 10.30 ppm. d) the spectrum at 72 h later shows the reference peak is constant throughout the reaction, and was also used as to monitor the reaction progress and shows a yield of 37%. The yield calculated by the increase and decrease of the proton (2) of phenyl ring and aldehyde, respectively, was 34%. Considering the potential errors of these methods, these two methods generated equivalent results throughout the duration of the assay.

The graph shows the yield in toluene reached 28% ($\pm 6\%$) over the three-day study, while the yield of the reaction was 9.5% ($\pm 2.5\%$) in chloroform (**Figure 2.24**). The data is smooth and reliable, which confirms that calculating the yield using ^1H NMR is reproducible. Hence, the results using ^1H NMR are more dependable than GC and this technique will be used for all further analysis.

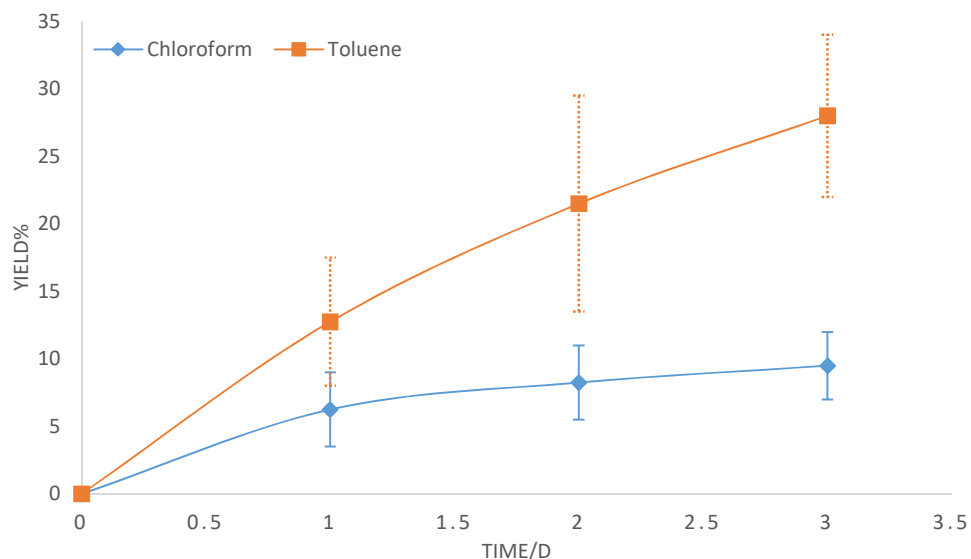


Figure 2-24. The catalysis controlled pyridine reaction was repeated in toluene and chloroform and monitored via ^1H NMR. The procedure of the reaction followed the amended protocol and was conducted in 1 mL of deuterated solvent and then replaced in the NMR tube. The reaction progress was monitored for three days by measuring the increase of the alkene peak and decrease of aldehyde peak. Combining the reactants in one vessel ensures that the reaction's conditions are maintained during the course of the experiment. This delivered more consistent and reproducible results.

The next step was conducting the catalysis reaction in toluene and chloroform using the pyridine cored HBP as catalyst and comparing it with the control. UV/Vis studies previously showed (section 2.4.4) weaker binding in both solvents using pyridine cored HBP due to steric hindrance, which was much weaker in chloroform due to reduced swelling and increased steric hindrance. This supports the hypothesis that results obtained from control reactions would be significantly better. However, if the region around the catalyst is poorly solvated then the structure of the copolymer may be important for catalysis, and the copolymer will therefore interact with all species during the reaction. If this is the case, then the progress in all solvents should be equal and less affected by the solvent, assuming internal space is constant. Assuming that the HBP structure is well solvated and improves the reaction progress, an alternative scenario is that the result will be better than control reaction.

The catalysis reaction using pyridine cored HBP may be slow, thus the reaction progress and yield was monitored over three days. The reactions were conducted as described previously, using the same concentration of starting materials and internal standard. The pyridine catalyst was replaced with the pyridine cored HBP such that the amount of pyridine corresponded to exactly 0.14 M, (calculation of pyridine concentrations was performed using a known amount of benzaldehyde, as described on section 2.3.6). The reactions were followed over three days and the percentage yield of product plotted and compared with the control reaction for each solvent individually (**Figure 2.25**).

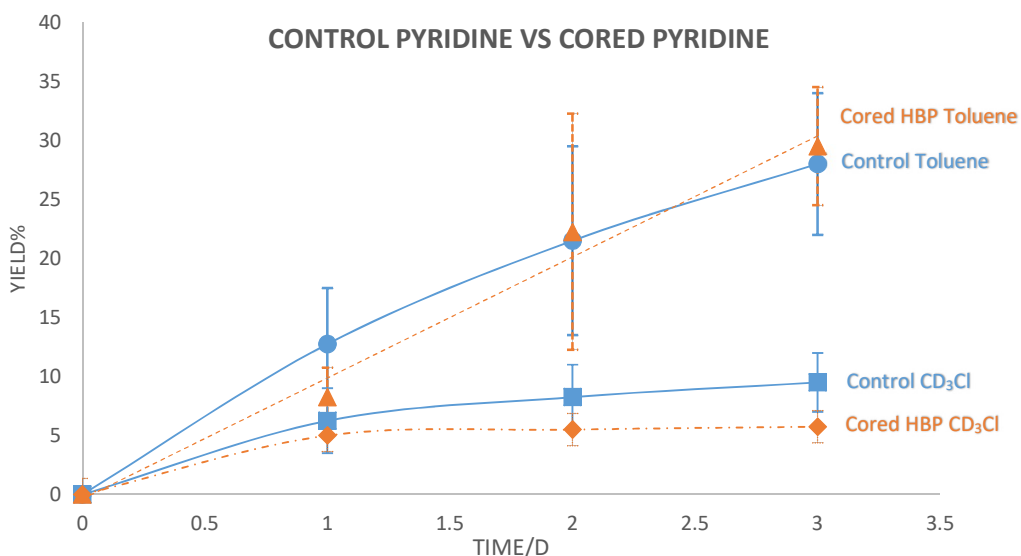


Figure 2-25. Comparison extent of conversion between control reactions and HBP reactions.

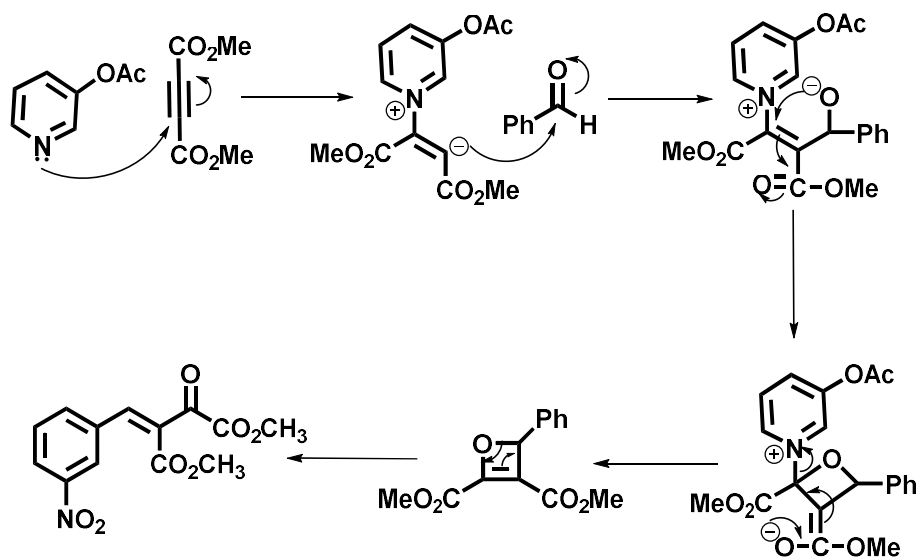
The above graphs demonstrate there are no differences between control reaction and HBP/cored reaction in either solvents, within the error of the assay. There is a small decrease for HBP reaction in chloroform, but essentially no real change. This confirms the HBP structure was too open, allowing solvents to access through it and reaction proceeds as it performed in bulk solvent. These results lead to understanding that the backbone of the HBP does not work as barrier to prevent solvent access as well as the reagents 3-nitrobenzaldehyde, and DMAD. Moreover, these results are conflicting with UV/Vis studies, it is likely that this occurred due to the porphyrin (ZnTAPP) enhancing the steric hindrance. This means that the small reagents could access the core more easily than the relatively large macrocycle porphyrin.

Interestingly, although chloroform is slightly higher in polarity, the reaction progress was better in toluene. These results prompted the study of the electronic effect using acetone, which has a polarity 10-times higher than toluene, and ethyl acetate, which has polarity between that of toluene and acetone.

Overall, this catalysis reaction was conducted in four solvents with different polarity: toluene, chloroform, acetone, and ethyl acetate. Other solvents were excluded due to unavailability and/or cost (**Table 2.7**). Assessing the reaction mechanism there is a number of charge species (**Scheme 2.19**). Therefore, pre-testing hypothesis suggests that the control reaction would be faster in acetone and ethyl acetate, if charge stabilization is important. The same experimental procedure used for toluene and chloroform was applied for acetone and ethyl acetate, firstly using control pyridine. Plots of all reactions showing concentration (yield in molarity) of the product are shown in **Figure 2.26**.

Solvent	Toluene	CHCl ₃	Ethyl acetate	Acetone
Polarity (δ_p)	1.4	3.1	5.3	10.4

Table 2-7. Polarity for some solvents at 25 °C.⁹¹



Scheme 2-19. Catalysis reaction mechanism.

The results after 24 hrs for the control reactions are shown below. Although the reaction was faster in toluene, it was only slightly faster than chloroform or acetone (the slowest). Indeed, when considering errors, it is apparent that there is no real effect of solvent polarity on the rate/yield of the reaction. As such we can conclude that the reaction does not involve high energy “formally” charged TS or intermediates.

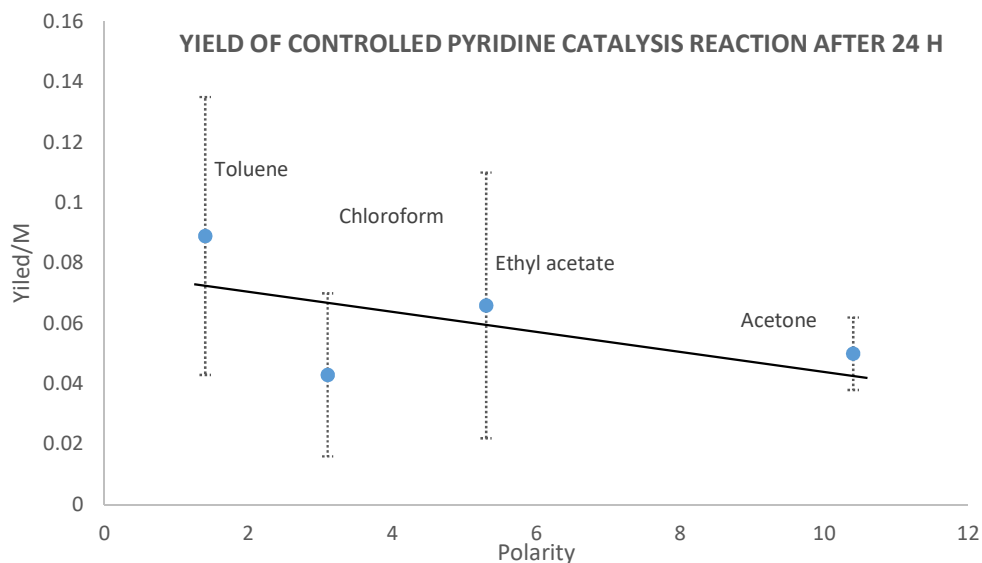


Figure 2-26. Progress of the control catalysis reaction in four different polar solvents after 24 hrs. Similar trends were observed at 48 and 72 hrs.

The investigation was continued to study the reaction using pyridine cored HBP in acetone and ethyl acetate. The reactions were carried out using the same procedure and concentrations applied for toluene and chloroform. The data after 24 hrs, 48 hrs and 72 hrs for all solvents is shown in **Figure 2.27**.

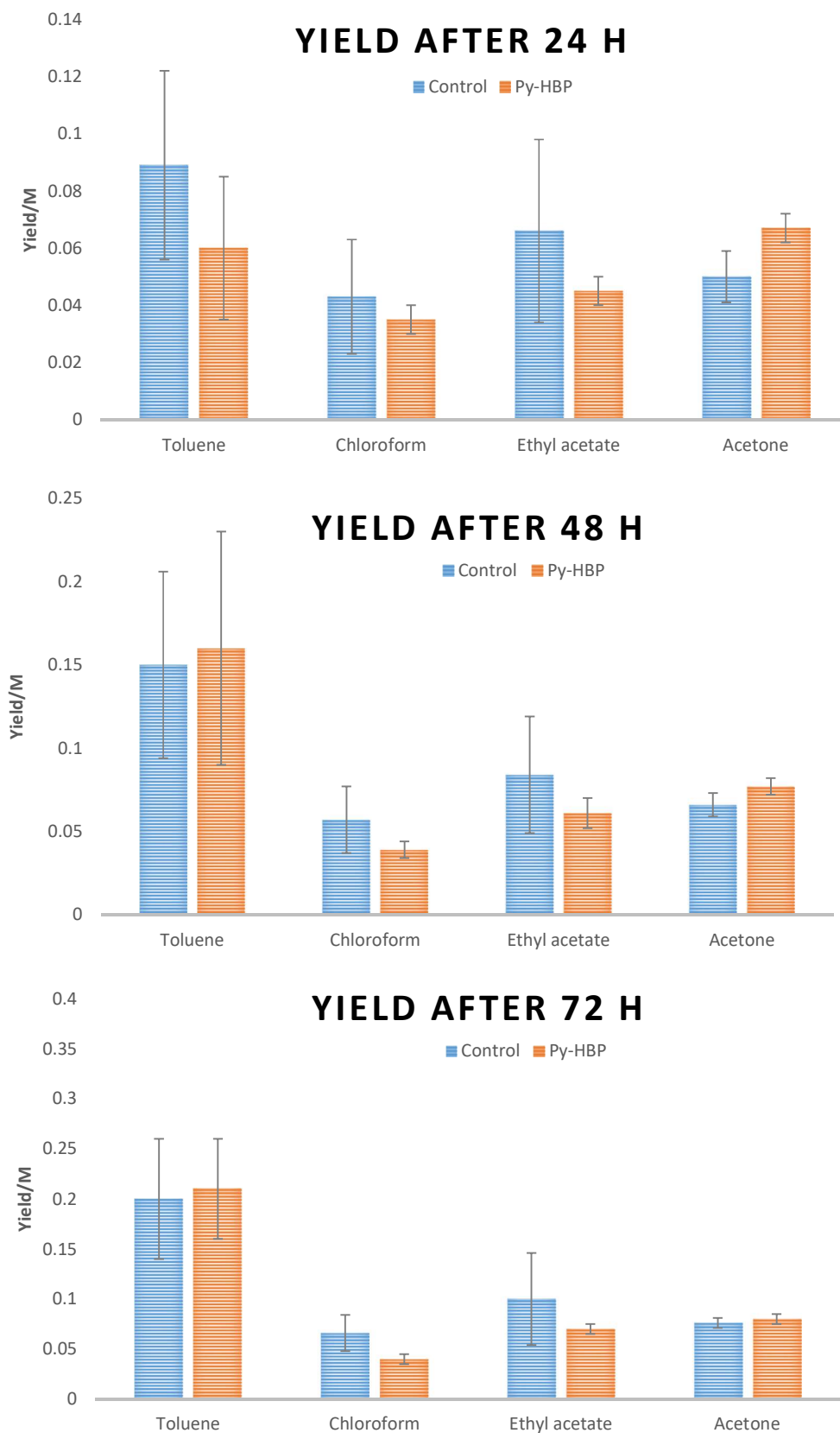


Figure 2-27. Progress of catalysis reactions of HBP and control catalysts.

As observed in all the above graphs, these results are the same as obtained from the control reaction. In addition, the HBP reactions generated yields very similar to those obtained in the control reactions. This tells us two things: the hyperbranched copolymer does not hinder the reaction by preventing substrate access, and the hyperbranched copolymer does not help the reaction. This means the HBP does not provide a superior or unique environment for the reaction. Nevertheless, the results are positive as the HBP can catalyse the reaction without a loss of activity and the catalyst can be removed easily by precipitation.

A final experiment was performed using the pyridine cored HBP in toluene and chloroform in order to study the possibility of reusing the hyperbranched copolymer. The reaction was repeated and left to stir for three days, after that it was precipitated in cold methanol and the solids collected. The copolymer then was collected in 85% mass yield. The ^1H NMR spectrum was recorded but did not show any pyridine peaks. GPC analysis provided the molecular weight of the copolymer was around 10000 Da, indicating that the polymer had not degraded. Therefore, the hyperbranched copolymer has only lost its 'catalytic' pyridine peak. This is probably due to the ester bond which binds the pyridine to the HBP. It is likely that this is a weak/reactive ester that is easily cleaved during the reaction or precipitation procedure. Therefore, the copolymer can be collected after the reaction, but due to loss of its catalytic group it cannot be reused.

2.6. Conclusion:

The work in this chapter involved three different aspects; synthesis of hyperbranched copolymer in order to improve the physical properties, probing the microenvironment of this copolymer using UV/Vis spectrophotometry, and applying the hyperbranched copolymer as a catalyst in different polar media.

A simple one-pot synthesis methodology was developed in the research for preparing the hyperbranched polymer with multiple peripheral units. Hyperbranched copolymers were prepared successfully based on 3,5-diacetoxybenzoic acid and stearic acid. This methodology offered a control in the level of co-monomer incorporated. Modifying the end group or adding a new functional group led to increased solubility of these hyperbranched polyarylesters. Additionally, the same strategy was used to synthesis pyridine cored analogue of the same HBP.

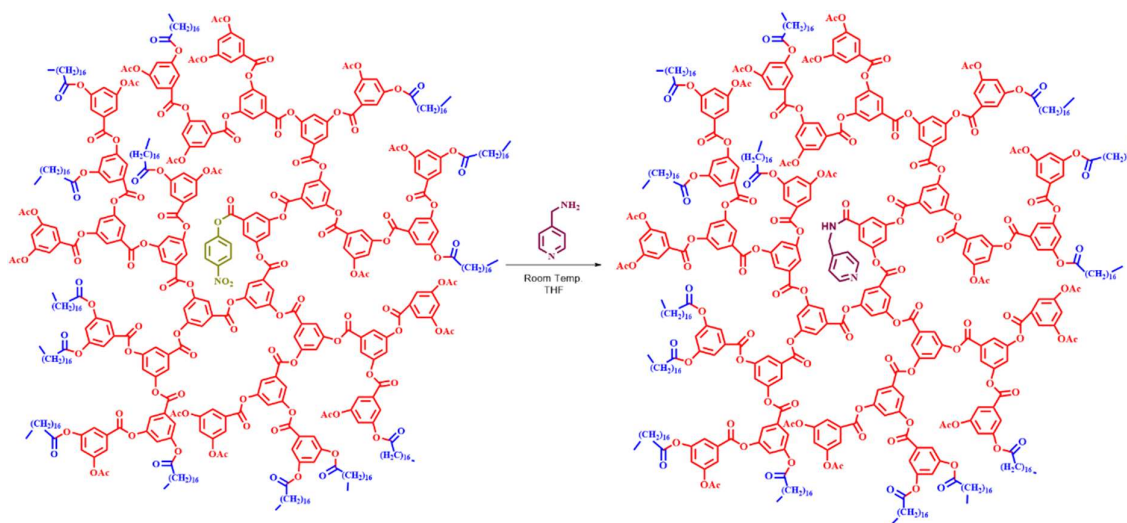
The pyridine cored hyperbranched copolymer was investigated to determine if it could provide a unique microenvironment in solvents such chloroform and toluene. Binding of zinc porphyrin to the hyperbranched copolymer was significantly weaker in both solvents, but much weaker in chloroform. These results confirm the presence of a steric barrier for the large porphyrin unit (i.e. dense packed structure). The differences in binding between toluene and chloroform may be due to the different levels of solvation within the internal region of the copolymer, which results in a greater swelling of the HBP in toluene; as such, there is more space, which leads to higher binding.

The solvent dependent steric effect was examined by conducting a catalysis reaction using pyridine and a pyridine cored HBP in toluene and chloroform. The reaction was followed by NMR using deuterated solvents. The progress of the reactions in each solvent showed there was no difference between the pyridine catalyst and the HBP catalyst. This means, despite the steric bulk surrounding the pyridine within HBP structure, the HBP did not provide a substantial steric barrier. Additional control and HBP reactions were conducted to investigate any electronic effects using the more polar solvents acetone and ethyl acetate. Similar results were obtained, which means the reaction did not involve any formally charge intermediates or TS.

Although no solvent or “dendritic” effects were observed, the HBP was able to catalyse the reaction and be recovered in a straightforward process after the reaction. Recovery and reuse experiments were carried out in toluene and chloroform using the pyridine cored hyperbranched copolymer. However, the ester bond between the pyridine and the hyperbranched copolymer was cleaved. Although synthesis of a HBP with a spacer between the ester functionality and the pyridine was attempted, incorporation did not take place.

Overall we can conclude that the polymer with molecular weight 6000 Da did not provide a significant controlled or steric environment that could affect the reactions. Although all the evidence leading up to this study, including binding and dense packing studies, suggested the chosen polymer would have the required structure, this was not the case. We believe this is due to the co-monomer reducing the degree of binding and raising the molecular weight at which dense packing occurred. Thus, more work needs to be done to obtain a new polymer with a higher molecular weight.

However, this research provided a route for hyperbranched polyarylesters with increased solubility in many solvents. Moreover, catalysis reactions using HBP took place without decreasing the yields. This HBP was also recovered completely but without the active pyridine site. To overcome this problem, and improve incorporation of pyridine, we propose to add a spacer within the hyperbranched copolymer using postsynthetic methodology (**Scheme 2.20**).⁹² This strategy should result in a pyridine cored HBP that can be collected and reused.



Scheme 2-20. Proposed post-synthetic reaction.

Chapter 3

Results and Discussion (II)

3. Light Harvesting Hyperbranched Copolymer Model:

3.1. Introduction:

Every day, the solar radiation that covers the Earth's surface in just one hour is enough to provide society's energy for an entire year. Attempting to harness this abundance of energy is of vital importance in order to reduce dependency on non-renewable energy resources (fossil fuels). Solar energy is a renewable energy resource and the most abundant available daily.⁹³ Organisms such as cyanobacteria, algae and plants play the crucial role of providing all of the biological energy for life through photosynthesis processes. This light harvesting system and photosynthesis are clearly important processes developed by nature. Furthermore, harvesting sunlight and transferring it to energy, including the conversion of carbon dioxide into oxygen, occurs in natural proteins that support multi-porphyrin arrays.^{94,95} The system is comprised of LH-I and LH-II complexes, which are perfectly symmetrical; purple bacteria is an example of organisms with such a system.^{96,97} However, by understanding the structure of the photosynthetic components of these phototrophs, as well as their functional complexes, then these systems could be replicated. The photosynthesis unit of purple bacteria is composed of two types of pigment proteins. The principle component of this pigment is chlorophyll (**Figure 3.1**).

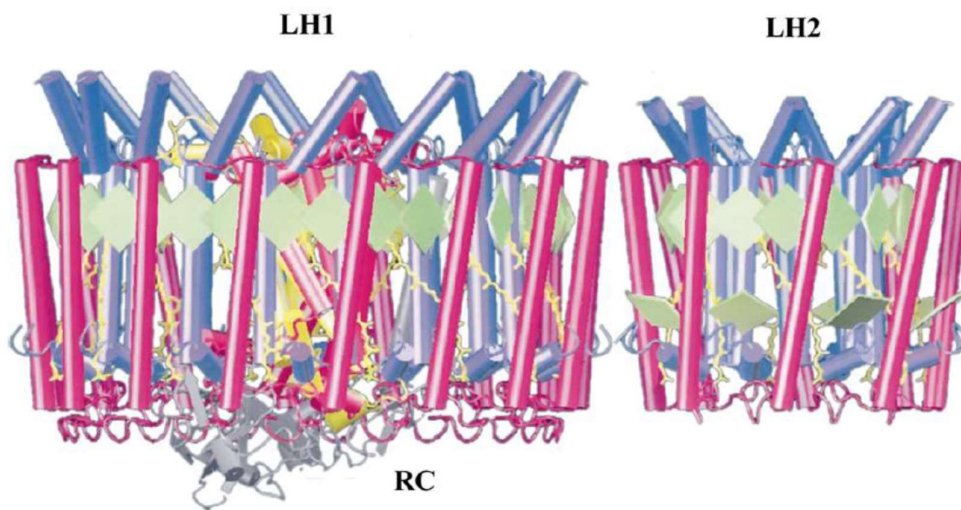


Figure 3-1. Two molecular models for pigment-protein complexes of the photosynthesis unit of the purple bacteria. Chlorophyll is shown as green squares.⁹⁸

These pigment-protein complexes are the photosynthetic reaction centres (RC) and the light harvesting antennae (LH). There are two types of light harvesting antennae; LH-I complex surrounds the RC with a ring of chlorophyll in a protein matrix. The second type is the LH-II complexes, which are on the outside and serve to increase the cross-section for photon absorption by the photosynthesis unit. Overall, chemical energy is being generated by absorption and transfer within the light harvesting antennae complexes, that migrates down from LH-II to LH-I, then into the reaction centre where it can be used to catalyse the conversion of carbon dioxide into oxygen (**Figure 3.2**).^{98,99}

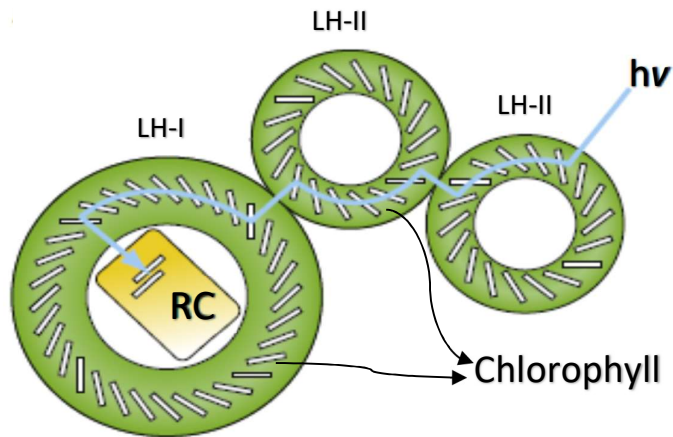


Figure 3-2. Natural light-harvesting system, through absorbing the light by LH-II and the path of transfer to the reaction centre via LH-I.⁹⁵

3.1.1. Multi-Porphyrin Arrays as Model Compound:

Chlorophyll, which is a functionalised porphyrin, plays the key role by capturing the light employed in these systems. This natural phenomenon of photosynthesis has been studied widely and research has focused on capturing and making use of solar energy. Therefore, it is no surprise that a variety of artificial LH antennae systems use porphyrin to mimic the energy transfer process of purple bacteria. The research includes incorporating multi-porphyrin arrays through covalent and non-covalent approaches.^{100–103}

Accordingly, many linear or bridged porphyrins have been reported, as well as three-dimensional system.^{104–107} Lindsey et al. and Gossaure et al. developed a ‘cross’ shaped pentamer and a ring-shaped hexamer respectively.^{108,109} These compounds consisted of a number of porphyrins linking together through covalent chemistry (**Figure 3.3**).

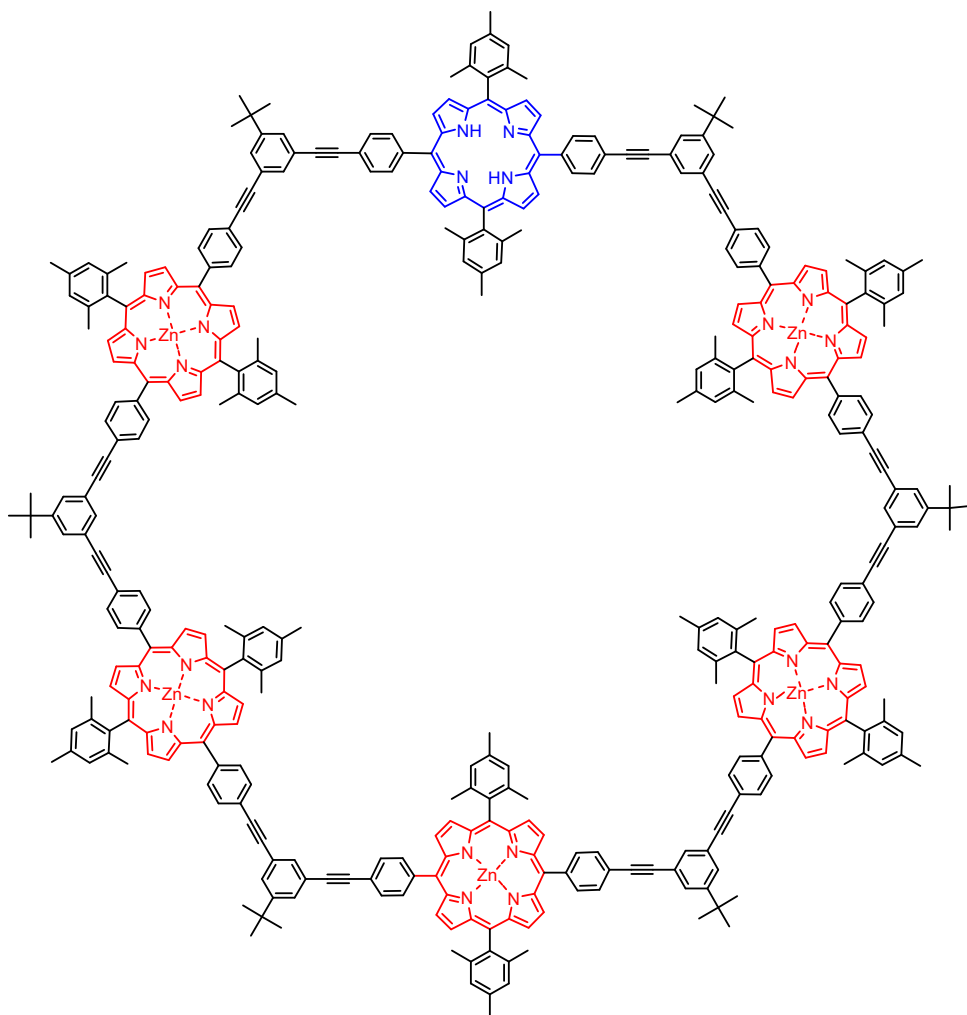


Figure 3-3. Ring-shaped hexamer porphyrin array prepared by Gossaure et al.

The structure of the compounds was ideal for capturing light and transferring the energy through the system. These processes were confirmed by observing an emission from free porphyrin resulting from an excitation of metal functionalised porphyrins. However, increasing the amount of porphyrin that was incorporated limited the ability to capture light.

On the other hand, non-covalent chemistry also has been used to synthesise multi-porphyrin arrays of greater complexity. Kobuke et al. reported a cyclic model of 12 porphyrins self-assembled from six metalloporphyrin dimers.¹¹⁰ These dimers were connected via metal to ligand interactions (**Figure 3.4**).

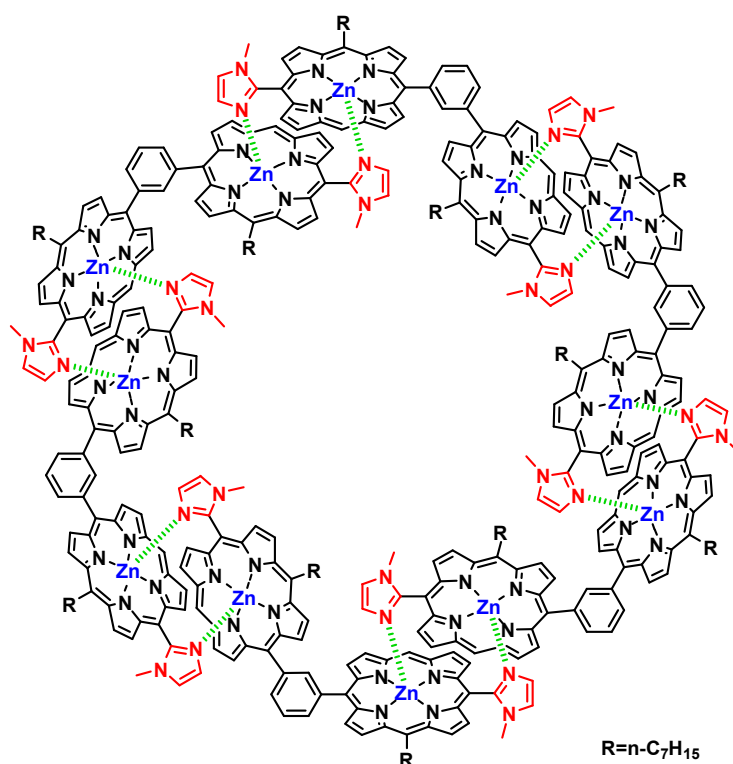


Figure 3-4. Cyclic supramolecular model including 12 porphyrin units which is self-assembled through ligand and metal interaction, prepared by Yoshiaki et al.

Although this represented a significant improvement in the design and synthesis of light harvesting models, no significant, light harvesting was obtained. Alternatively, dendritic polymers, such as dendrimers and hyperbranched polymers, could replace these conventional compounds. The backbone of these macromolecules can be used to mimic that of a protein and act as scaffold to support a number of chromophore units in a controlled structure.

3.1.2. Dendritic Polymers in Light Harvesting Systems:

The potential utilisation of dendritic polymers in many applications has made dendrimers and hyperbranched polymers prominent research subjects for over two decades. The structure of these tree-like macromolecules, possessing several chain ends that all emanate from a focal point, makes them attractive candidates for light-harvesting system. As discussed earlier, the energy transfer process of light-harvesting systems starts with the absorption and the transfer of photons using the chromophores. For example, the peripheral end groups could act as light absorbing chromophores (a) **Figure 3.5**. Chromophore units could also be positioned at (b) the core, (c) in the interior, or (d) within the interior.

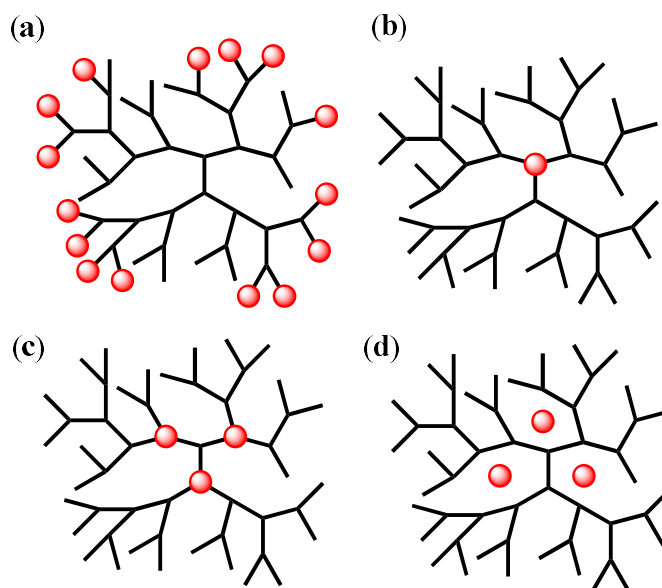


Figure 3-5. Possible position of chromophore unit at dendritic structure: (a) at the periphery, (b) at the core, (c) covalently bound in the interior, (d) encapsulated within the dendritic entity.

Controlling the method of synthesis employed in the preparation of dendrimers results in the symmetrical structure of this macromolecule. This makes it possible to mimic the highly arranged, ring-like structure of natural light harvesting complex, including porphyrin arrays.^{100,111–113} For example, Aida et al. synthesised a porphyrin core using a poly(benzyl ether) dendrimer. They showed that the energy absorbed by the peripheral dendrimer shell was efficiently transferred to the porphyrin at the focal point (**Figure 3.6**).¹¹⁴ The same researchers also developed a similar system incorporating multi-metalloporphyrins, which acted as energy donating units. The

whole system was attached to a porphyrin core which acted as an energy acceptor (**Figure 3.7**).^{115,116} These symmetrical architectures have been shown to exhibit efficient energy transfer. However, these types of macromolecules (dendrimer) are limited by the time-consuming nature of their synthesis.

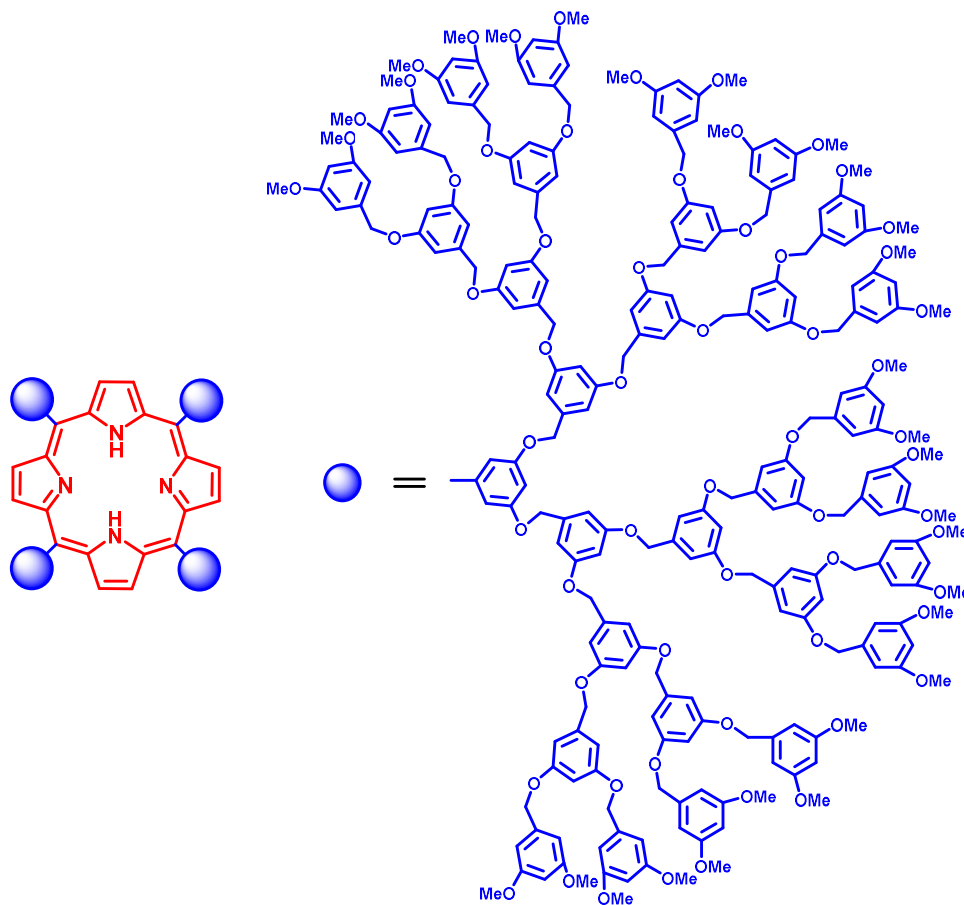


Figure 3-6. Schematic representation of porphyrins encapsulated by poly(benzyl ether) dendrimers.

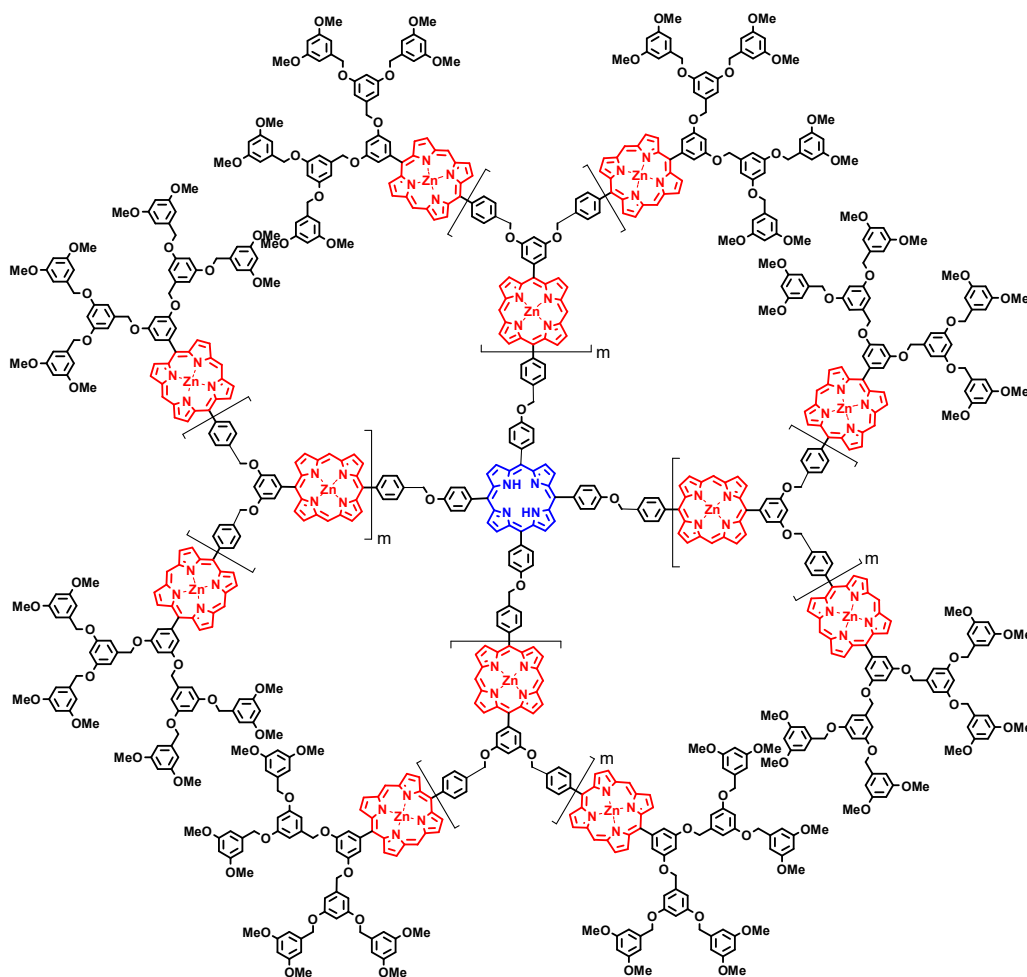


Figure 3-7. Multi-porphyrin dendrimer array containing a number of zinc porphyrins around a free base porphyrin core, where m = generation.

It is not necessarily important to obtain the well-ordered arrangements of porphyrins that are found in purple bacteria. Cyanobacteria and some other plants, exhibit their photosynthetic system via an apparently unsymmetrical porphyrin array.¹¹⁷ Consequently, the exploration of random systems has demonstrated that a highly symmetrical configuration is not necessary. This opens up the pathway for using hyperbranched polymers as light-harvesting porphyrin scaffolds.

Fréchet et al. reported the synthesis of a multi-porphyrin hyperbranched polyether via the ring-opening polymerisation of an $A_2 + B_3$ system (**Figure 3.8**).¹¹⁸ After a 10 day reaction time, the hyperbranched polymer contained up to ten porphyrin units and had a molecular weight around 10 kDa and PDI = 1.9. However, when trying to obtain a

higher molecular weight (>10 kDa) led to high polydispersity (>10). Other disadvantages of this synthesis included the long polymerisation period (of 10 days).

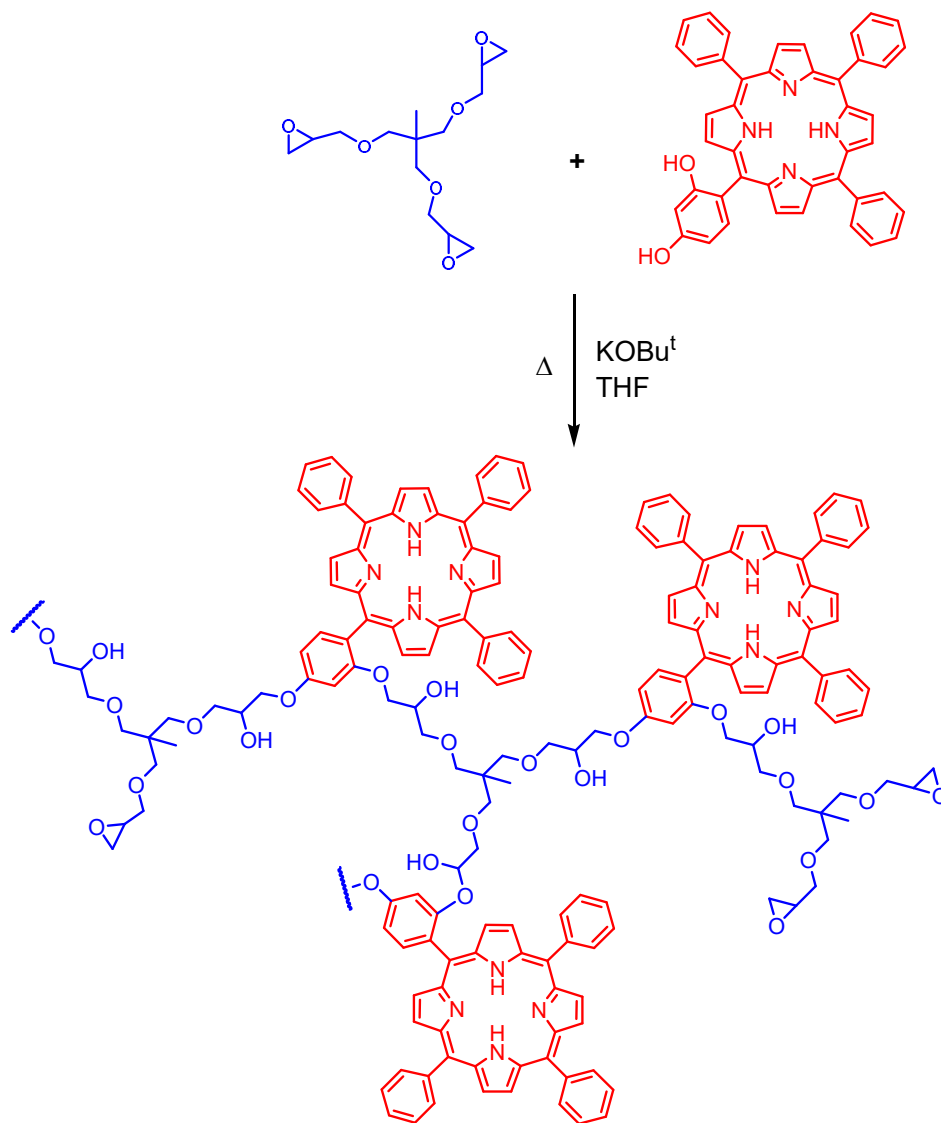


Figure 3-8. Synthesis of multi-porphyrin hyperbranched aliphatic polyether.

The work of Twyman's group generated a HBP containing multi-porphyrin by copolymerising the AB₂ monomer 3,5-diacetoxybenzoic acid, with the A₄ units of 4-tetracarboxyphenyl porphyrin (TCPP), as shown in **Figure 3.9**.⁶² The reaction was complete in 3 hours and the porphyrins were distributed everywhere within the HBP and with a total of 6 internal porphyrins and a molecular weight of 30 kDa with low polydispersity. Extra investigation illustrated a linear relationship between the molecular weight and number of incorporated porphyrins. In addition, metalation of

the porphyrin was conducted via inserting iron and zinc, which did not damage or cleave the HBP. Unfortunately, this HBP did not generate a high yield, reaching ~35%. The remaining products were cross linked species and oligomers. Furthermore, attempts were made to synthesise a polymer with a higher number of porphyrins, by modifying the reaction conditions and increasing the molar ratio of porphyrins, but these were unsuccessful due to increased cross-linking.

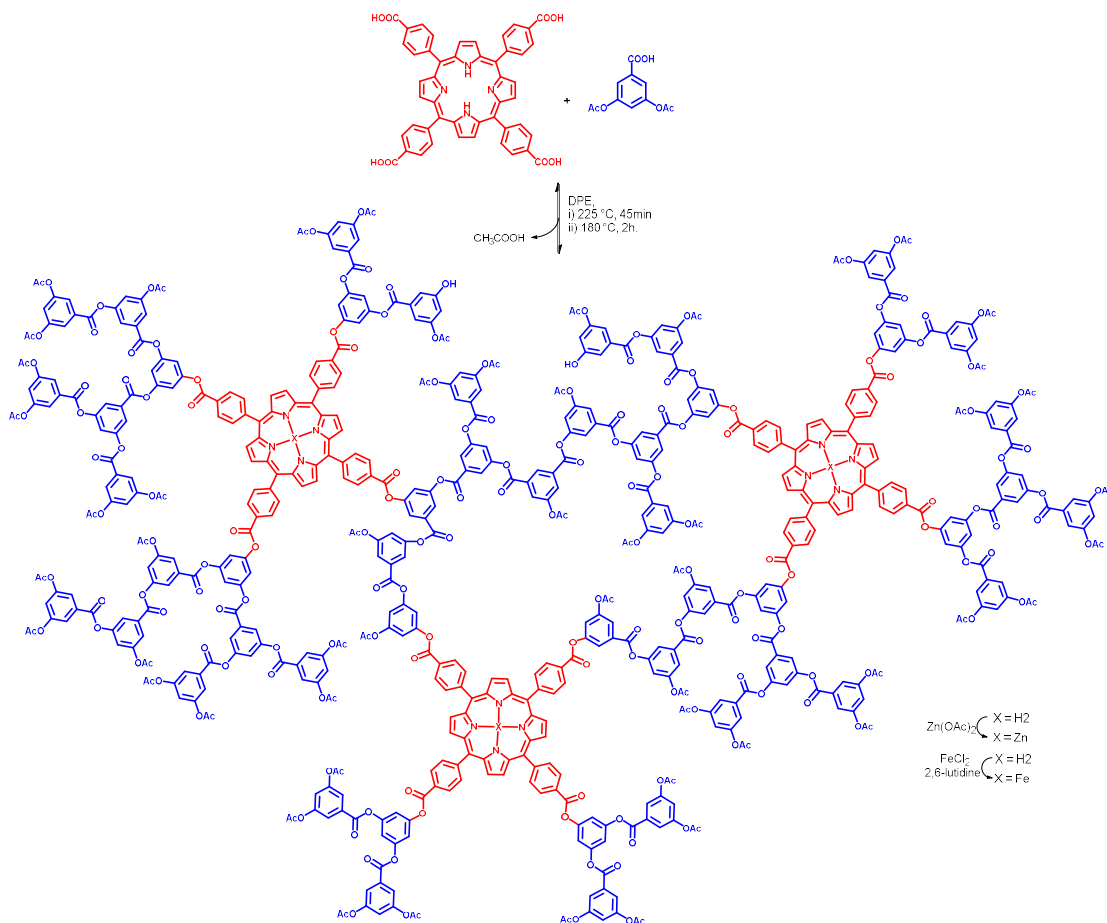


Figure 3-9. Synthesis of multi-porphyrin hyperbranched poly(3,5-diacetoxybenzoic acid).

3.2. Aims:

Although the covalent hyperbranched polymer model devised by Twyman suffers from low yield due to cross-linking, it avoided the drawbacks found in Fréchet's model, such as long reaction time and low molecular weight. Building up artificial light-harvesting systems using hyperbranched polymers as a scaffold requires peripheral multiple donor chromophores and a central acceptor moiety. Unfortunately, the methodologies involved for both syntheses discussed above preclude incorporation of the core molecule. In order to improve this design, the multifunctional porphyrin A_4 units (TCCP) can be replaced with a mono-functional A-unit co-monomer. This co-monomer will be located and attached at the surface of the system, which then acts as an energy-donating unit. Furthermore, combining with another porphyrin co-monomer possessing tetraacetoxy functionalised B_4 units will ensure that the hyperbranched polymer will possess a porphyrin core unit that can act as the energy acceptor unit (Figure 3.10).

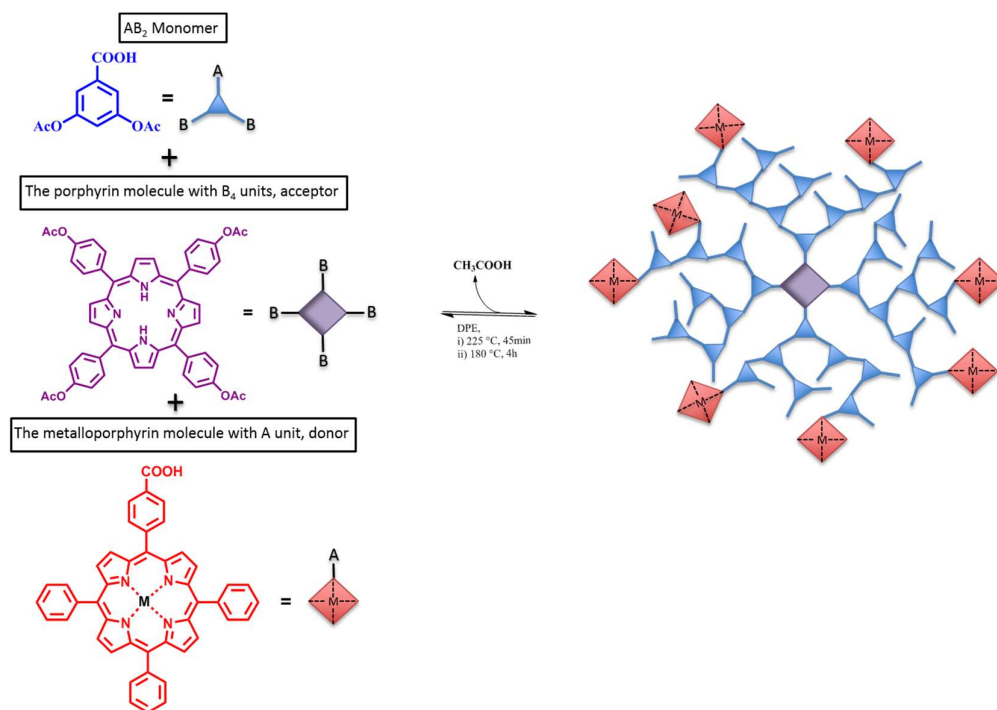


Figure 3-10. Representation of artificial light-harvesting system using covalent chemistry.

However, using covalent bonds means that modifications to the structure will be impossible after synthesis. Therefore, a new macromolecule will need to be made should different acceptors or donors be required. Also, if unexpected errors occur, the final product cannot be corrected without re-synthesising the whole system.

Non-covalent chemistry is an alternative approach that also mimics nature. Twyman et al. has demonstrated the use of non-covalent chemistry to incorporate multiple porphyrin units (porphyrin trimer) around a dendrimer. The dendrimer was used as scaffold, with pyridine groups located at its periphery. These pyridines coordinated metal functionalised porphyrins and generated a self-assembled multi-porphyrin array, as shown in **Figure 3.11**.

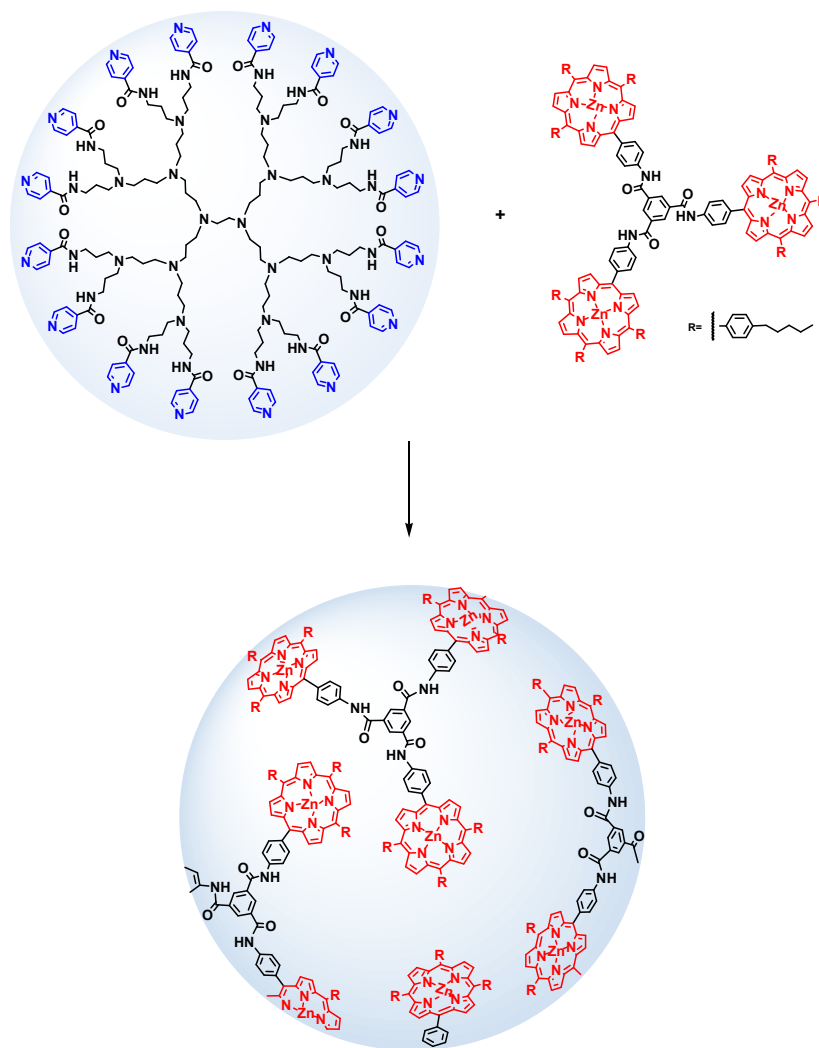


Figure 3-11. Non-covalent attraction between peripheral pyridine dendrimer and porphyrin trimers.

Taking inspiration from this non-covalent approach, the aim would be to synthesise a porphyrin-cored hyperbranched polymer that incorporates pyridine units into its structure. These pyridine molecules then would coordinate with external zinc functionalised porphyrins, which act as donors to a covalently incorporated porphyrin core as the acceptor (**Figure 3.12**).

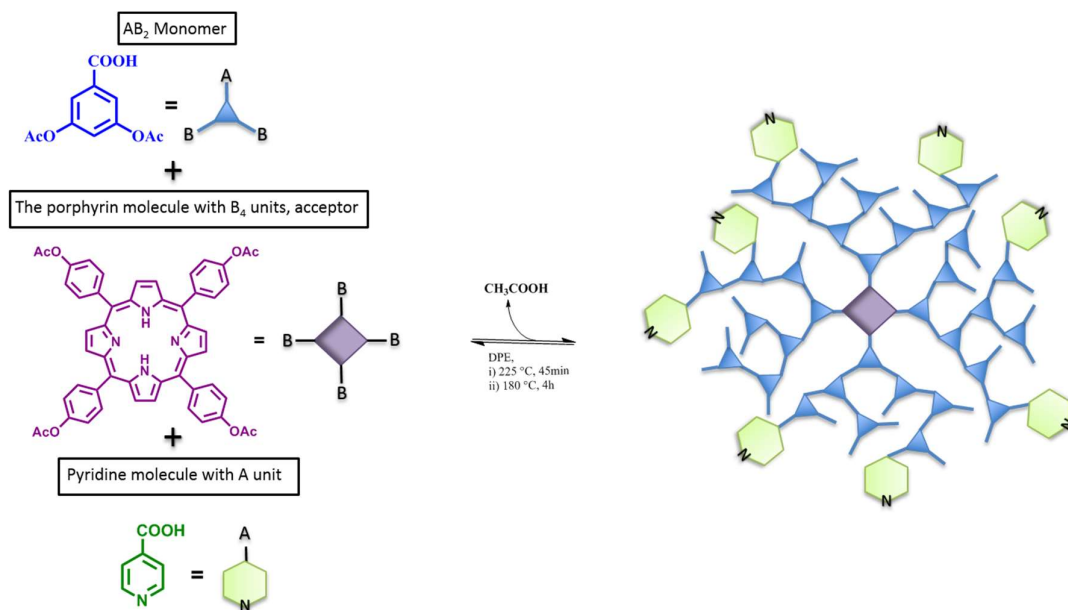


Figure 3-12. Targeted light harvesting system of multi-pyridine containing polymer.

A number of different zinc porphyrin macrocycles can then be used as donor molecules. These include zinc-functionalised porphyrin (ZnTPP) and a flexible zinc-functionalised dimer porphyrin (ZnTPP-ZnTPP). Hence, UV titrations can be used to evaluate the strength of the binding between the external metalloporphyrin and the peripheral pyridine. The value of this binding constant will reflect the feasibility of carrying out light-harvesting tests.

On the other hand, formation of the complex can be supported using NMR titration and diffusion NMR experiments. The ^1H NMR analysis would help to determine the non-covalently bound interaction between porphyrins and pyridine units, as well as help confirm stoichiometry. However, based on the size and structure of the molecules every compound exhibits a different diffusion pattern or spread through the solvent. The diffusion coefficients of the HBP and porphyrins will be determined both individually and as a complex. The diffusion coefficient values will be affected during

successful complexation with HBP. Therefore, determining the diffusion coefficient values will help to confirm that complexation takes place (**Figure 3.13**).

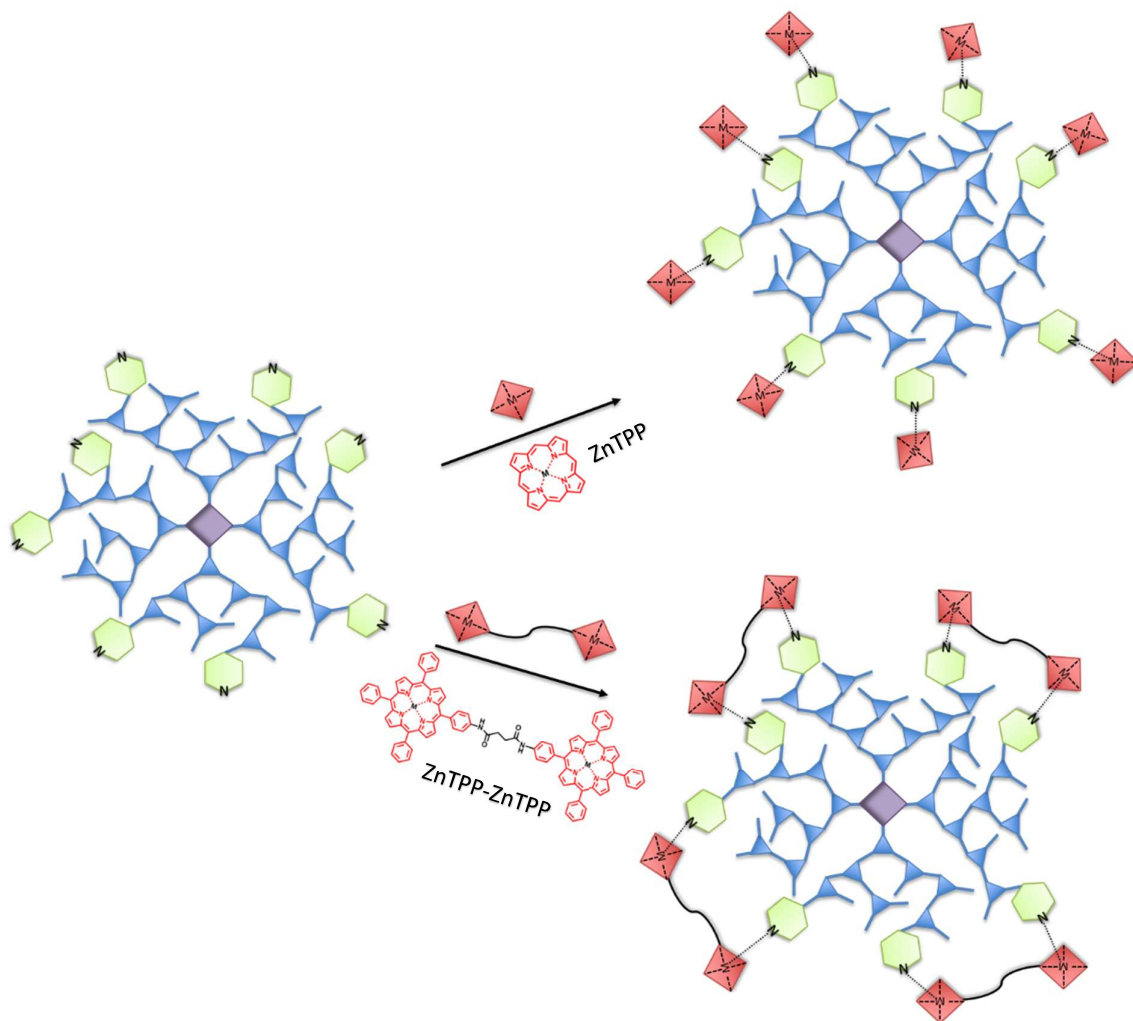


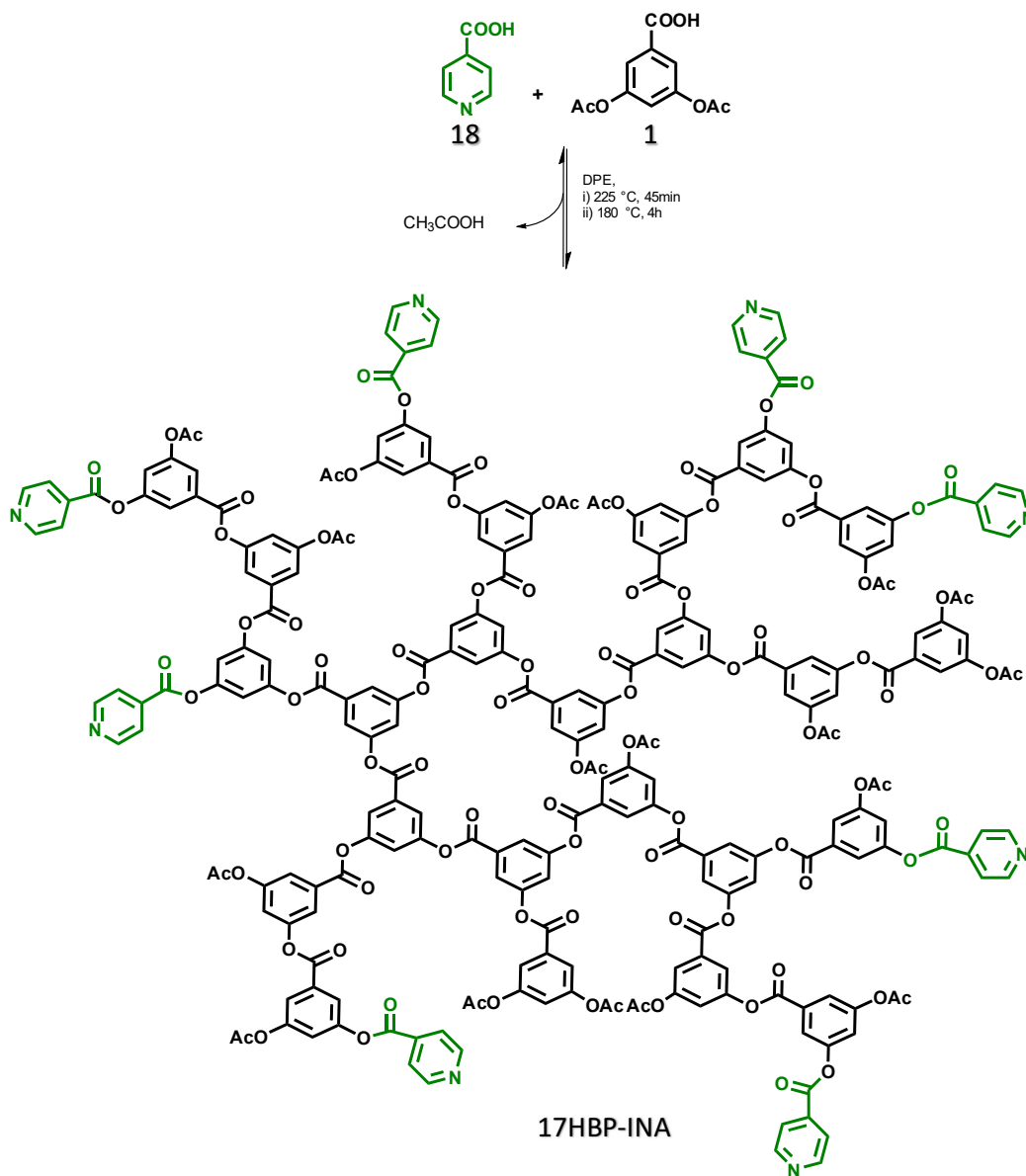
Figure 3-13. Schematic representation of the proposed supramolecular multi-porphyrin hyperbranched arrangement.

3.3. Copolymerisation of 3,5-Diacetoxybenzoic Acid and Isonicotinic Acid, **17HBP-INA**:

Having already developed and synthesised pyridine-cored hyperbranched polymers with multiple peripheral stearic acid functionalities, attention was focused towards a porphyrin-cored hyperbranched polymer system that also possessed multiple pyridyl units within the structure. In order to achieve this goal, isonicotinic acid (INA) was chosen. Porphyrin substituted with four -OAc functionalities, tetra(acetoxyphenyl)porphyrin (TAPP), was also chosen to produce a porphyrin-cored hyperbranched molecule, TAPP-HBP-INA.

However, UV titrations cannot be carried to get an indication of the strength of this non-covalent interaction between the TAPP-HBP-INA and porphyrins. This is because of the porphyrin at the core, which is not involved in the binding, has a Soret band which would prevent the Soret band of ZnTPP or ZnTPP-ZnTPP being visible. Therefore, any shifting in the Soret band during the complexation interaction would not be observed. In order to test our proposal, a simpler model was made without the porphyrin core; the copolymerisation of INA and 3,5-diacetoxybenzoic acid (17HBP-INA) was explored first. This comonomer was used at a 20% of molar ratio to retain the dendritic properties of the polymer (see section 2.1).

Using the general procedure discussed in the previous chapter, the copolymerisation experiment was conducted, as shown in **Scheme 3.1**. The isolated polymer was analysed by ^1H NMR which confirmed incorporation of INA, showing a broad singlet at 8.91 ppm, which corresponded to the pyridines' α H atoms. The β protons could not be seen as a discrete peak due to their presence coinciding with the polymer aromatics' region of 7.70–8.10 ppm. The molecular weight of 17HBP-INA, as obtained by GPC, was 9,000 Da, with a PDI of 1.5. The level of incorporation of INA was identified by integrating the pyridine peak and comparing this to the polymers' aromatic peaks in the ^1H NMR. The level of comonomer incorporation was around 15%, based on the molecular weight and level of incorporation the number of pyridines was estimated as 6-7.



Scheme 3-1. Synthesis of hyperbranched polymer with multiple outer pyridines.

3.4. Complexation of Multiple Zinc-Metalled Porphyrins with Pyridine Ligand containing Hyperbranched Polymer:

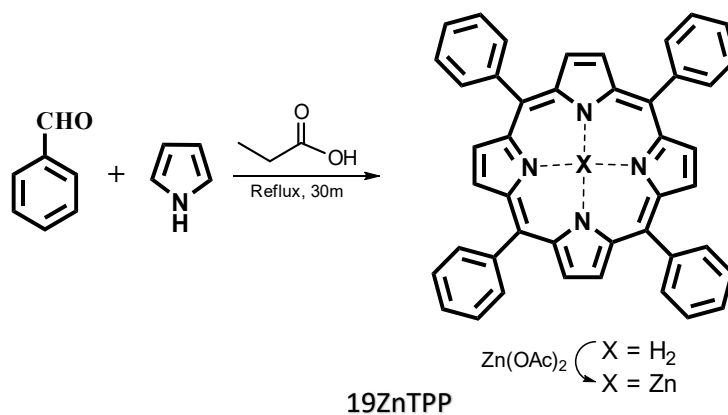
Having obtained a hyperbranched polymer with a number of pyridines (17HBP-INA), the next step was the formation of the self-assembled multiporphyrin system. The self-assembled process was carried out by mixing a solution of 17HBP-INA with a solution of porphyrins (including the monomeric porphyrin [ZnTPP] or dimeric porphyrin [ZnTPP-ZnTPP]). The mixtures were then monitored using three different techniques including UV/Vis spectrophotometry to quantify the binding constant. Also, ^1H NMR and diffusion NMR were used to confirm the complexation stoichiometry. However, metal functionalised porphyrins were synthesised first, as shown in the following.

3.4.1. Synthesis of Metal Functionalised Monomeric Porphyrin (19ZnTPP), and Metal Functionalised Dimeric Porphyrin (20ZnTPP-ZnTPP):

To carry out the self-assembly, the porphyrins needed to be prepared and functionalised with a zinc metal centre. The monomeric porphyrin (TPP) was synthesised by using the same procedure used to synthesise 15TAPP, described in the previous chapter (section 2.4.2); it is shown in **Scheme 3.2**. The yield of the product was 23% and was in the form of a purple solid. The ^1H NMR spectrum confirmed the desired compound was obtained, revealing a characteristic peak at minus (-) 2.76 ppm corresponding to the two internal, highly shielded N-H protons. A multiplet peak was present at 7.78 ppm, corresponding to 12 hydrogens from the phenyl ring (for *meta* and *para* protons), along with resonances attributed to the *ortho* protons, also in the phenyl ring, as doublets at 8.24 ppm. A singlet at 8.87 ppm from the pyrrole hydrogens on the porphyrin was also visible. Other techniques such as UV-Vis spectroscopy provided additional supporting evidence by displaying a Soret band at 417 nm with four weaker Q bands at 514 nm, 548.5 nm, 591 nm and 650 nm. Mass spectrometry showed the predicted value of a molecular ion peak at 615.

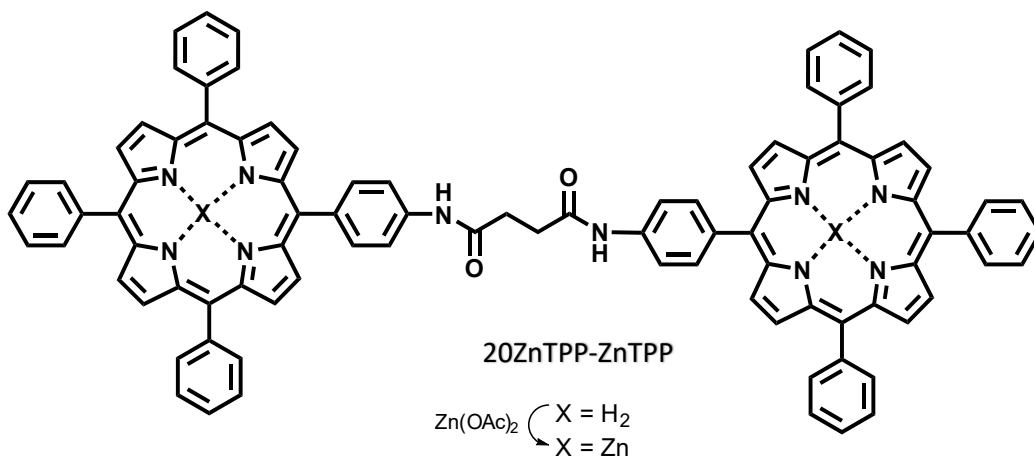
The metal insertion used to prepare 19ZnTPP was conducted in the same fashion as used to create metallate 16ZnTAPP (section 2.4.3) (**Scheme 3.2**). Successful insertion of zinc was confirmed by the ^1H NMR spectrum, which did not contain a proton peak

at minus (-) 2.76 ppm. Further confirmation was provided by UV/Vis spectrometry, in which the four Q bands of the starting material were replaced by two peaks at 547 and 586 nm. Mass spectrometry showed a molecular ion peak at $m/z = 677$, confirming the insertion of zinc.



Scheme 3-2. Synthesis of metal facturalised tetraphenyl porphyrin (19ZnTPP).

To obtain a complex with stronger binding capability, a zinc porphyrin dimer (20ZnTPP-ZnTPP) was provided by Greg Clixby. It was proposed that when one end of the dimer chromophore bound to the scaffold, then the other porphyrin would be more likely to bind, resulting in cooperative and strong binding. Overall, a nitro porphyrin was synthesised initially and then reduced to an amine porphyrin. After that, two equivalents of this amine porphyrin were then coupled with a difunctionalised linker, succinyl chloride, to form the porphyrin dimer (**Scheme 3.3**).



Scheme 3-3. Synthesis of metal facturalised dimer porphyrin (20ZnTPP-ZnTPP).

3.4.2. Binding Study:

A UV/Vis spectrophotometry experiment was conducted (by Greg Clixby) to determine the binding strengths of the porphyrins to the 17HBP-INA copolymer. A copolymer solution of 10^{-3} M concentration was prepared using a stock solution of porphyrins (19ZnTPP and 20ZnTPP-ZnTPP), which were prepared in DCM at a concentration of 10^{-6} M. The copolymer solution was then titrated into a cuvette containing the stock solution (i.e. experiments carried out at constant porphyrin concentration). The Soret band was observed to shift from 418 nm to 425 nm. Binding constants for the monomeric porphyrin (19ZnTPP) and dimeric porphyrin (20ZnTPP-ZnTPP) with copolymer (17HBP-INA) were obtained by plotting the variation of the bound peak in absorption as the concentration of pyridine increased. Fitting the data to a 1:1 binding analysis using GraphPad, allows the binding constants to be calculated (**Figure 3.14**).

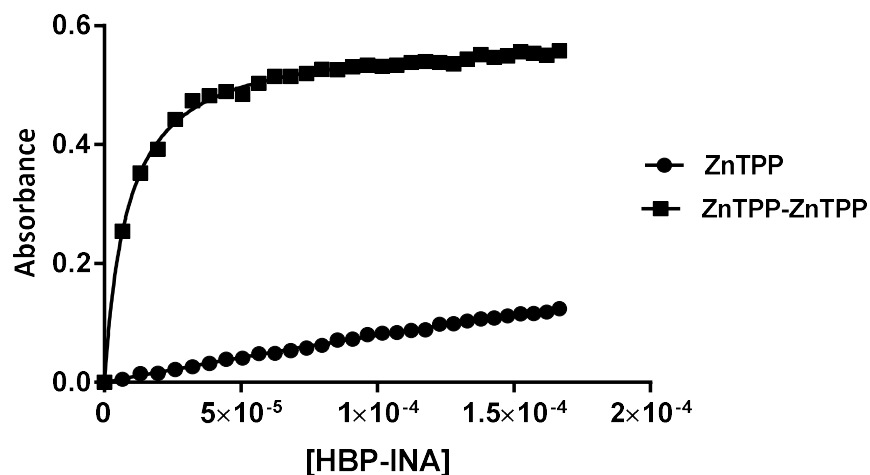


Figure 3-14. UV/Vis titration, HBP-INA concentration vs. absorbance of 13ZnTPP and 14ZnTPP-ZnTPP.

The interaction between the metalloporphyrins and pyridine ligands within the 17HBP-INA copolymer was much stronger for the dimeric porphyrin than the monomeric porphyrin. Therefore, one of the project's objectives was achieved by demonstrating that the binding constant increased to $1 \times 10^5 \text{ M}^{-1}$ for the dimer, 20ZnTPP-ZnTPP, compared to $1 \times 10^3 \text{ M}^{-1}$ for the monomer, 19ZnTPP. The results of this investigation demonstrated a proof of principle for this non-covalent self-assembled system. However, further conformation to support the UV study and to prove complexation and stoichiometry is also required.

3.4.3. Proof of Stoichiometry and Availability:

In the previous section UV/Vis spectra showed that the dimer porphyrin, 20ZnTPP-ZnTPP, had a 100-times better binding constant with a pyridyl unit contained on 17HBP-INA than 19ZnTPP. In this section, ^1H NMR titration was employed to provide further evidence that non-covalent chemistry was occurring between the metal functionalised porphyrins and 17HBP-INA. This was conducted also to confirm the stoichiometry by adding known concentrations of metalloporphyrins into known concentration of 17HBP-INA, verifying that 6-7 pyridine units existed (on the copolymer's 17HBP-INA periphery). Upon this mixing, complexation could be observed until saturation, at which point all available pyridines would be bound.

^1H NMR titration was conducted first between 17HBP-INA and 19ZnTPP. A solution of 17HBP-INA was prepared at a concentration of 1.4×10^{-3} M (1.12×10^{-6} mol) then placed in the NMR tube (7.84×10^{-6} mol due to 7 units of pyridine are existed around the copolymer). Another solution of 19ZnTPP was prepared with a concentration of 1.12×10^{-2} M. 0.1 mL of 19ZnTPP solution (1.12×10^{-6} mol) was then added to the NMR tube and the ^1H NMR spectrum obtained. The α and β protons of isonicotinic acid were observed to have shifted upfield (**Figure 3.15**). This process of adding 0.1 mL of porphyrin solution, followed by recording the ^1H NMR spectrum and observing the α and β shifts was repeated.

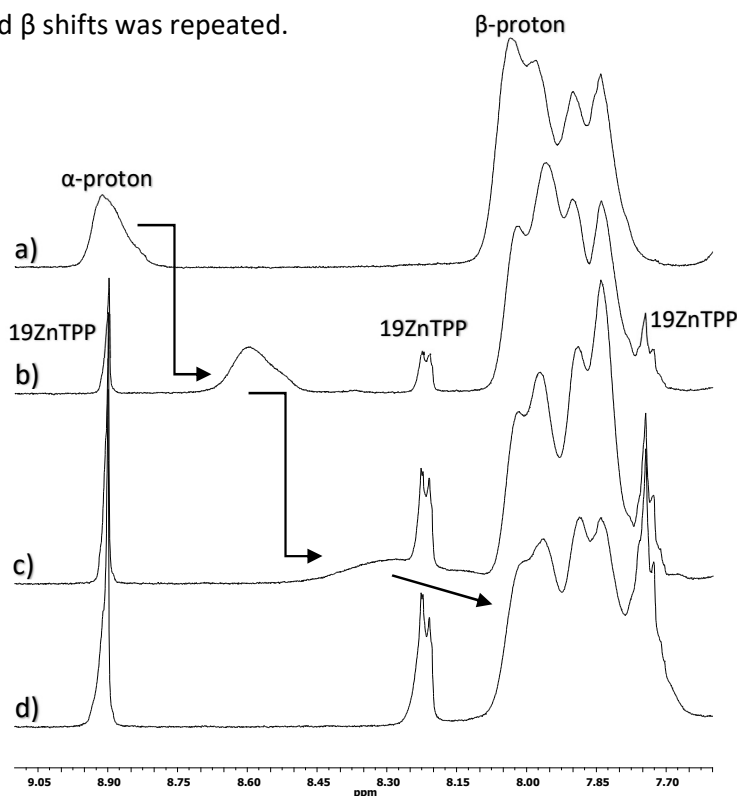


Figure 3-15. ^1H NMR titration of 17HBP-INA and 19ZnTPP. (a) ^1H NMR spectrum of the polymer with no addition of ZnTPP (b) alpha proton peak shift after addition 50 μL of ZnTPP (5.6×10^{-7} mol). (c) alpha proton peak merged with ZnTPP peak after addition 100 μL of ZnTPP (1.12×10^{-6} mol). (d) complete merging with polymer aromatics region after addition 150 μL of ZnTPP (1.68×10^{-6} mol).

Based on ^1H NMR titration spectra, the shift ($\Delta\delta$ -ppm) of the pyridyl α proton (from 8.92 ppm) was plotted against the number of equivalents of porphyrins added (**Figure 3.16**). The number of ZnTPP complexed to the copolymer was then estimated using the inflection point, which was around 7 ZnTPP per copolymer. This fits in well with total number of pyridines estimated by ^1H NMR. This gives us confidence that all of the pyridines have been complexed with ZnTPP unit, as shown in **Figure 3.17**. Considering this, pyridines are available and accessible for binding, which means they are relatively close to the surface.

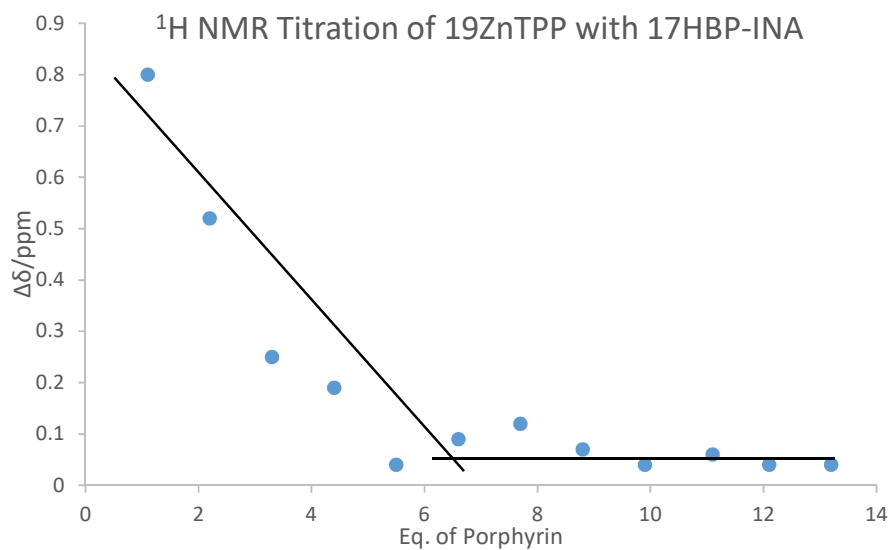


Figure 3-16. Plot of added ZnTPP vs change in shift. The stoichiometry of 19ZnTPP to 17HBP-INA was estimated from the onset of saturation.

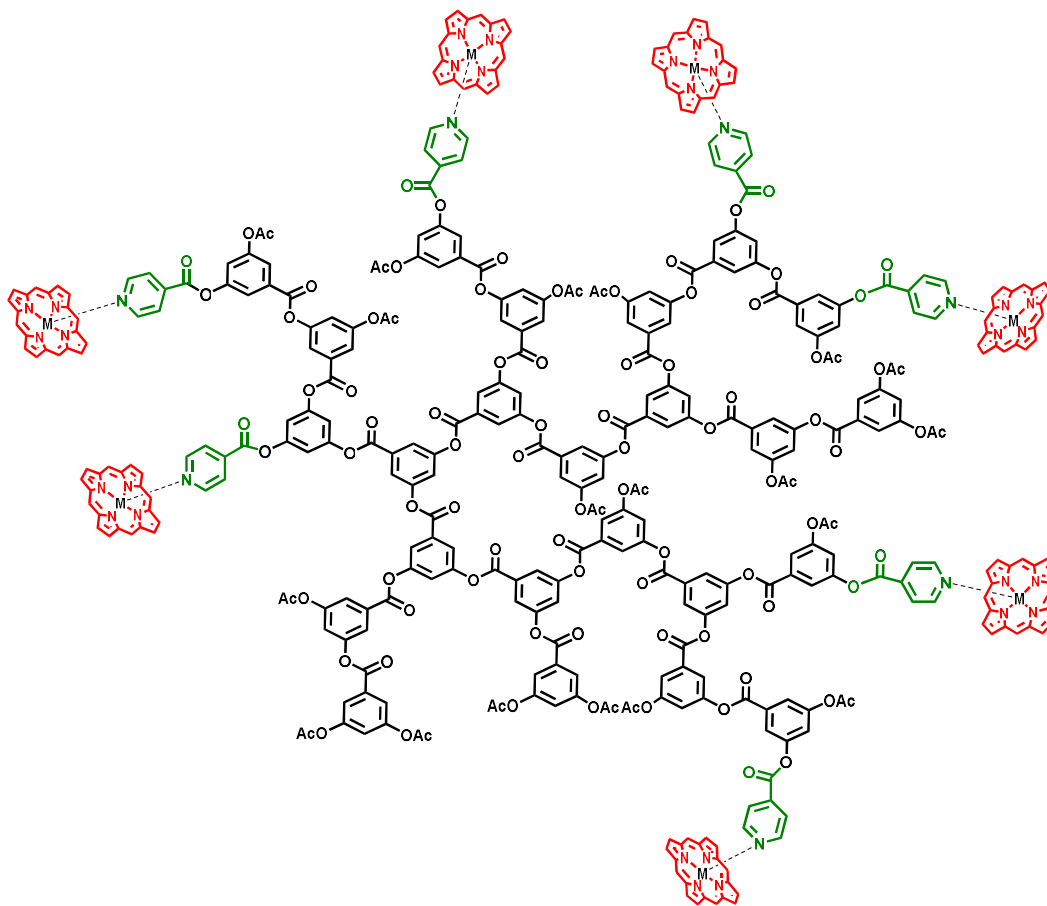


Figure 3-17. Representation of structure of 17HBP-INA complexed with 19ZnTPP.

The same experiment was repeated using the 17HBP-INA and the zinc functionalised porphyrin dimer, 20ZnTPP-ZnTPP. Due to each molecule having two porphyrins, the dimer porphyrin solution was prepared using half the concentration (5.6×10^{-3} M). Upon addition of the first 0.1 mL (5.6×10^{-7} mol) of dimeric porphyrin (20ZnTPP-ZnTPP), the peak corresponding to the α and β protons of isonicotinic acid were very broad and hard to see. When more aliquots were added, the peaks could no longer be seen as they moved under the polymer peak (**Figure 3.18**).

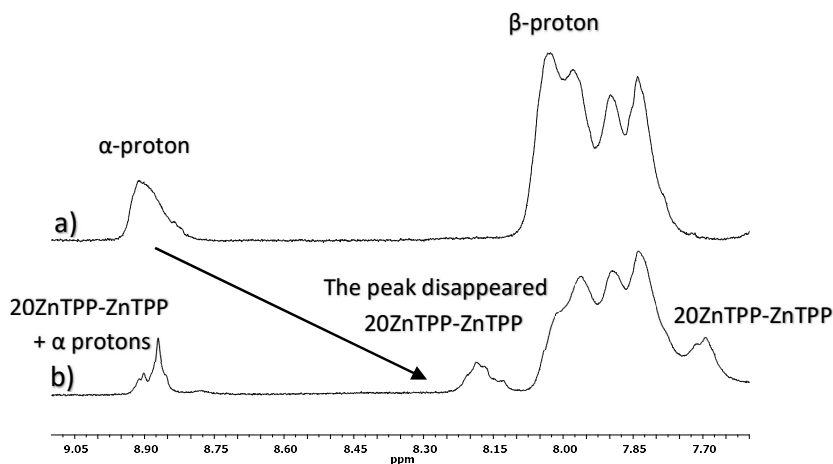


Figure 3-18. ^1H NMR titration of 17HBP-INA and 20ZnTPP-ZnTPP. (a) ^1H NMR spectrum of the polymer with no addition of ZnTPP-ZnTPP (b) No alpha proton peak is visible after the addition of 100 μL of ZnTPP-ZnTPP (5.6×10^{-7} mol).

Due to the strong binding, ^1H NMR could not be used, as it required relatively high concentrations of ligand and porphyrin. Therefore, in an effort to prove the stoichiometry of this complexation, a UV titration was employed (by Greg Clixby). We have previously used this method to determine the stoichiometry of a self-assembled porphyrin/dendrimer system.¹¹⁹ UV analysis was conducted by titrating 20ZnTPP-ZnTPP into 17HBP-INA, in 1 M aliquots of porphyrin and observing the shift in the porphyrin Q bands. Absorption of Soret band was very high so it was easier to follow the weaker Q band at 551 nm. The increase in bound peak vs porphyrin concentration, as well as the decrease in the free peak vs porphyrin concentration was plotted (**Figure 3.19**).

20ZnTPP-ZnTPP titrations into 17HBP-INA

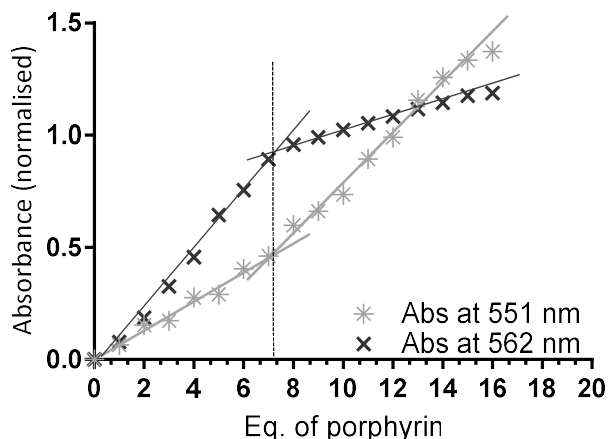


Figure 3-19. Titration plots of dimer (20ZnTPP-ZnTPP) added to 17HBP-INA (following the absorbance for bound porphyrin at 562 nm and free porphyrin at 551 nm).

Both plots in Figure 3.19 demonstrate a change occurring around 7 porphyrins, which indicate there are about 7 pyridines in the copolymer. This equals our previous NMR integration result and the NMR study using the monomeric porphyrin. Overall, we are satisfied that the copolymer has an average of 7 pyridines, as shown in **Figure 3.20**.

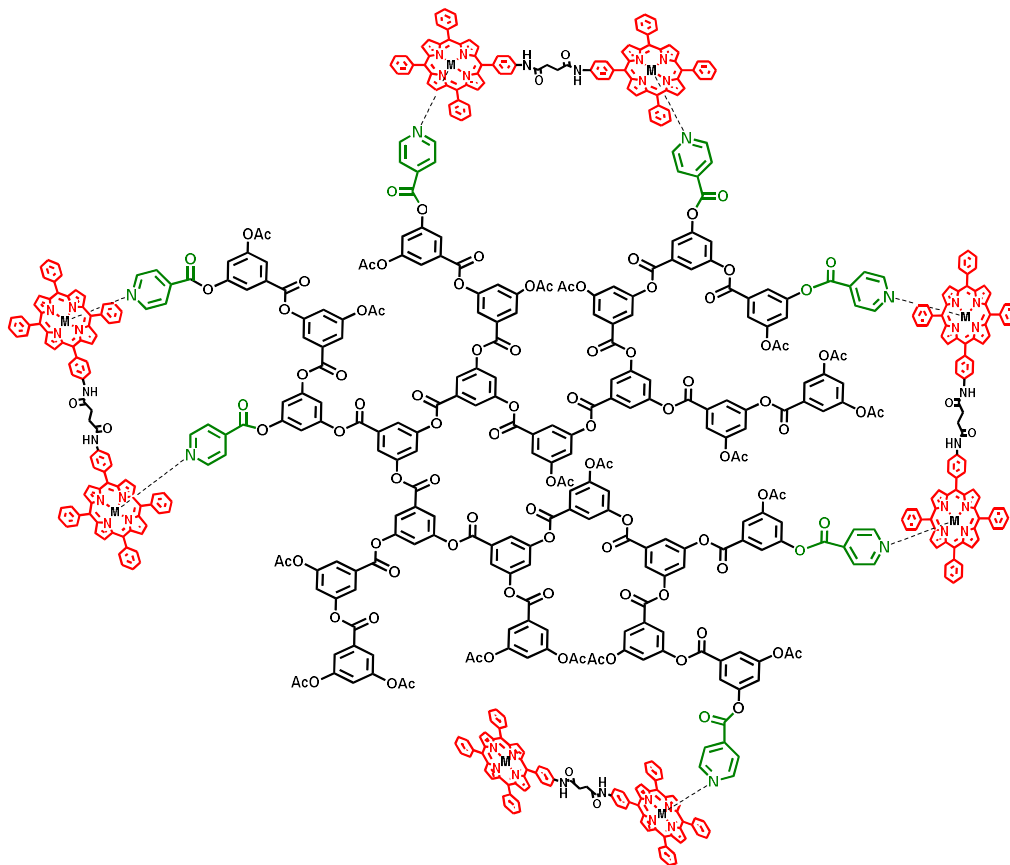


Figure 3-20. Representation of structure of 17HBP-INA complexed with 20ZnTPP-ZnTPP.

3.4.4. Proof of Self Assembled System:

Based on the size and structure of molecules, every compound exhibits a different diffusion rate in solution. We aimed to determine the diffusion coefficients of 17HBP-INA and porphyrins (including 19ZnTPP and 20ZnTPP-ZnTPP) individually then as a complex to show that a self-assembled system had formed, specifically, by looking for changes in the diffusion rate of the copolymer before and after adding the porphyrins. Adding the porphyrins to 17HBP-INA with certain molar equivalents of then analysing the results would help to observe increases and decreases in the diffusion coefficient values.

The diffusion study was conducted (by Greg Clixby), first between 17HBP-INA and 19ZnTPP. A solution of 17HBP-INA was prepared at a concentration of 1×10^{-2} M; the diffusion coefficient was recorded as $3.524 \times 10^{-9} \text{ m}^2\text{s}^{-1}$. Whereas, the diffusion coefficient of 19ZnTPP (4×10^{-1} M) was $5.284 \times 10^{-9} \text{ m}^2\text{s}^{-1}$. The 19ZnTPP demonstrates a 1.5-fold higher diffusion rate than the 17HBP-INA. However, once 1:1 equivalent of the 19ZnTPP with 17HBP-INA was mixed, the diffusion values decreased to be similar for both molecules (**Table 3.1**). This occurred as a consequence of the monomeric porphyrin becoming part of the polymer and at the same time, the size of the copolymer got bigger, which led both molecules to diffuse more slowly.

Equivalent of		Diffusion coefficient D ($\times 10^{-9} \text{ m}^2\text{s}^{-1}$)	
17HBP-INA	19ZnTPP	17HBP-INA	19ZnTPP
1	0	3.524	-
1	1	2.576	2.786
0	1	-	5.284

Table 3-1. Diffusion coefficient data of 17HBP-INA and 19ZnTPP individually, and in complex.

The 20ZnTPP-ZnTPP solution was prepared with a half concentration of 2×10^{-1} M. The experiment determined that 20ZnTPP-ZnTPP has a diffusion coefficient of $0.555 \times 10^{-9} \text{ m}^2\text{s}^{-1}$. However, a search of the literature indicates that the dimer tends to aggregate.¹²⁰ In order to investigate this, DLS was conducted for the dimer porphyrin and 17HBP-INA. Dynamic Light Scattering (DLS) is a technique classically used for measuring the size of particles typically in the submicron region, dispersed in a liquid. The basic principle of this machine is: the sample is illuminated by a laser beam and the fluctuations of the scattered light are detected at a known scattering angle by a fast photon detector. DLS analysis confirmed the aggregation of the dimer, showing its size to be $495.5 (\pm 59.8)$ nm, whereas it was $14.5 (\pm 1.5)$ nm for the copolymer (**Figure 3.21**).

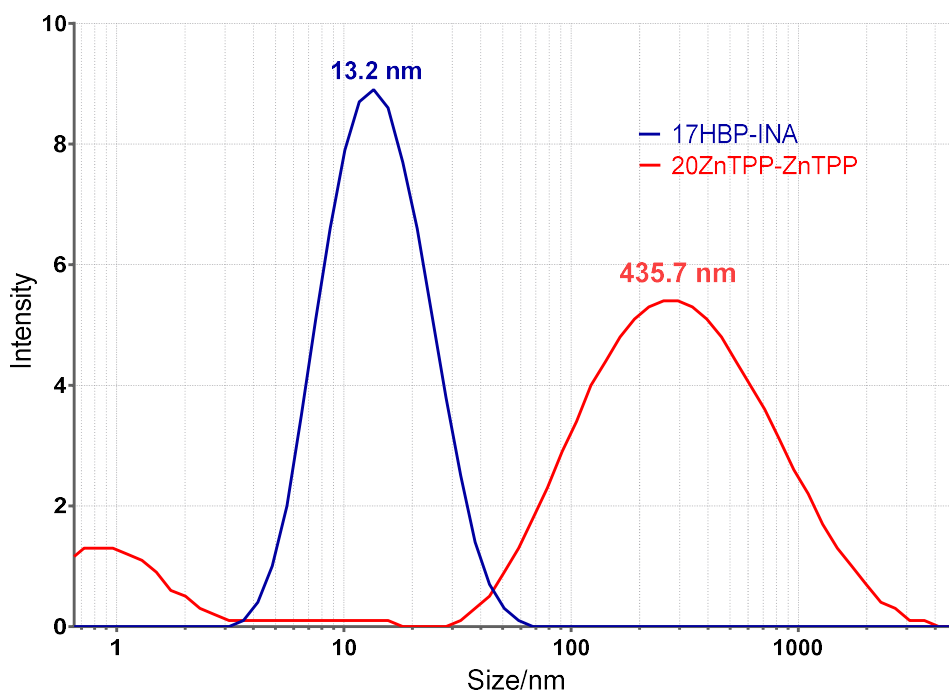


Figure 3-21. Size of hyperbranched polymer and porphyrin dimer, obtained from DLS experiments.

Aggregation of the dimer was broken up upon addition of dimeric porphyrin (0.2 equivalent) into excess of the copolymer (1 equivalent). The diffusion coefficients of the dimer increased to $3.090 \times 10^{-9} \text{ m}^2\text{s}^{-1}$ and decreased for the polymer to $3.126 \times 10^{-9} \text{ m}^2\text{s}^{-1}$. Adding more (0.6 equivalent) of the dimer, which is just below the saturation, the diffusion rate was approximately the same compared to that of the copolymer (**Table 3.2**). However, reaching 1:1 and 1:1.5 equivalents, there was a significant drop

in the diffusion values, which may suggest cross-linking has formed between the copolymers (**Figure 3.23**).

Equivalent of		Diffusion coefficient D ($\times 10^{-9} \text{m}^2\text{s}^{-1}$)	
17HBP-INA	20ZnTPP-ZnTPP	17HBP-INA	20ZnTPP-ZnTPP
1	0	3.524	-
1	0.2	3.126	3.090
1	0.6	3.027	3.020
1	1	0.360	0.384
1	1.5	0.128	0.135
0	1	-	0.555

Table 3-2. Diffusion coefficient data of 17HBP-INA and 20ZnTPP-ZnTPP individually, and as complex with different equivalents.

The DLS analysis confirmed cross-linking had formed in high concentration of dimer between the copolymers by showing the size as 43.7 (± 6.5) nm. While, 13.2 (± 1.4) nm was the size of the copolymer and the dimer with 1:0.6 ratio, which demonstrated no change compare to the polymer on its own as 14.5 (± 1.5) nm (**Figure 3.22**).

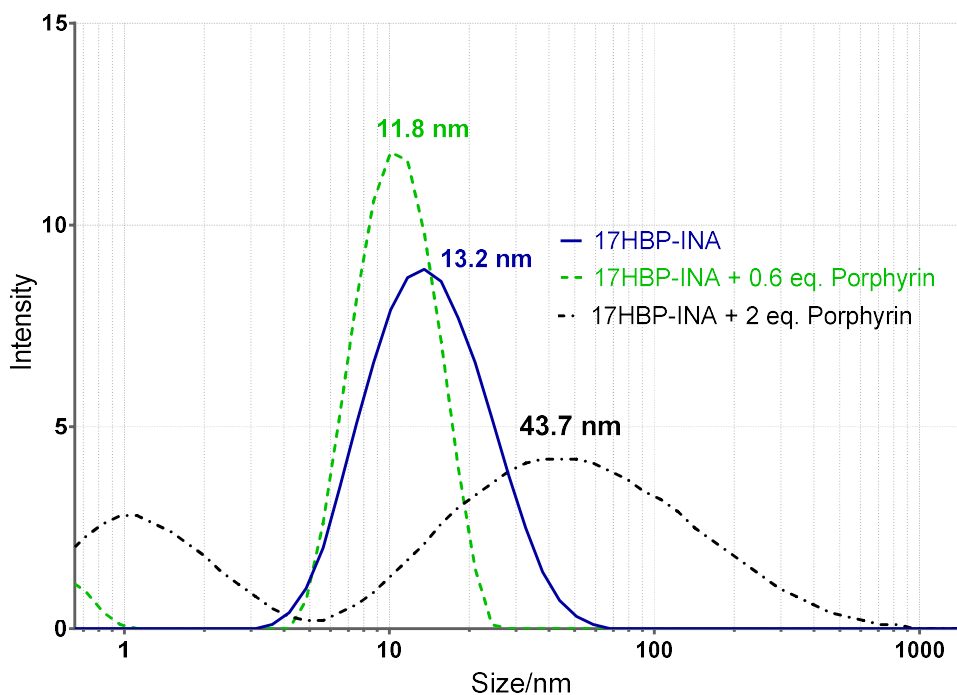


Figure 3-22. Size of hyperbranched polymer, porphyrin dimer, and different ratio of porphyrin to polymer obtained from DLS experiments.

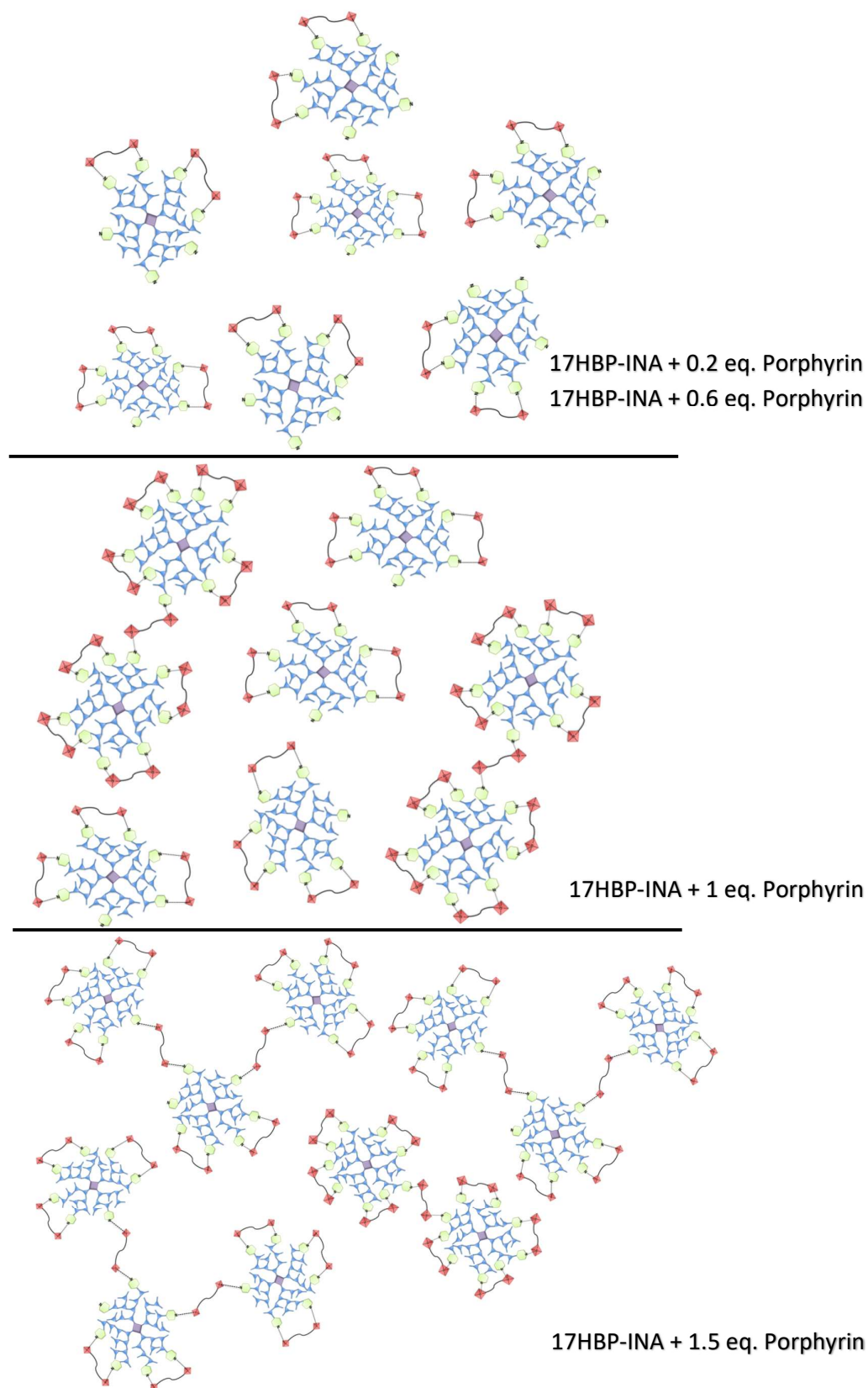


Figure 3-23. Representation of structure of cross-linking hyperbranched polymers (17HBP-INA), and complexation with dimer porphyrins (20ZnTPP-ZnTPP).

3.5. Copolymerisation of 3,5-diacetoxybenzoic acid with Isonicotinic Acid (INA) and Tetraacetoxyphenyl Porphyrin (TAPP); **21TAPP-HBP-INA**:

After proving that a hyperbranched copolymer (17HBP-INA) could be used as scaffold to support a number of porphyrins through non-covalent chemistry, attention was turned to the synthesis of a porphyrin-cored hyperbranched copolymer system (21TAPP-HBP-INA). The specific design would include the ability to bind multiple porphyrins via internal pyridyl units, but also to possess a porphyrin core. This design should allow light harvesting to occur between the complexed, terminal zinc porphyrins and the central porphyrin core. The design is shown schematically in **Figure 3.24**.

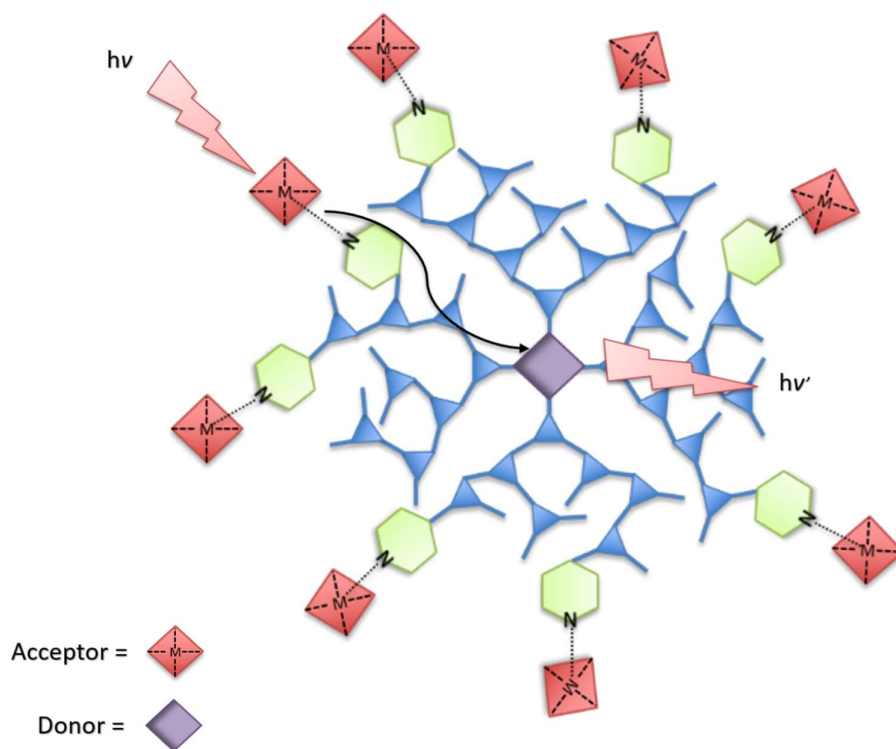
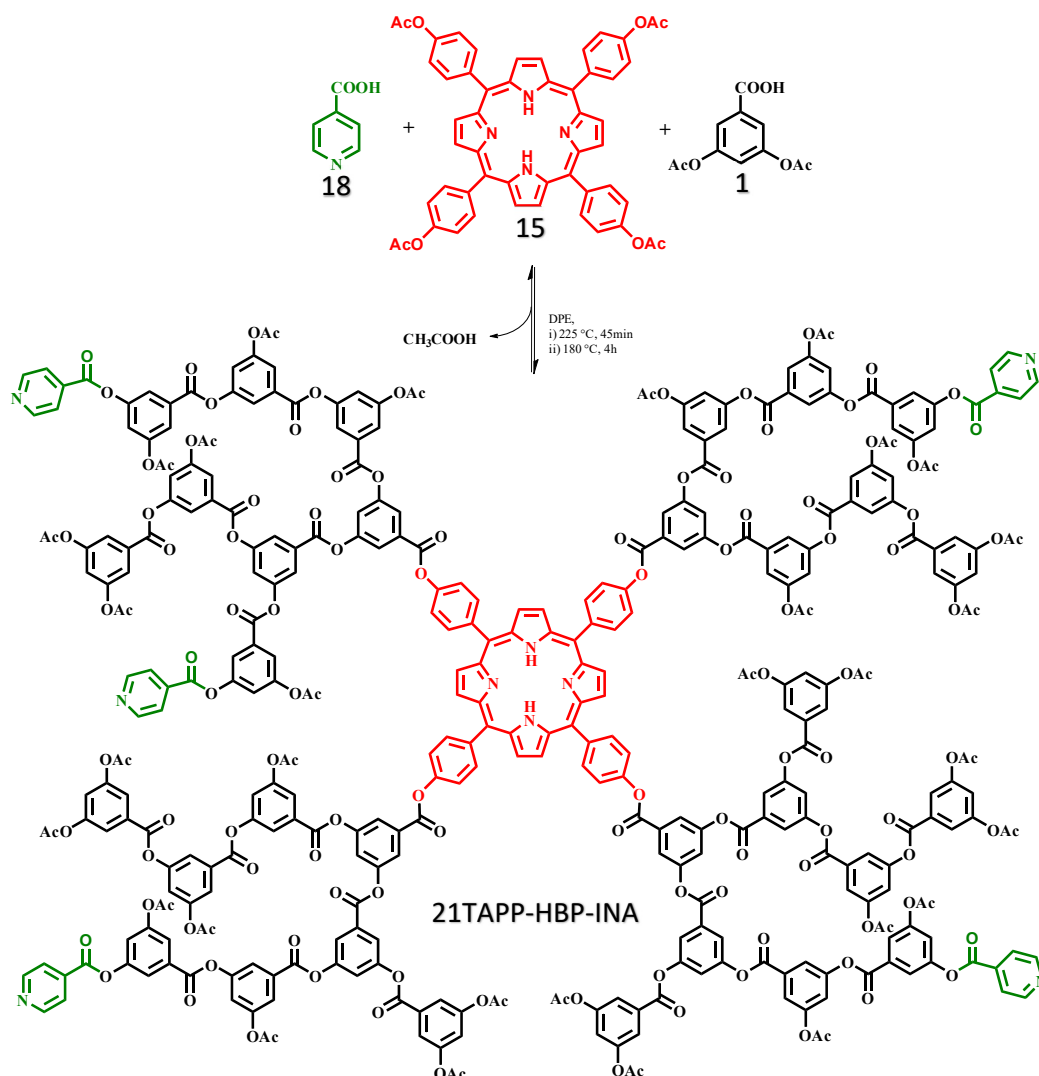


Figure 3-24. Simplified model of a light harvesting system.

3,5-Diacetoxybenzoic acid **1** was copolymerised with 20% INA **18** and 2.5% of TAPP **15** using the same polymerisation procedure developed and described in section 2.3.2; the process is shown schematically in **Scheme 3.4**. ^1H NMR confirmed that both porphyrin and INA were incorporated into the polymer by showing characteristic resonances for each molecule. However, in terms of porphyrin, the ^1H NMR results showed coincident sharp and broad resonances due to a mixture of 'free' and incorporated porphyrins (**Figure 3.25**).



Scheme 3-4. Synthesis of porphyrin cored hyperbranched polymer system incorporating with multiple pyridyl units.

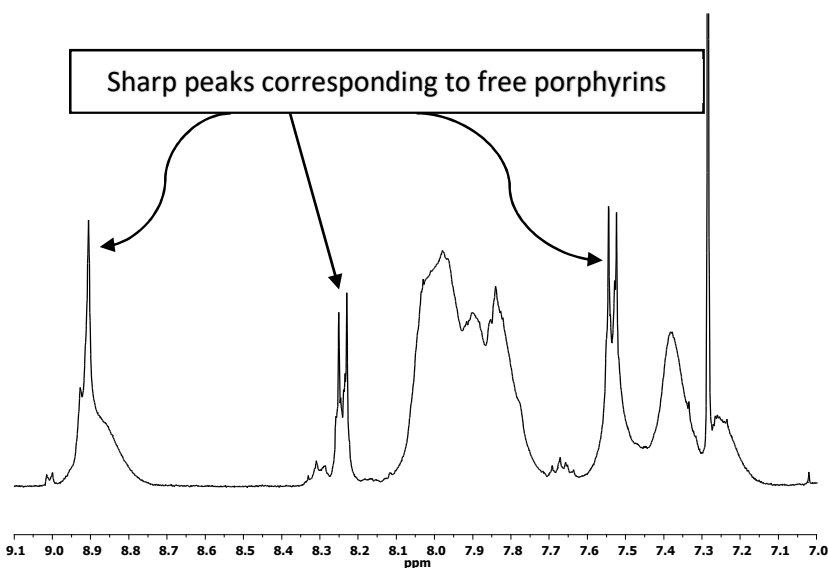


Figure 3-25. ^1H NMR of porphyrin cored hyperbranched polymer system before extra purification.

Unfortunately, these free porphyrins could not be separated using the conventional procedure. Therefore, size exclusion chromatography in the form of a Biobead column was used to separate the free porphyrin from the rest of the polymer mixture. Isolated solid provides an early indication of the presence of incorporated porphyrin from the copolymer colour. Subsequent analysis confirmed removal of free porphyrin as the sharp peaks corresponding to unincorporated porphyrin, were no longer present in the ^1H NMR. The UV/Vis spectrum supported the conclusion that porphyrin had been incorporated; the molecular weight of the 21TAPP-HBP-INA was assigned by GPC as 8,500 Da, with a PD of 2.1. The level of comonomer incorporation and loading were determined using ^1H NMR integration and found to be around 10%, which is estimated to be around 5 pyridine units.

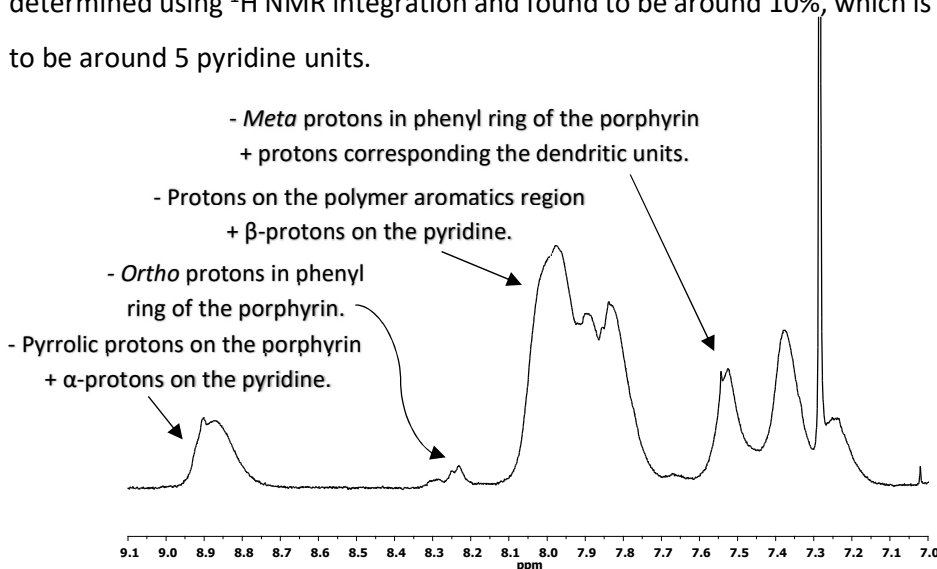


Figure 3-26. ^1H NMR of porphyrin cored hyperbranched polymer system after extra purification, using Biobead column.

3.6. Conclusion:

At the outset of the project, the aim was to use the hyperbranched polymer as a scaffold to support multi-porphyrin arrays. This was achieved by synthesising a hyperbranched copolymer that had pyridine units within its structure. The methodology presents an excellent method for assembling porphyrins around a globular structure. Specifically, hyperbranched copolymer was synthesised successfully with 7 pyridyl units at the peripheral of the 17HBP-INA structure. Two types of porphyrins (monomeric and dimeric) were synthesised and complexed with the HBP. UV/Vis spectrophotometry was used to determine the binding constants of $1 \times 10^3 \text{ M}^{-1}$ and of $1 \times 10^5 \text{ M}^{-1}$ for the monomeric and dimeric porphyrins respectively.

The average number of pyridine moieties existing with the copolymer was confirmed through stoichiometry measurements using ^1H NMR and UV titration. The data from these experiments conclude that all of the pyridine units within the copolymer are relatively in an equivalent environment and available for binding (i.e. fit in well with total number of pyridines estimated by ^1H NMR).

Formation of the self-assembly between the copolymer and the porphyrins was confirmed by diffusion NMR. The diffusion coefficients of both monomeric porphyrin and copolymer decreased to be almost the same when mixed at a 1:1 equivalent. Whereas, due to the aggregation of dimeric porphyrin, the finding of which was supported by DLS analysis, showed very slow diffusion. Upon addition of certain equivalent (0.2 and 0.6) of dimeric porphyrin into the copolymer (1 eq.), the diffusion difference reduced from 6-fold to be exactly the same diffusion for both. However, combining an excess of the dimer with the copolymer led to cross-linking, resulting in dimers or/and trimers bridging the porphyrin between the copolymers. DLS analysis provided further support that this cross-linking has taken place, showing a size of 43.7 (± 6.5) nm, compared to 13.2 (± 1.4) nm of 1 eq.:0.6 eq. of copolymer with dimer. In this respect, the molecule's structure is similar to the unsymmetrical light harvesting systems that exist in nature.

This project also reports a facile, single-step approach towards the construction of a porphyrin-cored hyperbranched polymer containing multiple pyridine residues. As such, this system possessed both donor and acceptor units and could perform light harvesting. Alternatively, phthalocyanine macrocycle could be introduced as the core acceptor chromophore, which would emit light at a longer wavelength and therefore expand the future work research. Work could be continued also to construct similar system with increased binding affinity for the terminal porphyrins (i.e. trimeric porphyrin). In addition, the methodology described above may be extended to a number of applications.

Chapter 4

4. Experimental Details:

4.1. General experimental Conditions:

4.1.1. Chemicals and Instruments:

All starting materials and solvents were obtained from; Sigma Aldrich, Alfa Aesar or VWR. Reagents and chemicals were used without further purification unless required. Dry solvents from Grubbs System. Preparative size exclusion chromatography was conducted using SX-1 biobead resin, obtained from Bio-rad.

4.1.2. Nuclear magnetic resonance spectroscopy (NMR):

NMR analyses were carried out in CDCl_3 , DMSO, MeOD, D_8 -Ethyl acetate, D_6 -Acetone and D_8 -Toluene, these solvents obtained from Sigma Aldrich, Alfa Aesar and VWR. ^1H NMR and ^{13}C NMR spectra were recorded on Bruker AM-250 MHz and AMX400 MHz under ambient conditions. The spectra of NMR were analysed using MestReNova software (version: 6.0.2-5475) and Topspin 3.0 NMR software.

4.1.3. Infra Red Spectroscopy (IR):

IR absorption spectra were recorded utilising a Perkin Elmer Spectrum RX FT - IR spectrophotometer in the range of $700 - 4000 \text{ cm}^{-1}$.

4.1.4. Ultra Violet-Visible (UV/Vis) Spectroscopy:

UV-Vis absorbance was recorded using a Specord S-600 spectrophotometer which analysed utilising WinASPECT software.

4.1.5. Analytical Gel Permeation Chromatography (GPC):

Analytical GPC was carried out at room temperature utilising a high molecular weight (HMW) column setup composing of 3x300mm PL gel 10um mixed-B, or a low molecular weight (LMW) column setup composing of 2x600mm PL gel 5um mixed-E. Calibration was achieved by using polystyrene standards and molecular weights are thus reported relative to these specific standards used. All samples were run using Fisher GPC grade THF, toluene was added to prepared sample as a flow marker before being injected.

The concentration of a sample was studied using an Erma ERC-7512 refractive index detector.

4.1.6. Mass Spectroscopy (MS):

Samples with a mass range 2-800 Da, Electrospray Ion Mass Spectrometry (ESI-MS) was used to record spectra.

4.1.7. Gas Chromatography (GC):

Gas chromatography results were obtained on a PerkinElmer Autosystem XL Gas Chromatograph. Samples were carried out using hydrogen gas flow using a Phenomenex ZB-624 (length 30 meters, ID: 0.32 mm, Film Thickness 1.80 μm). The injection temperature was 170 °C, the oven temperature remained at 40 °C for 5 minutes and then increased to 170 °C over a 20-minute period.

4.2. Synthesis:

4.2.1. General Procedure 1: Polymerisation/Copolymerisation:

Chemicals with difference ratio (such as 3,5-diacetoxybenzoic acid, stearic acid, 4-nitrophenyl acetate, etc) and diphenyl ether (equal to the total) were added into a round bottom flask which was evacuated and flushed with nitrogen. The mixture was then heated to 225 °C. After 45 mins, the temperature was reduced to 180 °C, and the reaction was placed under reduced pressure for 4 hours. The crude reaction mixture was dissolved in hot THF and poured into 500 mL methanol. The resulting brown solid was filtered and washed with cold methanol yielding crude polymer.

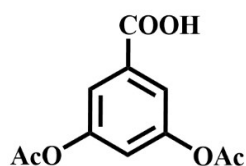
4.2.2. General Procedure 2: Synthesis of Porphyrins:

In a round bottom flask freshly distilled pyrrole and either 4-acetoxybenzaldehyde or benzaldehyde were added to refluxing propionic acid. The mixture was refluxed for a half hour and then allowed to cool to room temperature. The reaction mixture was filtered yielding purple solid crystals then washed with cold methanol till washings were colourless.

4.2.3. General Procedure 3: Synthesis of Zinc Functionalized Porphyrins:

Porphyrin was dissolved in DCM then $\text{Zn}(\text{OAc})_2 \cdot 2\text{H}_2\text{O}$ was added into the same round bottom flask fitted with condenser. The mixture was refluxed for a one hour and then allowed to cool to 25 °C. Unreacted zinc acetate dihydrate was removed *via* filtration. Solvent was then removed via rotary evaporation to obtain zinc functionalized porphyrin.

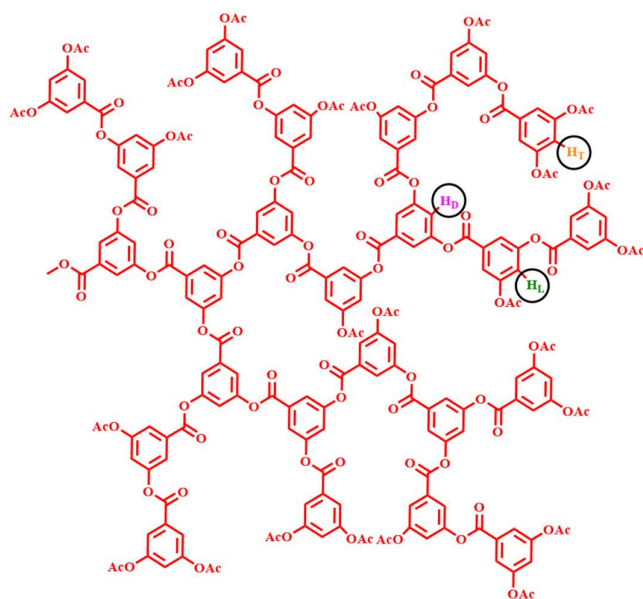
4.2.4. Synthesis of 3,5-Diacetoxybenzoic Acid **1**, AB₂ monomer:



A 500 mL round bottom flask was charged with 3,5-dihydroxybenzoic acid (77.00 g, 0.50 mol) and acetic anhydride (200 mL). The reaction mixture was heated to reflux, as the temperature increased the dihydroxy acid gradually dissolved into solution and the mixture was left to reflux for 6 hours. A brown solution was obtained containing a small amount of insoluble material; the excess acetic anhydride and acetic acid by-product were removed under reduced pressure, the compound dissolved in refluxing chloroform (200 mL) and filtered hot. Petroleum ether (300 mL) was then added to the mother liquor, precipitating a white solid. The mixture was left overnight; the white product was isolated by filtration and thoroughly washed with petroleum ether.

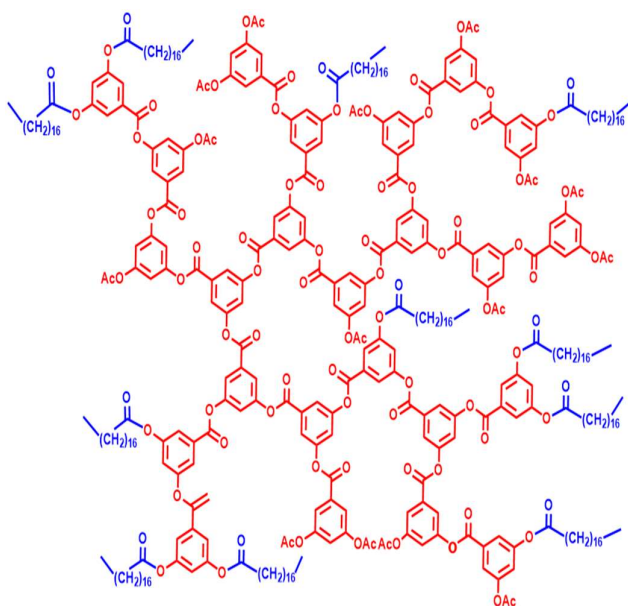
Yield: 40 g, 34%; ¹H NMR (CDCl₃) δ 2.33 (s, 6H, -CH₃), 7.22 (t, *J* = 2.5 Hz, 1H, Ar *p*-CH), 7.74 (d, *J* = 2.5 Hz, 2H, Ar *o*-CH), 10.19 (br s, 1H, -COOH); ¹³C NMR (CDCl₃) δ 21.0, 120.8, 121.0, 131.4, 151.0, 168.8, 170.1; IR (cm⁻¹) 1690 (COOR), 1769, 2400-3400 (COOH); MH⁺ = 237g/mol.

4.2.5. Polymerisation of 3,5-Diacetoxybenzoic Acid, **2HBP**:



Following general procedure 1, 3,5-diacetoxybenzoic acid **1** (1.70 g, 7.14 mmol) and diphenyl ether (1.70 g) were mixed and polymerised.

Yield: 1 g, 59% by mass; ¹H NMR (CDCl₃) δ 2.30 (s, 3H, -CH₃), 7.11-7.60 (br t, 1H, Ar *p*-CH), 7.70-8.10 (br m, 2H, Ar *o*-CH); GPC M_n = 9150, PDI = 11.00.

4.2.6. Copolymerisation of 3,5-Diacetoxybenzoic acid and Stearic acid, **4HBP-****SA%:**

4HBP-SA 10%: Following general procedure 1, 3,5-diacetoxybenzoic acid **1** (1.70 g, 7.14 mmol), stearic acid **3** (10% - 560 mg, 2.00 mmol) and diphenyl ether (1.70 g) were mixed and polymerised.

Yield: 2.77 g, 50% by mass; $^1\text{H NMR}$ (CDCl_3) δ 0.85 (br s, 3H, [SA] $\sim\text{COOCH}_2\text{CH}_2[\text{CH}_2]_{13}\text{CH}_3$), 1.15-1.40 (br s, 26H, [SA] $\sim\text{COOCH}_2\text{CH}_2[\text{CH}_2]_{13}\text{CH}_3$), 1.78 (br s, 2H, [SA] $\sim\text{COOCH}_2\text{CH}_2[\text{CH}_2]_{13}\text{CH}_3$), 2.25-2.43 (br s, 3H, [HBP] CH_3), 2.58 (br s, 2H, [SA] $\sim\text{COOCH}_2\text{CH}_2[\text{CH}_2]_{13}\text{CH}_3$), 7.20-7.60 (br t, 1H, [HBP] Ar $p\text{-CH}$), 7.77-8.09 (br m, 2H, [HBP] Ar $o\text{-CH}$); GPC $M_n = 7750$, PDI = 2.5.

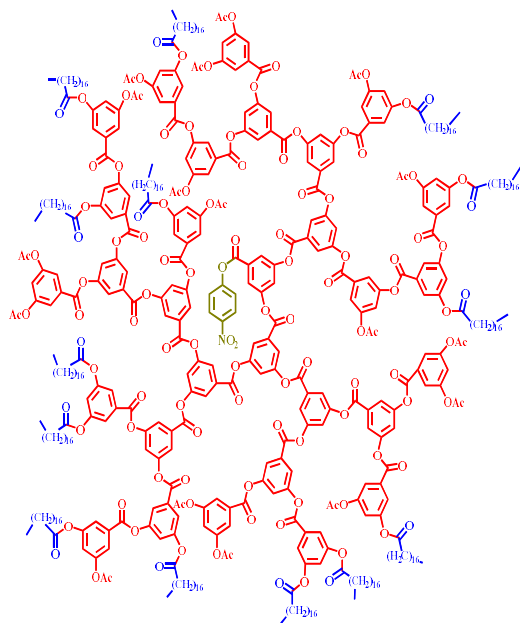
4HBP-SA 20%: Following general procedure 1, 3,5-diacetoxybenzoic acid **1** (1.70 g, 7.14 mmol), and stearic acid **3** (20% - 1.14 g, 4.00 mmol) and diphenyl ether (3 g) were mixed and polymerised.

Yield: 3.47 g, 56% by mass; $^1\text{H NMR}$ (CDCl_3) δ 0.85 (br s, 3H, [SA] $\sim\text{COOCH}_2\text{CH}_2[\text{CH}_2]_{13}\text{CH}_3$), 1.15-1.40 (br s, 26H, [SA] $\sim\text{COOCH}_2\text{CH}_2[\text{CH}_2]_{13}\text{CH}_3$), 1.78 (br s, 2H, [SA] $\sim\text{COOCH}_2\text{CH}_2[\text{CH}_2]_{13}\text{CH}_3$), 2.25-2.43 (br s, 3H, [HBP] CH_3), 2.58 (br s, 2H, [SA] $\sim\text{COOCH}_2\text{CH}_2[\text{CH}_2]_{13}\text{CH}_3$), 7.20-7.60 (br t, 1H, [HBP] Ar $p\text{-CH}$), 7.77-8.09 (br m, 2H, [HBP] Ar $o\text{-CH}$); GPC $M_n = 27600$, PDI = 5.1.

4HBP-SA 40%: Following general procedure 1, 3,5-diacetoxybenzoic acid **1** (1.70 g, 7.14 mmol), and stearic acid **3** (40% - 2.38 g, 8.00 mmol) and diphenyl ether (4 g) were mixed and polymerised.

Yield: 3.95g, 53% by mass; $^1\text{H NMR}$ (CDCl_3) δ 0.85 (br s, 3H, [SA] $\sim\text{COOCH}_2\text{CH}_2[\text{CH}_2]_{13}\text{CH}_3$), 1.15-1.40 (br s, 26H, [SA] $\sim\text{COOCH}_2\text{CH}_2[\text{CH}_2]_{13}\text{CH}_3$), 1.78 (br s, 2H, [SA] $\sim\text{COOCH}_2\text{CH}_2[\text{CH}_2]_{13}\text{CH}_3$), 2.25-2.43 (br s, 3H, [HBP] CH_3), 2.58 (br s, 2H, [SA] $\sim\text{COOCH}_2\text{CH}_2[\text{CH}_2]_{13}\text{CH}_3$), 7.20-7.60 (br t, 1H, [HBP] Ar $p\text{-CH}$), 7.77-8.09 (br m, 2H, [HBP] Ar $o\text{-CH}$); GPC $M_n = 3100$, PDI = 1.9.

4.2.7. 4-Nitrophenyl Acetate Cored Hyperbranched Copoly (3,5-Diacetoxybenzoic acid) and (Stearic acid), **7NPA-HBP-SA**%:



7NPA-HBP-SA (1:40:8): Following general procedure 1, 3,5-diacetoxybenzoic acid **1** (2.08 g, 8.70 mmol), stearic acid **3** (20% - 500 mg, 1.70 mmol), 4-nitrophenyl acetate **5** (2.5% - 40 mg, 0.2 mmol) and diphenyl ether (2.60 g) were mixed and polymerised.

Yield: 1.90 g, 73% by mass; $^1\text{H NMR}$ (CDCl_3) δ 0.85 (br s, 3H, [SA] $\sim\text{COOCH}_2\text{CH}_2[\text{CH}_2]_{13}\text{CH}_3$), 1.15-1.40 (br s, 26H, [SA] $\sim\text{COOCH}_2\text{CH}_2[\text{CH}_2]_{13}\text{CH}_3$), 1.78 (br s, 2H, [SA] $\sim\text{COOCH}_2\text{CH}_2[\text{CH}_2]_{13}\text{CH}_3$), 2.25-2.43 (br s, 3H, [HBP] CH_3), 2.58 (br s, 2H, [SA] $\sim\text{COOCH}_2\text{CH}_2[\text{CH}_2]_{13}\text{CH}_3$), 7.20-7.60 (br t, 1H, [HBP] Ar *p*-CH), 7.77-8.09 (br m₄, 2H, [HBP] Ar *o*-CH), 8.35 (d, 2H, [NPA] Ar *m*-CH); GPC $M_n = 2850$, PDI = 3.3.

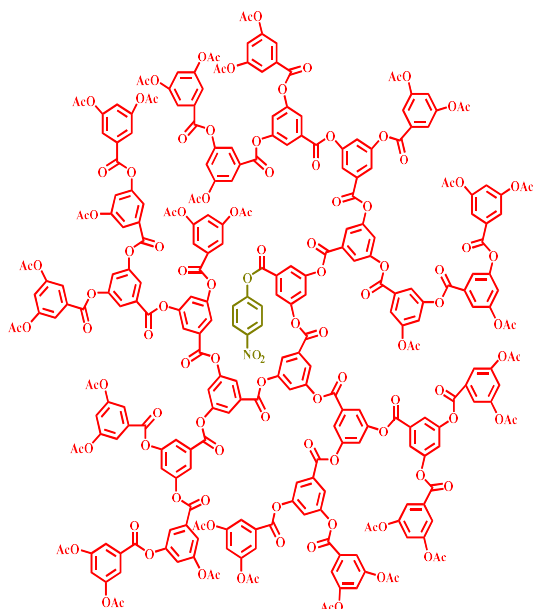
7NPA-HBP-SA (1:20:4): Following general procedure 1, 3,5-diacetoxybenzoic acid **1** (1.04 g, 4.30 mmol), stearic acid **3** (20% - 250 mg, 0.8 mmol), 4-nitrophenyl acetate **5** (5% - 40 mg, 0.2 mmol) and diphenyl ether (1.35 g) were mixed and polymerised.

Yield: 770 mg, 57% by mass; $^1\text{H NMR}$ (CDCl_3) δ 0.85 (br s, 3H, [SA] $\sim\text{COOCH}_2\text{CH}_2[\text{CH}_2]_{13}\text{CH}_3$), 1.15-1.40 (br s, 26H, [SA] $\sim\text{COOCH}_2\text{CH}_2[\text{CH}_2]_{13}\text{CH}_3$), 1.78 (br s, 2H, [SA] $\sim\text{COOCH}_2\text{CH}_2[\text{CH}_2]_{13}\text{CH}_3$), 2.25-2.43 (br s, 3H, [HBP] CH_3), 2.58 (br s, 2H, [SA] $\sim\text{COOCH}_2\text{CH}_2[\text{CH}_2]_{13}\text{CH}_3$), 7.20-7.60 (br t, 1H, [HBP] Ar *p*-CH), 7.77-8.09 (br m₄, 2H, [HBP] Ar *o*-CH), 8.35 (d, 2H, [NPA] Ar *m*-CH); GPC $M_n = 17050$, PDI = 2.6.

7NPA-HBP-SA (1:10:2): Following general procedure 1, 3,5-diacetoxybenzoic acid **1** (520 mg, 2 mmol), stearic acid **3** (20% - 125 mg, 0.4 mmol), 4-nitrophenyl acetate **5** (10% - 40 mg, 0.2 mmol) and diphenyl ether (685 mg) were mixed and polymerised.

Yield: 345 mg, 50% by mass; $^1\text{H NMR}$ (CDCl_3) δ 0.85 (br s, 3H, [SA] $\sim\text{COOCH}_2\text{CH}_2[\text{CH}_2]_{13}\text{CH}_3$), 1.15-1.40 (br s, 26H, [SA] $\sim\text{COOCH}_2\text{CH}_2[\text{CH}_2]_{13}\text{CH}_3$), 1.78 (br s, 2H, [SA] $\sim\text{COOCH}_2\text{CH}_2[\text{CH}_2]_{13}\text{CH}_3$), 2.25-2.43 (br s, 3H, [HBP] CH_3), 2.58 (br s, 2H, [SA] $\sim\text{COOCH}_2\text{CH}_2[\text{CH}_2]_{13}\text{CH}_3$), 7.20-7.60 (br t, 1H, [HBP] Ar *p*-CH), 7.77-8.09 (br m₄, 2H, [HBP] Ar *o*-CH), 8.35 (d, 2H, [NPA] Ar *m*-CH); GPC $M_n = 14550$, PDI = 2.2.

4.2.8. Polymerisation of 3,5-Diacetoxybenzoic Acid with 4-Nitrophenyl acetate core, **6NPA-HBP%**:



6HBP-NPA 2.5%: Following general procedure 1, 3,5-diacetoxybenzoic acid **1** (2.08 g, 8.7 mmol), 4-nitrophenyl acetate **5** (2.5% - 40 mg, 0.2 mmol) and diphenyl ether (2.15 g) were mixed and polymerised.

Yield: 1.70 g, 80% by mass; $^1\text{H NMR}$ (CDCl_3) δ 2.25-2.43 (br s, 3H, [HBP] CH_3), 7.20-7.60 (br t, 1H, [HBP] Ar *p*-CH), 7.77-8.09 (br m₄, 2H, [HBP] Ar *o*-CH), 8.35 (d, 2H, [NPA] Ar *m*-CH); GPC $M_n = 22000$, PDI = 3.02.

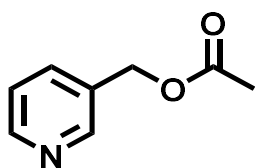
6HBP-NPA 5%: Following general procedure 1, 3,5-diacetoxybenzoic acid **1** (1.04 g, 4.3 mmol), 4-nitrophenyl acetate **5** (5% - 40 mg, 0.2 mmol) and diphenyl ether (1.10 g) were mixed and polymerised.

Yield: 850 mg, 78% by mass; $^1\text{H NMR}$ (CDCl_3) δ 2.25-2.43 (br s, 3H, [HBP] CH_3), 7.20-7.60 (br t, 1H, [HBP] Ar *p*-CH), 7.77-8.09 (br m₄, 2H, [HBP] Ar *o*-CH), 8.35 (d, 2H, [NPA] Ar *m*-CH); GPC $M_n = 14600$, PDI = 2.14.

6HBP-NPA 10%: Following general procedure 1, 3,5-diacetoxybenzoic acid **1** (520 mg, 2.1 mmol), 4-nitrophenyl acetate **5** (10% - 40 mg, 0.2 mmol) and diphenyl ether (560 mg) were mixed and polymerised.

Yield: 400 mg, 71% by mass; $^1\text{H NMR}$ (CDCl_3) δ 2.25-2.43 (br s, 3H, [HBP] CH_3), 7.20-7.60 (br t, 1H, [HBP] Ar *p*-CH), 7.77-8.09 (br m₄, 2H, [HBP] Ar *o*-CH), 8.35 (d, 2H, [NPA] Ar *m*-CH); GPC $M_n = 7600$, PDI = 3.52.

4.2.9. Synthesis of Pyridine 3-(Acetoxymethyl), **AMPy9**:

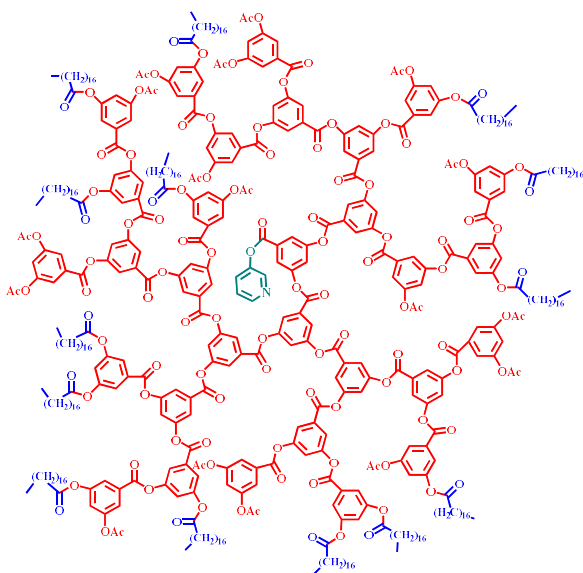


A 2-necked round bottom flask was fitted with a reflux condenser, 3-pyridinemethanol (20 g, 183 mmol), triethylamine (33 mL), anhydrous THF (600 mL) and a magnetic stirrer bar. The flask was stirred under N_2 for 10 mins before acetyl chloride (33 ml, 458 mmol) was added wise drop via syringe, stirring was then continued under nitrogen at room temperature for 30 mins. The reaction mixture (contained brown oil and white solid) was filtered, the white solid was washed with THF and disposed of. The brown oil was dissolved in DCM (100 mL), washed with saturated sodium hydrogen carbonate solution (200 mL), the distilled water (200 mL). This washing process was then repeated a second time and the DCM layer collected. MgSO_4 was added to absorb any remaining

traces of water in the solution and then removed via vacuum filtration. Finally, all the solvent was extracted via rotary evaporation yielding the product as brown oil.

Yield: 18.44 g, 65%; $^1\text{H NMR}$ (CDCl_3) δ 2.12 (s, 3H, $-\text{CH}_3$), 5.14 (s, 2H, CH_2), 7.32 (m, 1H, Ar 5- CH), 7.71 (dt, $J = 8.0, 1.5$ Hz, 1H, Ar 4- CH), 8.59 (d, $J = 5.0$ Hz, 1H, Ar 6- CH), 8.63 (s, 1H, Ar 2- CH); $^{13}\text{C NMR}$ (CDCl_3) δ 20.8, 63.6, 123.4, 131.6, 136.1, 149.5, 149.6, 170.6; IR (cm^{-1}) 1744 (C=O); $\text{MH}^+ = 152\text{g/mol}$.

4.2.10. 3-Acetoxypyridine Cored Hyperbranched Copoly (3,5-Diacetoxybenzoic acid) and (Stearic acid), **11Py-HBP-SA**:



7.20-7.60 (br t, 1H, [HBP] Ar *p*- CH), 7.77-8.09 (br m₄, 2H, [HBP] Ar *o*- CH), 8.58 (br m, 2H, [APy] Ar $\alpha+\beta$ - CH); GPC $M_n = 10000$, PDI = 2.44.

11Py-HBP-SA.1 (1:40:8):

Following general procedure 1, 3,5-diacetoxybenzoic acid **1** (5.00 g, 21 mmol), stearic acid **3** (20% 1.19 g, 4.2 mmol), 3-acetoxypyridine **12** (2.5% 71.9 mg, 525 μmol) and diphenyl ether (6.30 g) were mixed and polymerised.

Yield: 4.11 g, 65% by mass; $^1\text{HNMR}$ (CDCl_3) δ 0.85 (br s, 3H, [SA] $\sim\text{COOCH}_2\text{CH}_2[\text{CH}_2]_{13}\text{CH}_3$), 1.15-1.40 (br s, 26H, [SA] $\sim\text{COOCH}_2\text{CH}_2[\text{CH}_2]_{13}\text{CH}_3$), 1.78 (br s, 2H, [SA] $\sim\text{COOCH}_2\text{CH}_2[\text{CH}_2]_{13}\text{CH}_3$), 2.25-2.43 (br s, 3H, [HBP] CH_3), 2.58 (br s, 2H, [SA] $\sim\text{COOCH}_2\text{CH}_2[\text{CH}_2]_{13}\text{CH}_3$), 7.20-7.60 (br t, 1H, [HBP] Ar *p*- CH), 7.77-8.09 (br m₄, 2H, [HBP] Ar *o*- CH), 8.58 (br m, 2H, [APy] Ar *m*- CH); GPC $M_n = 10000$, PDI = 2.44.

11Py-HBP-SA.1 (1:10:2): Following general procedure 1, 3,5-diacetoxybenzoic acid **1** (5.00 g, 21 mmol), stearic acid **3** (20% 1.19 g, 4.2 mmol), 3-acetoxypyridine **12** (10% 287 mg, 2.1 mmol) and diphenyl ether (6.50 g) were mixed and polymerised.

Yield: 4.20 g, 64% by mass; $^1\text{HNMR}$ (CDCl_3) δ 0.85 (br s, 3H, [SA] $\sim\text{COOCH}_2\text{CH}_2[\text{CH}_2]_{13}\text{CH}_3$), 1.15-1.40 (br s, 26H, [SA] $\sim\text{COOCH}_2\text{CH}_2[\text{CH}_2]_{13}\text{CH}_3$), 1.78 (br s, 2H, [SA] $\sim\text{COOCH}_2\text{CH}_2[\text{CH}_2]_{13}\text{CH}_3$), 2.25-2.43 (br s, 3H, [HBP] CH_3), 2.58 (br s, 2H, [SA] $\sim\text{COOCH}_2\text{CH}_2[\text{CH}_2]_{13}\text{CH}_3$), 7.20-7.60 (br t, 1H, [HBP] Ar *p*- CH), 7.77-8.09 (br m₄, 2H, [HBP] Ar *o*- CH), 8.58 (br m, 2H, [APy] Ar *m*- CH); GPC $M_n = 6000$, PDI = 2.73.

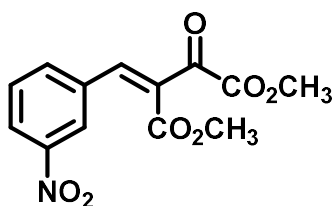
11Py-HBP-SA.3 (1:10:2): Following general procedure 1, 3,5-diacetoxybenzoic acid **1** (10.00 g, 42 mmol), stearic acid **3** (20% 2.38 g, 8.3 mmol), 3-acetoxypyridine **12** (10% 570 mg, 4.1 mmol) and diphenyl ether (13 mg) were mixed and polymerised.

Yield: 9.11 g, 70% by mass; $^1\text{H NMR}$ (CDCl_3) δ 0.85 (br s, 3H, [SA] $\sim\text{COOCH}_2\text{CH}_2[\text{CH}_2]_{13}\text{CH}_3$), 1.15-1.40 (br s, 26H, [SA] $\sim\text{COOCH}_2\text{CH}_2[\text{CH}_2]_{13}\text{CH}_3$), 1.78 (br s, 2H, [SA] $\sim\text{COOCH}_2\text{CH}_2[\text{CH}_2]_{13}\text{CH}_3$), 2.25-2.43 (br s, 3H, [HBP] CH_3), 2.58 (br s, 2H, [SA] $\sim\text{COOCH}_2\text{CH}_2[\text{CH}_2]_{13}\text{CH}_3$), 7.20-7.60 (br t, 1H, [HBP] Ar *p*- CH), 7.77-8.09 (br m₄, 2H, [HBP] Ar *o*- CH), 8.58 (br m, 2H, [APy] Ar *m*- CH); GPC $M_n = 5000$, PDI = 2.82.

11Py-HBP-SA.4 (1:5:1): Following general procedure 1, 3,5-diacetoxybenzoic acid **1** (10.00 g, 42 mmol), stearic acid **3** (20% 2.38 g, 8.3 mmol), 3-acetoxypyridine **12** (20% 1.14 g, 8.3 mmol) and diphenyl ether (13.5 mg) were mixed and polymerised.

Yield: 8.50 g, 62% by mass; $^1\text{H NMR}$ (CDCl_3) δ 0.85 (br s, 3H, [SA] $\sim\text{COOCH}_2\text{CH}_2[\text{CH}_2]_{13}\text{CH}_3$), 1.15-1.40 (br s, 26H, [SA] $\sim\text{COOCH}_2\text{CH}_2[\text{CH}_2]_{13}\text{CH}_3$), 1.78 (br s, 2H, [SA] $\sim\text{COOCH}_2\text{CH}_2[\text{CH}_2]_{13}\text{CH}_3$), 2.25-2.43 (br s, 3H, [HBP] CH_3), 2.58 (br s, 2H, [SA] $\sim\text{COOCH}_2\text{CH}_2[\text{CH}_2]_{13}\text{CH}_3$), 7.20-7.60 (br t, 1H, [HBP] Ar *p*-CH), 7.77-8.09 (br m, 2H, [HBP] Ar *o*-CH), 8.58 (br m, 2H, [APy] Ar *m*-CH); GPC $M_n = 5000$, PDI = 2.58.

4.2.11. Preparation of 2-oxo-3-benzylidenesuccinate, **13**:

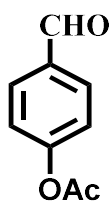


In 100 mL around bottom flask, A solution of 3-nitrobenzaldehyde (1.05 g, 7 mmol) and dimethyl acetylenedicarboxylate (1 g, 7 mmol) were mixed under nitrogen atmosphere in dry DME (10 mL). 20% molar ratio of 4-dimethylaminopyridine (0.17 g, 1.4 mmol) was added and the reaction then stirred for 1h at room temperature. The solvent was removed via rotary

evaporation and purification was done using column chromatography with eluent ratio of DCM containing with 10% petroleum ether gave 2-oxo-3-benzylidenesuccinates.

Yield: 119 mg, 6%. $^1\text{H NMR}$ (CDCl_3) δ 3.71 (s, 3H, OCH_3), 3.83 (s, 3H, OCH_3), 7.14 (s, 1H, =CH), 7.74 (t, $J = 8.0$ Hz, 1H, Ar 5-CH), 8.26 (dt, $J = 7.5, 1.5$ Hz, 1H, Ar 4-CH), 8.48 (m, 1H, Ar 6-CH), 8.70 (t, $J = 2$ Hz, 1H, Ar 2-CH); $^{13}\text{C NMR}$ (CDCl_3) δ 52.8, 53.5, 123.4, 128.0, 130.1, 131.5, 133.9, 136.9, 144.2, 148.5, 162.9, 164.2, 190.3; Elem. Anal. for $\text{C}_{13}\text{H}_{11}\text{O}_7\text{N}$ found: C= 54.26%, H= 4.2%, N= 4.58% (calculated: C= 53.25%, H= 3.78%, N= 4.78%); $\text{MH}^+ = 294\text{g/mol}$.

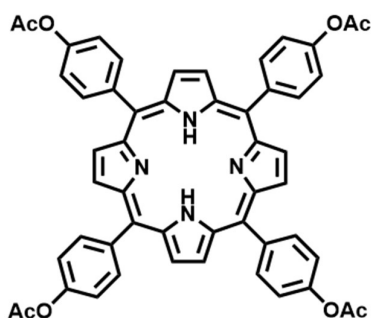
4.2.12. Preparation of 4-Acetoxybenzaldehyde, **14**:



A tow necked 1000 mL a round bottom flask was charged with triethylamine (30 mL, 215 mmol), 4-hydroxybenzaldehyde (20.00 g, 167 mmol) and anhydrous THF (600 mL). The mixture was stirred under nitrogen for 10 minutes before acetyl chloride (30 mL, 422 mmol) was added dropwise *via* syringe, stirring was then continued under nitrogen at room temperature for 30 minutes. The reaction mixture was filtered, the white solid was washed with THF and disposed of. The brown liquid

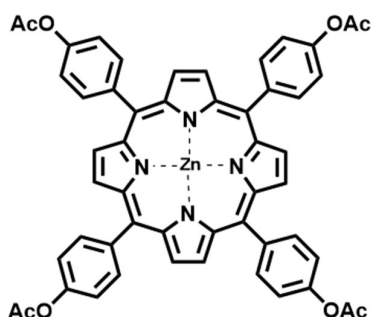
was collected and reduced on a rotary evaporator, the remaining brown oil was dissolved in dichloromethane (100 mL), washed with saturated sodium hydrogen carbonate solution (200 mL), and then distilled water (200 mL). This washing process was then repeated, while the organic layer collected and dried over excess of magnesium sulphate.

Yield: 16.3 g, 60%; $^1\text{H NMR}$ (CDCl_3) δ 2.31 (s, 3H, CH_3), 7.38 (d, $J = 5.5$ Hz, 2H, Ar *m*-CH), 7.95 (d, $J = 5.5$ Hz, 2H, Ar *o*-CH), 10.00 (s, 1H, COH); $^{13}\text{C NMR}$ (CDCl_3) δ 21.1, 122.3, 131.2, 133.9, 155.3, 168.7, 191.0; $\text{MH}^+ = 165\text{g/mol}$.

4.2.13. Synthesis of 4-Acetoxyphenyl Porphyrin, **15TAPP**:

Following general procedure 2, freshly distilled pyrrole (5.54 mL, 80 mmol) and 4-acetoxybenzaldehyde (13.13 g, 80 mmol) were added to refluxing propionic acid (300 mL) were mixed and synthesised.

Yield: 4.0 g, 24%; $^1\text{H NMR}$ (CDCl_3) δ -2.81 (s, 2H, NH), 2.53 (s, 12H, CH_3), 7.54 (d, $J=8.50$, 8H, phenylic $m\text{-CH}$), 8.25 (d, $J=8.50$, 8H, phenylic $o\text{-CH}$), 8.92 (s, 8H, pyrrolic $\beta\text{-H}$); $^{13}\text{C NMR}$ (DMSO) δ 21.1, 119.4, 119.9, 131.6, 134.9, 140.0, 149.3, 150.1, 169.3 UV/Vis (CH_2Cl_2) $\text{nm} = 417.5$ (λ_{max}), 515.5, 551.5, 591.5, 648.5; $\text{MH}^+ = 847\text{g/mol}$.

4.2.14. Porphyrin Zinc Complex, **16ZnTAPP**:

Following general procedure 3, 15TAPP (0.5 g, 0.59 mmol) was dissolved in DCM (75 mL) then $\text{Zn}(\text{OAc})_2 \cdot 2\text{H}_2\text{O}$ (1.4 g, 6.37 mmol) were added. Further purification was performed using column chromatography with a solvent system of dichloromethane containing 2% methanol by volume.

Yield: 250 mg, 47%; $^1\text{H NMR}$ (DMSO) δ 2.51 (s, 12H, CH_3), 7.56 (d, $J = 8.50$ Hz, 8H, phenylic $m\text{-CH}$), 8.21 (d, $J = 8.50$ Hz, 8H, phenylic $o\text{-CH}$), 8.81 (s, 8H, pyrrolic $\beta\text{-H}$); $^{13}\text{C NMR}$ (DMSO) δ 21.1, 119.4, 119.9, 131.6, 134.9, 140.0, 149.3, 150.0, 169.3; UV/Vis (CH_2Cl_2) $\text{nm} = 420.5$ (λ_{max}), 547.5, 586; $\text{MH}^+ = 909\text{g/mol}$.

4.2.15. Pyridine Catalysed Control Reaction of DMAD with 3-Nitrobenzaldehyde (in 5 mL standard solvent):

In round-bottomed flask 3-nitrobenzaldehyde (528 mg, 3.5 mmol), dimethyl acetylene dicarboxylate, DMAD, (497 mg, 3.5 mmol), and naphthalene (448 mg, 3.5 mmol) were added in presence of a dry solvent (5 mL), including toluene, chloroform, DMF, ethyl acetate, and DME. 3-Acetoxy pyridine 20% molar equivalent (95 mg, 0.7 mmol) was added to the reaction mixture. The colourless reaction mixture altered to a reddish brown solution and the reaction mixture was left stirring at room temperature for four days. During the reaction period, samples were taken regularly to be analysed using GC and $^1\text{H NMR}$.

$^1\text{H NMR}$ (CDCl_3) δ Product: 7.18 (s, 1H, $=\text{CH}$), 8.69 (s, 1H, Ar 2- CH), Substrate: 10.16 (s, 1H, COH).

4.2.16. Pyridine Catalysed Control Reaction of DMAD with 3-Nitrobenzaldehyde (in 1 mL deuterated solvent):

In a NMR tube 3-nitrobenzaldehyde (105 mg, 0.7 mmol), dimethyl acetylene dicarboxylate, DMAD, (99 mg, 0.7 mmol), and benzyl methyl ether (42.7 mg, 0.35 mmol) were added and dissolved in a deuterated solvent (1 mL), including toluene, chloroform, ethyl acetate, and acetone. 3-Acetoxy pyridine, 20% molar equivalent, (19 mg, 0.14 mmol) was added to the reaction mixture. The colourless reaction mixture changed to a reddish brown solution and the reaction mixture was left in the shaker machine at room temperature for four days. During the reaction period, ^1H NMR analysis was conducted.

^1H NMR (EtOAc- d_8) δ Standard: 4.55 (s, 2H, Ar- CH_2 -O), Product: 7.27 (s, 1H, = CH), 8.80 (t, 1H, Ar 2- CH), Substrate: 10.32 (s, 1H, COH).

^1H NMR (Acetone- d_6) δ Standard: 4.45 (s, 2H, Ar- CH_2 -O), Product: 7.12 (s, 1H, = CH), 8.67 (t, 1H, Ar 2- CH), Substrate: 10.20 (s, 1H, COH).

^1H NMR (Tol- d_8) δ Standard: 4.25 (s, 2H, Ar- CH_2 -O), Product: 8.71 (t, 1H, Ar 2- CH), Substrate: 9.40 (s, 1H, COH).

^1H NMR (CDCl_3) δ Standard: 4.42 (s, 2H, Ar- CH_2 -O), Product: 7.12 (s, 1H, = CH), 8.65 (t, 1H, Ar 2- CH), Substrate: 10.10 (s, 1H, COH).

4.2.17. Cored Pyridine Catalysis Reaction of DMAD with 3-Nitrobenzaldehyde (in 1 mL deuterated solvent):

In a NMR tube 3-nitrobenzaldehyde (105 mg, 0.7 mmol), dimethyl acetylene dicarboxylate, DMAD, (99 mg, 0.7 mmol), and benzyl methyl ether (42.7 mg, 0.35 mmol) were added and dissolved in a deuterated solvent (1 mL), including toluene, chloroform, ethyl acetate, and acetone. Cored pyridine hyperbranched copolymer (11Py-HBP-SA.3), 20% molar equivalent, (600 mg, 0.14 M) was added to the reaction mixture. The colourless reaction mixture changed to a reddish brown solution and the reaction mixture was left in the shaker machine at room temperature for four days. During the reaction period, ^1H NMR analysis was conducted.

^1H NMR (EtOAc- d_8) δ Standard: 4.55 (s, 2H, Ar- CH_2 -O), Product: 7.27 (s, 1H, = CH), 8.80 (t, 1H, Ar 2- CH), Substrate: 10.32 (s, 1H, COH).

^1H NMR (Acetone- d_6) δ Standard: 4.45 (s, 2H, Ar- CH_2 -O), Product: 7.12 (s, 1H, = CH), 8.67 (t, 1H, Ar 2- CH), Substrate: 10.20 (s, 1H, COH).

^1H NMR (Tol- d_8) δ Standard: 4.25 (s, 2H, Ar- CH_2 -O), Product: 8.71 (t, 1H, Ar 2- CH), Substrate: 9.40 (s, 1H, COH).

^1H NMR (CDCl_3) δ Standard: 4.42 (s, 2H, Ar- CH_2 -O), Product: 7.12 (s, 1H, = CH), 8.61 (t, 1H, Ar 2- CH), Substrate: 10.10 (s, 1H, COH).

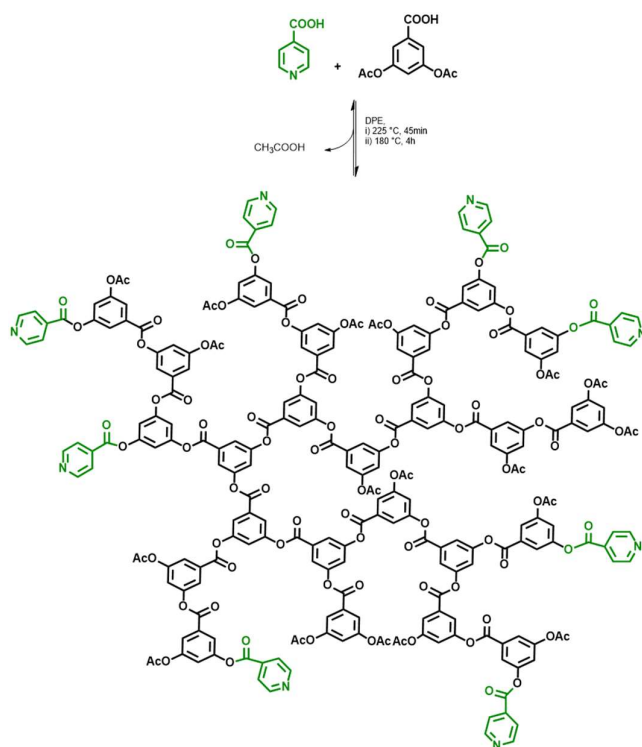
4.2.18. Recovery Experiment of Cored Pyridine Catalyst (in 3mL normal solvent):

In a round-bottomed flask 3-nitrobenzaldehyde (315 mg, 2.1 mmol), dimethyl acetylene dicarboxylate, (DMAD) and (295 mg, 2.1 mmol) were added and dissolved in 3 mL of standard solvent (including toluene and chloroform). Cored pyridine hyperbranched copolymer 20% molar equivalent (1.8 g, 0.14 M) was added to the reaction mixture. The colourless reaction mixture altered to a reddish brown solution and the reaction mixture was left stirring at room temperature for three days. The crude reaction mixture was precipitated overnight into 500 mL methanol. The resulting white solid was filtered and washed with cold methanol yielding crude polymer.

Yield: 1.55 g, 85% by mass; $^1\text{H NMR}$ (CDCl_3) δ 0.85 (br s, 3H, [SA] $\sim\text{COOCH}_2\text{CH}_2[\text{CH}_2]_{13}\text{CH}_3$), 1.15-1.40 (br s, 26H, [SA] $\sim\text{COOCH}_2\text{CH}_2[\text{CH}_2]_{13}\text{CH}_3$), 1.78 (br s, 2H, [SA] $\sim\text{COOCH}_2\text{CH}_2[\text{CH}_2]_{13}\text{CH}_3$), 2.25-2.43 (br s, 3H, [HBP] CH_3), 2.58 (br s, 2H, [SA] $\sim\text{COOCH}_2\text{CH}_2[\text{CH}_2]_{13}\text{CH}_3$), 7.20-7.60 (br t, 1H, [HBP] Ar $p\text{-CH}$), 7.77-8.09 (br m₄, 2H, [HBP] Ar $o\text{-CH}$); GPC $M_n = 10000$, PDI = 2.1.

4.2.19. Copolymerisation of 3,5-Diacetoxbenzoic Acid and Isonicotinic Acid,

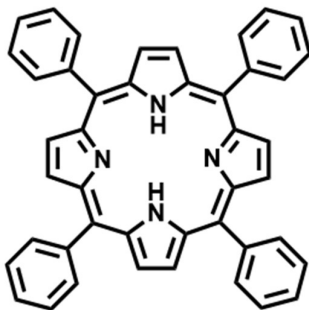
17HBP-INA:



Following general procedure 1, 3,5-diacetoxbenzoic acid **1** (2.00 g, 8.40 mmol), isonicotinic acid **18** (20% - 206 mg, 1.68 mmol), and diphenyl ether (2.20 g) were mixed and polymerised.

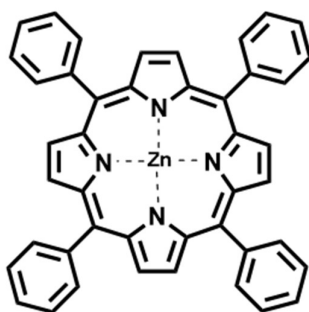
Yield 1.35g, 61% by mass; $^1\text{H NMR}$ (CDCl_3) δ 2.34 (br s, 3H, [HBP] CH_3), 7.20-7.60 (br t, 1H, [HBP] Ar $p\text{-CH}$), 7.77-8.10 (br m₄, 2H, [HBP] Ar $o\text{-CH}$ + 2H, [INA] Ar $\beta\text{-CH}$), 8.91 (br s, 2H, [INA] Ar $\alpha\text{-CH}$); GPC $M_n = 9000$, PDI = 1.5.

4.2.20. Synthesis of Tetraphenyl Porphyrin, TPP:



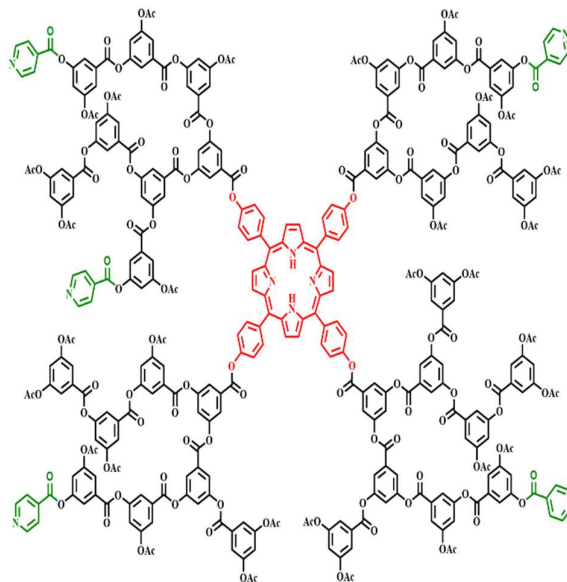
Following general procedure 2, freshly distilled pyrrole (7 mL, 100 mmol) and benzaldehyde (10 g, 100 mmol) were added to refluxing propionic acid (350 mL) were mixed and synthesised.

Yield: 3.5 g, 23%; $^1\text{H NMR}$ (CDCl_3) δ -2.76 (s, 2H, NH), 7.78 (m, 12H, phenylic $m\text{-CH}$ + $p\text{-CH}$), 8.24 (dd, $J=7.50$, 8H, phenylic $o\text{-CH}$), 8.87 (s, 8H, pyrrolic $\beta\text{-H}$); $^{13}\text{C NMR}$ (CDCl_3) δ 120.2, 126.7, 127.7, 134.6, 142.2; UV/Vis (CH_2Cl_2) $\text{nm} = 417$ (λ_{max}), 514, 548.5, 591, 650; $\text{MH}^+ = 615\text{g/mol}$.

4.2.21. Synthesis of Tetraphenyl Porphyrin, **19ZnTPP**:

Following general procedure 3, TPP (300 mg, 0.488 mmol) was dissolved in DCM (75 mL) then $\text{Zn}(\text{OAc})_2 \cdot 2\text{H}_2\text{O}$ (100 mg, 0.45 mmol) were added.

Yield: 278 mg, 92%; $^1\text{H NMR}$ (CDCl_3) δ 7.80 (m, 12H, phenylic $m\text{-CH}$ + $p\text{-CH}$), 8.26 (dd, $J=7.50$, 8H, phenylic $o\text{-CH}$), 8.99 (s, 8H, pyrrolic $\beta\text{-H}$); $^{13}\text{C NMR}$ (CDCl_3) δ 120.2, 126.7, 127.7, 134.6, 142.2; UV/Vis (CH_2Cl_2) $\text{nm} = 418.5$ (λ_{max}), 547, 586; $\text{MH}^+ = 677\text{g/mol}$.

4.2.22. Copolymerisation of 3,5-diacetoxybenzoic acid with Isonicotinic Acid (INA) and Tetraacetoxyphenyl Porphyrin (TAPP); **21TAPP-HBP-INA**:

Following general procedure 1, 3,5-diacetoxybenzoic acid **1** (5.00 g, 21 mmol), isonicotinic acid **18** (20% 520 mg g, 4.2 mmol), TAPP **15** (2.5% 440 mg, 0.525 mmol) and diphenyl ether (5.70 g) were mixed and polymerised.

Yield: 1.4 g, 24% by mass; $^1\text{H NMR}$ (CDCl_3) δ -2.81 (s, 2H, [TAPP] NH), 2.25-2.43 (br s, 3H, [HBP] CH_3), 7.20-7.60 (br t, 1H, [HBP] Ar $p\text{-CH}$), 7.77-8.09 (br m, 2H, [HBP] Ar $o\text{-CH}$), 8.25 (br, 8H, [TAPP] phenylic $o\text{-CH}$), 8.85 (br, 2H, [INA] Ar $\alpha\text{-CH}$) + (s, 8H, [TAPP] pyrrolic $\beta\text{-H}$); UV/Vis (CH_2Cl_2) λ_{max} $\text{nm} = 419, 515, 549, 592, 648$; GPC $M_n = 8500$, PDI = 2.11.

Chapter 5

5. Reference:

- 1 G. Odian, *Principles of polymerization*, John Wiley & Sons, Fourth Edi., 2004.
- 2 M. Irfan and M. Seiler, *Ind. Eng. Chem. Res.*, 2010, **49**, 1169–1196.
- 3 W. Jiang, Y. Zhou and D. Yan, *Chem. Soc. Rev.*, 2015, **44**, 3874–3889.
- 4 U. Boas, J. B. Christensen and P. M. H. Heegaard, *J. Mater. Chem.*, 2006, **16**, 3785–3798.
- 5 C. Gao and D. Yan, *Prog. Polym. Sci.*, 2004, **29**, 183–275.
- 6 D. A. Tomalia and J. M. J. Fréchet, *J. Polym. Sci. Part A Polym. Chem.*, 2002, **40**, 2719–2728.
- 7 Y. H. Kim, *J. Polym. Sci. Part A Polym. Chem.*, 1998, **36**, 1685–1698.
- 8 B. Voit, *J. Polym. Sci. Part A Polym. Chem.*, 2000, **38**, 2505–2525.
- 9 M. Jikei and M. Kakimoto, *Prog. Polym. Sci.*, 2001, **26**, 1233–1285.
- 10 A. Sunder, Johannes Heinemann and H. Frey, *Chem. Eur. J.*, 2000, **6**, 2499–2506.
- 11 B. Klajnert and M. Bryszewska, *Acta Biochim. Pol.*, 2001, **48**, 199–208.
- 12 A. Carlmark, C. Hawker, A. Hult and M. Malkoch, *Chem. Soc. Rev.*, 2009, **38**, 352–362.
- 13 S. M. Grayson and J. M. J. Fréchet, *Chem. Rev.*, 2001, **101**, 3819–3867.
- 14 E. BUHLEIER, W. WEHNER and F. VÖGTLE, *Synthesis (Stuttg.)*, 1978, **2**, 155–158.
- 15 D. A. Tomalia, H. Baker, M. Hall, G. Kallos, S. Martin, J. Roeck, J. Ryder and P. Smith, *Polym. J.*, 1985, **17**, 117–132.
- 16 G. R. Newkome, Z. Yao, G. R. Baker and M. J. Saunders, *J. Am. Chem. Soc.*, 1986, **18**, 849–850.
- 17 C. J. Hawker, R. Lee and J. M. J. Fréchet, *J. Am. Chem. Soc.*, 1991, **113**, 4583–4588.
- 18 D. Hölter, A. Burgath and H. Frey, *Acta Polym.*, 1997, **48**, 30–35.
- 19 S. P. Armes, Lecture 2 ;Department of Chemistry; University of Sheffield, 2009.
- 20 C. J. Hawker, P. J. Farrington, M. E. Mackay, K. L. Wooley and J. M. J. Fréchet, *J. Am. Chem. Soc.*, 1995, **117**, 4409–4410.
- 21 S. R. Turner, F. Walter, B. I. Voit and T. H. Mourey, *Macromolecules*, 1994, **27**, 1611–1616.
- 22 K. L. Wooley, J. M. J. Fréchet and C. J. Hawker, *Polymer (Guildf.)*, 1994, **35**, 4489–4495.
- 23 C. J. Hawker, E. E. Malmstrom, C. W. Frank and J. P. Kampf, *J. Am. Chem. Soc.*,

- 1997, **119**, 9903–9904.
- 24 D. Gennes, P.G. and H. Hervet, *J. Phys. Lett. Paris*, 1983, **44**, 351.
- 25 S. Rosenfeldt, N. Dingenouts, D. Pötschke, M. Ballauff, A. J. Berresheim, K. Müllen and P. Lindner, *Angew. Chemie - Int. Ed.*, 2004, **43**, 109–112.
- 26 J. F. Jansen, E. M. M. de Brabander-van den Berg and E. W. Meijer, *Science (80-)*, 1994, **266**, 1226–1229.
- 27 R. L. Lescanec and M. Muthukumar, *Macromolecules*, 1990, **23**, 2280–2288.
- 28 U. Boas, J. B. Christensen and P. M. H. Heegaard, *J. Mater. Chem.*, 2006, 3785–3798.
- 29 D. A. Tomalia, H. Baker, J. Dewald, M. Hall, G. Kallos, S. Martin, J. Roeck, J. Ryder and P. Smith, *Polym. J.*, 1985, **17**, 117–132.
- 30 C. J. Hawker and J. M. J. Fréchet, *J. Am. Chem. Soc.*, 1990, **112**, 7638–7647.
- 31 L. J. Twyman, A. S. H. King and I. K. Martin, *Chem. Soc. Rev.*, 2002, **31**, 69–82.
- 32 P. J. Flory, *J. Am. Chem. Soc.*, 1952, **74**, 2718–2723.
- 33 Y. H. Kim and O. W. Webster, *Am. Chem. Soc. Polym. Prepr. Div. Polym. Chem.*, 1988, **29**, 310–311.
- 34 B. I. Voit, *Comptes Rendus Chim.*, 2003, **6**, 821–832.
- 35 C. Schlenk, A. W. Kleij, H. Frey and G. Van Koten, *Organometallics*, 2000, **3773**, 3445–3447.
- 36 C. J. Hawker, R. Lee and J. M. J. Frechet, *J. Am. Chem. Soc.*, 1991, **113**, 4583–4588.
- 37 K. E. Uhrich, C. J. Hawker, J. M. J. Fréchet and S. R. Turner, *Macromolecules*, 1992, **25**, 4583–4587.
- 38 C. J. Hawker and F. Chu, *Macromolecules*, 1996, **29**, 4370–4380.
- 39 J. F. Miravet and J. M. J. Frechet, *Macromolecules*, 1998, **31**, 3461–3468.
- 40 C. R. Yates and W. Hayes, *Eur. Polym. J.*, 2004, **40**, 1257–1281.
- 41 M. Jikei, S. H. Chon, M. A. Kakimoto, S. Kawauchi, T. Imase and J. Watanebe, *Macromolecules*, 1999, **32**, 2061–2064.
- 42 J. M. J. Fréchet, M. Henmi, I. Gitsov, S. Aoshima, M. Leduc and R. B. Grubbs, *Sci*, 1995, **269**, 1080–1083.
- 43 K. Matyjaszewski, S. G. Gaynor, A. Kulfan and M. Podwika, *Macromolecules*, 1997, **30**, 5192–5194.
- 44 M. Suzuki, A. Ii and T. Saegusai, *Macromolecules*, 1992, **25**, 7071–7072.
- 45 A. Sunder, R. Hanselmann, H. Frey and R. Mülhaupt, *Macromolecules*, 1999, **32**, 4240–4246.

- 46 M. Liu, N. Vladimirov and J. M. J. Fréchet, *Macromolecules*, 1999, **32**, 6881–6884.
- 47 K. Inoue, *Prog. Polym. Sci.*, 2000, **25**, 453–571.
- 48 F. Vögtle, S. Gestermann, R. Hesse, H. Schwierz and B. Windisch, *Prog. Polym. Sci.*, 2000, **25**, 987–1041.
- 49 H. N. Patel and P. M. Patel, *Int. J. Pharma Bio Sci.*, 2013, **4**, 454–463.
- 50 R. Dong, Y. Zhou and X. Zhu, *Acc. Chem. Res.*, 2014, **47**, 2006–2016.
- 51 W. Wu, R. Tang, Q. Li and Z. Li, *Chem. Soc. Rev.*, 2015, **44**, 3997–4022.
- 52 A.-M. Caminade, D. Yan and D. K. Smith, *Chem. Soc. Rev.*, 2015, **44**, 3870–3873.
- 53 R. Dong, L. Zhou, J. Wu, C. Tu, Y. Su, B. Zhu, H. Gu, D. Yan and X. Zhu, *Chem. Commun.*, 2011, **47**, 5473.
- 54 Y. Shi, C. Tu, R. Wang, J. Wu, X. Zhu and D. Yan, *Society*, 2008, 1782–1785.
- 55 G. Tong, T. Liu, S. Zhu, B. Zhu, D. Yan, X. Zhu and L. Zhao, *J. Mater. Chem.*, 2011, **21**, 12369–12374.
- 56 S. S. Sheiko, M. Gauthier and M. Möller, *Macromolecules*, 1997, **30**, 2343–2349.
- 57 A. Asif, C. Huang and W. Shi, *Colloid Polym. Sci.*, 2004, **283**, 200–208.
- 58 M. Sono, M. P. Roach, E. D. Coulter and J. H. Dawson, *Chem. Rev.*, 1996, **96**, 2841–2888.
- 59 L. J. Twyman and X. Zheng, *Supramol. Chem.*, 2016, **28**, 617–623.
- 60 L. J. Twyman and Y. Ge, *Chem. Commun. (Camb.)*, 2006, 1658–1660.
- 61 K. K. Dyal, Phd Thesis ,Department of Chemistry, University of Sheffield, 2015.
- 62 L. J. Twyman, A. Ellis and P. J. Gittins, *Macromolecules*, 2011, **44**, 6365–6369.
- 63 C. C. Tzschucke, C. Markert, W. Bannwarth, S. Roller, A. Hebel and R. Haag, *Angew. Chemie - Int. Ed.*, 2002, **41**, 3964–4000.
- 64 K. Kirkorian, A. Ellis and L. J. Twyman, *Chem. Soc. Rev.*, 2012, **41**, 6138–59.
- 65 D. Wang and D. Astruc, *Coord. Chem. Rev.*, 2013, **257**, 2317–2334.
- 66 C. A. McNamara, M. J. Dixon and M. Bradley, *Chem. Rev.*, 2002, **102**, 3275–3300.
- 67 I. F. J. Vankelecom, *Chem. Rev.*, 2002, **102**, 3779–3810.
- 68 T. J. Dickerson, N. N. Reed and K. D. Janda, *Chem. Rev.*, 2002, **102**, 3325–3344.
- 69 A.-M. Caminade, P. Servin, R. Laurent and J.-P. Majoral, *Chem. Soc. Rev.*, 2008, **37**, 56–67.
- 70 L. Gade, *Dendrimer Catalysis*, 2006.

- 71 A. Ellis and L. J. Twyman, *Macromolecules*, 2013, **46**, 7055–7074.
- 72 X. Zheng, I. R. Oviedo and L. J. Twyman, *Macromolecules*, 2008, **41**, 7776–7779.
- 73 A. Ellis, D. Gooch and L. J. Twyman, *J. Org. Chem.*, 2013, **78**, 5364–5371.
- 74 X. Zhu, Y. Zhou and D. Yan, *J. Polym. Sci. Part B Polym. Phys.*, 2011, **49**, 1277–1286.
- 75 M. Alsharif, PhD Thesis, Department of Chemistry, University of Sheffield, 2015.
- 76 V. Nair, A. R. Sreekanth and A. U. Vinod, *Org. Lett.*, 2001, **3**, 3495–3497.
- 77 S. R. Turner, B. I. Voit and T. H., *Macromolecules*, 1993, **26**, 4617–4623.
- 78 W. J. Feast and N. M. Stainton, 1995, **5**, 405–411.
- 79 L. J. Twyman, Y. Ge and P. J. Gittins, *Supramol. Chem.*, 2006, **18**, 357–360.
- 80 P. J. Gittins, J. Alston, Y. Ge and L. J. Twyman, *Macromolecules*, 2004, **37**, 7428–7431.
- 81 P. J. Gittins, PhD Thesis, Department of Chemistry, University of Sheffield, 2005.
- 82 C. C. Liao, C. S. Wang, H. S. Sheu and C. K. Lai, *Tetrahedron*, 2008, **64**, 7977–7985.
- 83 E. Malmström, M. Johansson, a. Hult, E. Malmström, M. Johansson and a. Hult, *Macromolecules*, 1995, **28**, 1698–1703.
- 84 Y. Zheng, S. Li, Z. Weng and C. Gao, *Chem. Soc. Rev.*, 2015, **44**, 4091–4130.
- 85 J. Liu, Y. Zhong, J. W. Y. Lam, P. Lu, Y. Hong, Y. Yu, Y. Yue, M. Faisal, H. H. Y. Sung, I. D. Williams, K. S. Wong and B. Z. Tang, *Macromolecules*, 2010, **43**, 4921–4936.
- 86 S. Shamsudin, PhD Thesis, Department of Chemistry, University of Sheffield, 2012.
- 87 S. Hecht, N. Vladimirov and J. M. J. Fréchet, *J. Am. Chem. Soc.*, 2001, **123**, 18–25.
- 88 A. D. Adler, F. R. Longo, J. D. Finarelli, J. Goldmacher, J. Assour and L. Korsakoff, *J. Org. Chem.*, 1967, **32**, 476–476.
- 89 P. Rothmund, *J. Am. Chem. Soc.*, 1936, **58**, 625–627.
- 90 A. Ellis, PhD Thesis, Department of Chemistry, University of Sheffield, 2011.
- 91 F. M. Allan and P. D. Barton, *CRC Handbook of solubility parameters and other cohesion parameters*, Boca Raton, Florida: CRC, 1983.
- 92 P. J. Gittins and L. J. Twyman, *J. Am. Chem. Soc.*, 2005, **127**, 1646–1647.
- 93 N. S. Lewis, *Sci.*, 2007, **315**, 798.

- 94 H. Imahori, *J. Phys. Chem. B*, 2004, **108**, 6130–6143.
- 95 I. McConnell, G. Li and G. W. Brudvig, *Chem. Biol.*, 2010, **17**, 434–447.
- 96 A. Freer, S. Prince, K. Sauer, M. Papiz, A. Hawthornthwaite-lawless, G. Mcdermott, R. Cogdell and N. W. Isaacs, *Structure*, 1996, **4**, 449–462.
- 97 G. Mcdermott, M. Prince, A. A. Freer, A. M. Hawthornthwaite-lawless, M. Z. Papiz, R. J. Cogdell and N. W. Isaacs, *Nature*, 1995, **374**, 517.
- 98 X. Hu and K. Schulten, *Biophys. J.*, 1998, **75**, 683–694.
- 99 T. Mirkovic, E. E. Ostroumov, J. M. Anna, R. Van Grondelle and G. D. Scholes, *Chem. Rev.*, 2017, **117**, 249–293.
- 100 M. Kozaki, S. Suzuki and K. Okada, *Chem. Soc. Japan*, 2013, **42**, 1112–1118.
- 101 M. C. Balaban, A. Eichho, G. Buth and R. Hauschild, *J. Phys. Chem. B*, 2008, **112**, 5512–5521.
- 102 H. B. Baudin, J. Davidsson, S. Serroni, A. Juris, V. Balzani, S. Campagna and L. Hammarstro, *J. Phys. Chem. A*, 2002, **106**, 4312–4319.
- 103 T. Hori, N. Aratani, A. Takagi and T. Matsumoto, *Chem. Eur. J.*, 2006, **12**, 1319–1327.
- 104 V. S. Lin, S. G. Dimagno and M. J. Therien, *Science.*, 1994, **264**, 1105.
- 105 R. W. Wagner and J. S. Lindsey, *J. Am. Chem. Soc.*, 1994, **116**, 9759–9760.
- 106 J. Hsiao, B. P. Krueger, R. W. Wagner, T. E. Johnson, J. K. Delaney, D. C. Mauzerall, G. R. Fleming, J. S. Lindsey, D. F. Bocian, R. J. Donohoe, N. Carolina, S. Uni, N. Carolina and R. V May, *J. Am. Chem. Soc.*, 1996, **118**, 11181–11193.
- 107 R. W. Wagner, T. E. Johnson, J. S. Lindsey and N. Carolina, *J. Am. Chem. Soc.*, 1996, **118**, 11166–11180.
- 108 O. Mongin, A. Schuwey, M. Vallot and A. Gossauer, *Tetrahedron Lett.*, 1999, **40**, 8347–8350.
- 109 S. Prathapan, T. E. Johnson and J. S. Lindsey, *J. Am. Chem. Soc.*, 1993, **115**, 7519–7520.
- 110 R. Takahashi and Y. Kobuke, *J. Am. Chem. Soc.*, 2003, **125**, 2372–2373.
- 111 A. Adronov and J. M. J. Fréchet, *Chem. Commun.*, 2000, 1701–1710.
- 112 A. Nantalaksakul, D. R. Reddy, C. J. Bardeen and S. Thayumanavan, *Photosynth. Res.*, 2006, **87**, 133–150.
- 113 V. Balzani, P. Ceroni, M. Maestri and V. Vicinelli, *Curr. Opin. Chem. Biol.*, 2003, **7**, 657–665.
- 114 D. Jiang and T. Aida, *J. Am. Chem. Soc.*, 1998, **120**, 10895–10901.
- 115 M. Choi, T. Aida, T. Yamazaki and I. Yamazaki, *Chem. Eur. J.*, 2002, **8**, 2667–2678.

- 116 M. Choi, T. Yamazaki, I. Yamazaki and T. Aida, *Angew. Chem. Int. Ed.*, 2004, **43**, 150–158.
- 117 P. Jordan, P. Fromme, H. T. Witt, O. Klukas, W. Saenger and N. Krauß, *Nature*, 2001, **411**, 909–917.
- 118 S. Hecht, T. Emrick and J. M. J. Fr, 2000, 313–314.
- 119 P. Ballester, R. M. Gomila, C. A. Hunter, A. S. King and L. J. Twyman, *Chem. Commun.*, 2003, 38–39.
- 120 H. L. Anderson, *Inorg. Chem.*, 1994, **33**, 972–981.